

Comparative Study of OWTG Standards

Prepared for JIP Sponsorship

MMI Project No. MMW528

Submitted by
MMI Engineering, Inc.
Oakland, California

June 29, 2009

THIS DOCUMENT IS THE PROPERTY OF
MMI ENGINEERING AND THE JIP SPONSORSHIP

The information contained herein is bound by the various confidentiality agreements of the project sponsorship and should be distributed only within your organizations. It may not be lent, copied or conveyed to any third party without prior written consent from MMI Engineering. Use of the material herein by any third party is strictly at the sole risk of such party.

TABLE OF CONTENTS

LIST OF TABLES..... I

LIST OF FIGURES.....II

LIST OF SYMBOLS IV

EXECUTIVE SUMMARY 1

1.0 INTRODUCTION..... 1

 1.1 OVERVIEW 1

 1.2 REPORT STRUCTURE 1

 1.3 BACKGROUND..... 2

 1.4 OBJECTIVE 4

2.0 METHODOLOGY..... 5

 2.1 TYPES OF COMPARISONS..... 6

 2.1.1 *Direct Comparison* 6

 2.1.2 *Comparative Reliability*..... 6

 2.2 RANGE OF CASE STUDIES..... 13

 2.2.1 *Structure Type*..... 14

 2.2.2 *Site Conditions*..... 15

 2.2.3 *Case Study Combinations* 16

 2.3 STUDY TEAM 17

3.0 SUMMARY OF AVAILABLE GUIDELINES 19

 3.1 BACKGROUND..... 19

 3.2 API RP 2A 21

 3.3 IEC 61400-3 22

 3.4 ISO 23

 3.5 COMPARISON OF API AND IEC GUIDELINES..... 24

 3.5.1 *Wind Fatigue* 24

 3.5.2 *Load Cases* 24

 3.5.3 *Wake Induced Velocities*..... 25

 3.5.4 *Extrapolation of Stochastic Ultimate Loads* 25

 3.5.5 *Slam Loading*..... 25

 3.5.6 *Wave Kinematics Correction*..... 25

4.0 INHERENT RELIABILITY 27

 4.1 ASSUMPTIONS AND PREMISE..... 27

 4.2 DEVELOPMENT OF LIMIT STATE EQUATION – API & IEC 27

 4.2.1 *Independent Wave and Wind Loads*..... 27

 4.2.2 *Wave and Wind Loads* 34

 4.3 LOAD AND RESISTANCE VARIABLES 35

 4.4 PRELIMINARY RELIABILITY INDICES 36

5.0 REGIONAL COMPARISON OF RELIABILITY INDICES 38

6.0 SITE SPECIFIC COMPARISONS 44

 6.1 TURBINE SPECIFICATIONS 44

 6.1.1 *Turbine Size* 44

6.1.2	<i>Tower Properties</i>	46
6.1.3	<i>Turbine Operating Requirements</i>	47
6.2	SITE CONDITIONS	48
6.2.1	<i>Location and Water Depth</i>	48
6.2.2	<i>Support Structure Configuration</i>	51
6.2.3	<i>Oceanographic Data</i>	57
6.2.4	<i>Other Site Assumptions</i>	66
6.3	ANALYSIS METHODOLOGY	66
6.3.1	<i>Coupled Wave and Wind Load Analyses</i>	68
6.3.2	<i>Equivalent Monopile Properties for FAST Analyses</i>	72
6.3.3	<i>FAST Wave and Wind Load Analyses</i>	73
6.3.4	<i>Breaking Wave Forces</i>	73
6.3.5	<i>Additional Drag and Inertia</i>	78
6.4	MASSACHUSETTS CASE	79
6.4.1	<i>Wind and Wave Load Analyses with FAST</i>	80
6.4.2	<i>Total Wind and Wave Load Demand</i>	81
6.4.3	<i>Strength Checks</i>	83
6.4.4	<i>Capacity Analysis</i>	87
6.4.5	<i>Reliability Analysis</i>	89
6.5	TEXAS CASE	98
6.5.1	<i>Design Requirements for Resonance Avoidance</i>	98
6.5.2	<i>Wind and Wave Load Analyses with FAST</i>	99
6.5.3	<i>Total Wind and Wave Load Demand</i>	99
6.5.4	<i>Strength Checks</i>	100
6.5.5	<i>Capacity Analysis</i>	111
6.5.6	<i>Reliability Analysis</i>	112
7.0	SUMMARY AND CONCLUSIONS	118
7.1	KEY FINDINGS	118
7.1.1	<i>Inherent Safety Level in API and IEC</i>	118
7.1.2	<i>Effect of Period of Vibration Requirements</i>	119
7.1.3	<i>Effect of Operating versus Extreme Load Conditions</i>	119
7.1.4	<i>Effect of Breaking Waves</i>	119
7.1.5	<i>Regional Reliability Comparison</i>	120
7.2	RECOMMENDATIONS	120
	REFERENCES	122
	APPENDIX A: STEADY-STATE RESPONSE OF THE NREL 5MW BASELINE WIND TURBINE	124
	APPENDIX B: DRAG AND INERTIA COEFFICIENTS FOR LARGE DIAMETER TURBINE COMPONENTS	125
	APPENDIX C: STUDY ON THE SENSITIVITY OF LOAD ANALYSIS RESULTS TO THE NUMBER OF SIMULATIONS	131
	APPENDIX D: COMPARISON OF API AND IEC GUIDELINES	132
D.1	ENVIRONMENTAL CRITERIA AND PERFORMANCE REQUIREMENTS	132
D.1.1	<i>Wind</i>	132
D.1.2	<i>Sea State</i>	133
D.2	DIRECT COMPARISON BY TOPIC	134

<i>D.2.1 Planning.....</i>	<i>134</i>
<i>D.2.2 Design Criteria.....</i>	<i>138</i>
<i>D.2.3 Member Design.....</i>	<i>143</i>
<i>D.2.4 Fatigue.....</i>	<i>145</i>
<i>D.2.5 Foundation.....</i>	<i>146</i>
APPENDIX E: CODE CHECKS FOR MONOPILE (PER API AND IEC).....	147
APPENDIX F: CODE CHECKS FOR IEC TRIPOD.....	152
APPENDIX G: CODE CHECKS FOR API TRIPOD.....	167
APPENDIX H: EFFECT OF NONLINEARITY.....	182

LIST OF TABLES

<i>Table 1: Relationship of reliability index with probability of failure and return period</i>	8
<i>Table 2: Net safety factors for API and IEC</i>	31
<i>Table 3: 100-year to 50-year load ratio threshold to compare API to IEC</i>	31
<i>Table 4: Reliability indices for wind and wave loads</i>	36
<i>Table 5: Coefficient of variation across regions and for specific site data for MA and TX sites</i>	41
<i>Table 6: Reliability index comparison across MA and TX Sites, along with other regions with different Metocean CoV</i>	42
<i>Table 7: Properties of the NREL 5-MW baseline wind turbine</i>	46
<i>Table 8: Undistributed blade structural properties</i>	46
<i>Table 9: Tower dimensions [10]</i>	47
<i>Table 10: Metocean criteria for MA site</i>	65
<i>Table 11: Metocean criteria for TX site</i>	65
<i>Table 12: FAST input data for MA site</i>	81
<i>Table 13: Structural loads at MA site</i>	82
<i>Table 14: Monopile design loads for MA site</i>	84
<i>Table 15: Member utilization ratio</i>	85
<i>Table 16: Lateral load and overturning capacity for the monopile</i>	88
<i>Table 17: FAST input data for TX site</i>	99
<i>Table 18: Structural loads at TX site</i>	100
<i>Table 19: Member dimensions in API and IEC tripods</i>	102
<i>Table 20: Unfactored design loads for the members of the IEC tripod</i>	103
<i>Table 21: Unfactored design loads for the members of the API tripod</i>	104
<i>Table 22: Factored design loads and utilization ratios for the members of the IEC tripod (power production)</i>	105
<i>Table 23: Factored design loads and utilization ratios for the members of the IEC tripod (parked/idling)</i>	105
<i>Table 24: Design loads and utilization ratios for the members of the API tripod (power production)</i>	106
<i>Table 25: Design loads and utilization ratios for the members of the API tripod (parked/idling)</i>	106
<i>Table 26: Utilization ratio summary</i>	107
<i>Table 27: Capacity analysis results</i>	112
<i>Table 28: Reliability index for tripod for TX site</i>	117
<i>Table 29: API and IEC standards for wind</i>	132
<i>Table 30: API and IEC standards for sea state</i>	133
<i>Table 31: API and IEC comparison (planning)</i>	135
<i>Table 32: API and IEC comparison (design criteria)</i>	139
<i>Table 33: API and IEC/ISO comparison (member design)</i>	144
<i>Table 34: API and IEC comparison for fatigue</i>	145
<i>Table 35: API and IEC comparison for foundation</i>	146
<i>Table 36: Base shear for the broken waves</i>	182

LIST OF FIGURES

Figure 1: Indication of failure probability given load and resistance probability distributions.....	9
Figure 2: Specification of a factored load for design relative to a given load percentile.....	10
Figure 3: Specification of a factored resistance relative to a given resistance percentile.....	10
Figure 4: Types of support structures.....	15
Figure 5: Case study combinations.....	16
Figure 6: Project organization chart.....	17
Figure 7: Timeline for the development of API RP-2A.....	19
Figure 8: Reference guidelines/standards used by IEC 61400-3.....	20
Figure 9: Wind speed comparison for MA and TX sites.....	39
Figure 10: Wave height comparison for MA and TX sites.....	40
Figure 11: Campbell diagram.....	48
Figure 12: Location of MA site.....	49
Figure 13: Location of TX site.....	50
Figure 14: Parametric study for determining monopile dimensions.....	52
Figure 15: Monopile with a 4s period.....	53
Figure 16: Tripod with 4s period.....	56
Figure 17: Gumbel Fit to Site-Specific Wind Speed Data for MA Site (Y-Axis is Wind Speed). The Upper and Lower Bounds Around the Gumbel Fit Represent the 95% Confidence Bounds on the Fitted Data.....	58
Figure 18: Fitted Gumbel to significant wave height tropical storm data (y-axis is Hs in meters). The upper and lower bounds around the Gumbel fit, represent the 95% confidence bounds on the fitted data.....	59
Figure 19: Correlation of wind speed and Hs for tropical storms.....	60
Figure 20: MA site relation of maximum wave height in a tropical storm with the Hs value of that storm.....	61
Figure 21: The average zero-crossing period in a storm related to Hs, the wave period for the maximum wave height is assumed to be $1.2 \times T_z$	61
Figure 22: Surge height as a function of significant wave height for MA site.....	62
Figure 23: Maximum wave height related to Hs for tropical storms for TX site.....	63
Figure 24: Surge height related to Hs for tropical storms for TX site.....	63
Figure 25: The average zero-crossing wave period ($T_{max} = 1.2 \times T_z$) related to Hs in tropical storms for TX site.....	64
Figure 26: Methodology flowchart.....	67
Figure 27: Grid points for the wind velocity data and force components acting on a blade.....	69
Figure 28: Plot showing the contributions of drag and inertia forces separately to the total time history of wave force for one wave cycle (t/T is the time expressed as a fraction of the wave period T).....	71
Figure 29: Tower and monopile model properties.....	72
Figure 30: Breaking waves at MA site. (T_{app} is the apparent wave period.).....	74
Figure 31: Breaking waves at TX site.....	75
Figure 32: Concept of breaking wave.....	76
Figure 33: Impulse input force.....	77
Figure 34: Impulse input force.....	78
Figure 35: Additional drag and inertia forces.....	78
Figure 36: Monopile model in CAP.....	84
Figure 37: Monopile details (final design).....	86
Figure 38: Results of a typical capacity analysis. (Left: Load-displacement curve; Right: deflected shape with nonlinear events.).....	88
Figure 39: Mudline overturning moment (OTM) versus wind speed for the smallest storm analyzed. (There is no breaking wave phenomenon for this small storm.).....	91
Figure 40: Mudline OTM vs wind speed for the largest storm analyzed. (Includes breaking wave effect.).....	92
Figure 41: Loads on blade and wave loads only as a function of W_s , shown for all Hs values analyzed.....	93
Figure 42: Loads on blade and wave load as a function of Hs.....	94
Figure 43: Total loads (including all applicable components) vs. wind speed. (1 hour average, at 10m reference height.).....	95
Figure 44: All components included as a function of Hs.....	96

Figure 45: Total load and capacity for MA site as a function of wind speed. (Failure mechanism is different for operating vs. parked modes.).....	97
Figure 46: Total load and capacity for MA site as a function of wave height	98
Figure 47: Tripod model in CAP. (Left: Oblique model view; Right: Loads applied to the model.)	102
Figure 48: Utilization ratios.....	107
Figure 49: IEC tripod details (final design)	109
Figure 50: API tripod details (final design)	110
Figure 51: Results of a typical capacity analysis. (Bottom: load-displacement curve; Top: deflected shape with nonlinear events at important steps.).....	111
Figure 52: Mudline overturning moment due to aerodynamic wind load and hydrodynamic wave loads. (No breaking wave effect included yet.).....	113
Figure 53: Loads from aerodynamic and hydrodynamic effects (excluding breaking wave effects) vs. H_s	114
Figure 54: Total load (including all effects) vs wind speed for different H_s values.....	114
Figure 55: Total load (including all effects) vs H_s for different wind speed values.....	115
Figure 56: Total load and capacity as a function of wind speed (as reference: $W_{s_{50yr}} \approx 39\text{m/s}$, $W_{s_{100yr}} \approx 44\text{m/s}$)	115
Figure 57: Total load and capacity as a function of H_s (as reference: $H_{s_{50yr}} \approx 8.7\text{m}$, $H_{s_{100yr}} \approx 9.74\text{m}$).....	116
Figure 58: Change in acceleration due to different environmental conditions	182
Figure 59: Change in square of velocity due to different environmental conditions	183
Figure 60: Change in force due to different environmental conditions	183

LIST OF SYMBOLS

A	Area (projected or cross section)
c	Influence coefficient
C	Wave celerity
C_A	Normalized hydrodynamic-added-mass coefficients
C_D	Viscous drag coefficients
C_{ds}	Steady state flow drag coefficient at post-critical Reynolds numbers
C_M	Inertia coefficient
C_S	Shape coefficient
C_X	Water height above mean still water at numerical limit for stream
C_Y	Water height above mean still water at physical limit for breaking
D	Diameter
D_{mp}	Monopile diameter
E	Young's modulus
\tilde{F}_y	Ultimate bending capacity normalized by its nominal or characteristic value
f_a	Acting axial stress (API design)
F_a	Allowable axial stress
f_b	Acting bending stress (API and IEC/ISO design)
f_c	Acting compressive stress (IEC/ISO design)
F_t	Allowable tensile stress
F_b	Allowable bending stress
F_v	Allowable beam shear stress
F_{xe}	Elastic local buckling stress
F_{xc}	Inelastic local buckling stress
f_v	Acting shear stress (API and IEC/ISO design)
F_y	Yield strength
H_b	Wave height at the breaking location
H_{max}	Maximum wave height
H_s	Significant wave height
H_X	Wave height at numerical limit for stream

H_Y	Wave height at physical limit for breaking
I	Moment Inertia
K	Keulegan-Carpenter Number
k	Effective length factor
γ_m	Material factor
γ_f	Partial load factor
\tilde{L}_a	Normalized annual maximum 1-hour mean wind load
\tilde{L}_w	Normalized annual maximum hydrodynamic load
L	Load
L	Unbraced length
L_{BW}	Aerodynamic blade load and the hydrodynamic wave load calculated using FAST
L_c	Characteristic Load
L_{code}	Load for a given code
L_{Corr}	Additional load where a correction to Stream function is warranted
L_f	Design Load
L_n	Nominal Load
L_p	Design load at percentile p
L_{Slam}	Wave slam load
L_{tower}	Wind load on the tower
M_b	Base over-turning moment
M_t	Tower top over-turning moment
P_f	Annual failure probability
q	Displacement degree of freedom of tower/monopile node
R_{mp}	Radius of the monopile
R	Resistance (or capacity)
R_c	Characteristic Capacity
R_{code}	Resistance at percentile p for a given code
R_f	Design Resistance
R_n	Nominal Capacity

R_p	Resistance at percentile p
r	Radius of gyration
S	Load effects (or Elastic section modulus)
SF	Allowable stress reduction factor
T	Random variable representing the turbulence effect
t	Thickness
T_{\max}	Zero crossing wave period corresponding to maximum wave height in a storm
T_z	Average zero crossing wave period
u	Velocity (water particle or wind)
U_m	Maximum water particle velocity normal to the cylinder axis
V	Displaced volume of the cylinder per unit length
V_b	Base shear force
V_t	Tower top shear force
W_s	Average wind speed
X_{BW}	Model uncertainty and variability for aerodynamic load on blade and hydrodynamic load from drag and inertia from wave particle kinematics acting on the foundation.
X_h	Model error due to hydrodynamic load
X_a	Model error due to aerodynamic load
X_{dyn}	Model error due to turbulent loading
X_m	Uncertainty in the capacity model
X_{Corr}	Model uncertainty for the load correction applied to Stream
X_{Slam}	Model uncertainty for slam loads
X_{Tower}	Model uncertainty on tower wind load
α	Relative contribution of wave load to the total wave and wind load
β	Reliability index
η_b	Maximum elevation of the free water surface above the still water level
λ	Curling factor
ρ	Density (water or air)
Z	Plastic section modulus

EXECUTIVE SUMMARY

There are currently no guidelines that have been accepted by U.S. agencies for the design of offshore wind power generators in U.S. Outer Continental Shelf (OCS) waters. The International Electrotechnical Commission (IEC) has developed guidelines specifically for the design requirements of offshore wind turbines. It has been proposed that the IEC guidelines be adopted by the U.S. wind power industry as the governing standard for offshore systems. This study provides a due diligence review of the IEC guideline to assess its applicability for conditions that exist in U.S. OCS waters. This included targeted case studies that addressed different site conditions and types of support structures.

The study was completed to provide a baseline comparison of the IEC design requirements for offshore wind turbines (IEC 61400-3) and the American Petroleum Institute (API) recommended practice for the design of fixed offshore platforms (API RP-2A). This comparison was specifically performed to address the effects of applying either the 50-year storm condition used by the IEC or the 100-year storm condition used by the API. Particular emphasis was placed on the assessment of hurricane and tropical storm hazards that exist in the Gulf of Mexico and along the east coast of the U.S. and how these hazards affect the application of either design guideline.

The study has compared the standards in terms of structural reliability for extreme storm conditions. The comparison starts with a generic assessment of each guideline and ends with site specific case studies. The results of the study show that the IEC and API design methodologies generate similar levels of structural reliability for the conditions included in this study. This is partly due to similarities in the fundamental philosophies of the guidelines and also a result of other design requirements that tend to deemphasize the influence of the extreme storm criteria.

The study also found that the levels of reliability that are achieved when using the IEC or API guidelines are significantly affected by the annual variability, or coefficient of variation (CoV), in tropical storm severity. Areas like the Gulf of Mexico exhibit large variability in storm severity, which results in a greater difference in the definition of 100- and 50-year storm conditions (i.e., wave heights and wind speeds). In this situation, the application of the API

design recipe generally results in marginally higher levels of reliability. Conversely, in areas where the CoV is relatively small (e.g. the North Sea), the use of the IEC design recipe generally results in a marginally higher reliability.

The case studies show that, for the specific conditions included in the study, the requirement to provide a support structure that is stiff enough to avoid dynamic resonance with the rotor dictates the design of the support structure. As a result, the designs were found to generate capacities that were much greater than required for the extreme storm levels (i.e., versus 100-year load for API and 50-year load for IEC). Consequently, the reliability index for both the monopile and the tripod were found to be high for both API and IEC designs. In the Gulf of Mexico case study, API resulted in a marginally higher reliability index due to the relatively large CoV of the metocean environment.

The site specific comparison included in the study has shown that the potential exposure to tropical storms significantly impacts the structural reliability of wind power systems. This was found not only for the Gulf of Mexico site, which was expected, but also for the Northeast location.

The case studies have also shown that the need to avoid dynamic resonance with rotor frequency, amongst other issues, can affect the design of the support structure, resulting in high reliability indices regardless of the design recipe that is used. These design factors have, to some extent, offset the adverse impact of the higher CoVs associated with the tropical storms included in the case studies. It is likely that a set of conditions could be defined (i.e., latitude, water depth, support structure type and turbine size) where the support structure design would be controlled predominantly by extreme storm conditions. In these situations, the levels of reliability that would be produced using either the API or IEC design recipes would be substantially lower than those indicated for the case studies documented herein. Also, these situations could produce reliability levels that are less than the target levels inherent to API or IEC.

The U.S. wind power industry will need to address the minimum performance requirements for offshore wind power, which directly correlate to safety levels for ultimate and fatigue strength. These performance requirements can then be used to establish the design requirements, using

either an IEC or API approach that will achieve an acceptable level of structural reliability. This study has included sensitivity analysis using both guidelines to illustrate the means to achieve this goal.

1.0 INTRODUCTION

1.1 OVERVIEW

This report documents the results of a Joint Industry Project (JIP) that was undertaken to address design standards needed for the development of offshore wind turbine generation (OWTG) in the United States. This project was sponsored by the U.S. Minerals Management Service, the National Renewable Energy Laboratory, GE Energy-Wind, Southern Company, Clipper Wind, BP and ABS.

This work was executed in phases over a period of two years as the sponsorship and associated funding levels were defined. The first phase of the work included a definition of the specific study objectives and an identification of the design guidelines that would be used as the basis of the comparison. This first phase assessment addressed the functional similarities and differences in the codes and compared the levels of structural reliability that are obtained using the two selected design guidelines in a generic application to offshore wind support structures.

The second phase of the work included a more extensive comparison of structural reliability and addressed the significance of tropical storm hazards. The second phase performed two site specific comparisons to enhance understanding of the effects of structure type, water depth, and environmental conditions on structural reliability. This site specific work required the selection of two hypothetical wind farm locations and the development of wind and wave data for each site. The results of the second phase of work have been integrated with those of the first phase and are documented herein as one comprehensive study report.

1.2 REPORT STRUCTURE

The report is structured similar to the sequence in which the scope of work was completed.

- Section 2 provides a summary of the general approach to the work, the objectives of each of the study tasks, the study team and responsibilities. This section does not provide details regarding specific analytical methods that were applied during the study; this information is provided in each section that presents specific analytical results.

- Section 3 summarizes the results of the direct comparison (i.e., Task 1 of the study) of the API and IEC design guidelines.
- Section 4 provides a detailed review of the methodology that was used in all reliability analysis. This section also provides the results of the comparison of the inherent levels of reliability generated with each guideline (i.e., Task 2 of the study).
- Section 5 provides the assessment of regional environmental conditions (i.e., tropical, extra-tropical, and continuous storms) on the reliability comparison (i.e., Task 3.2 of the study).
- Section 6 provides the results of the site specific case studies (i.e., Task 4 of the study). This section provides the details of the analysis methodologies used to define the loads and other structural requirements for each case, summaries of structural response simulations, capacity analysis and final reliability comparisons. This section also provides the oceanographic data that was developed to support both the regional sensitivity assessment of reliability and the site specific case studies (i.e., Task 3.1 of the study).
- Section 7 of the report provides a summary of the conclusions, recommendations, and key findings of the study.
- Details of the specific aspects of the work, such as wind force simulation time history results, are provided as Appendices to the report.

1.3 BACKGROUND

While the U.S. has a long history of onshore wind power development, offshore wind power resources remain largely untapped. At the time of this study, there are a few offshore wind farms proposed for U.S. waters but none have yet been constructed. Offshore wind represents a relatively new resource that can be developed with the use of today's very large, high efficiency, turbines.

The U.S. Minerals Management Service (MMS) has been established as the lead regulatory authority for offshore wind power developments on the U.S. Outer Continental Shelf (OCS). This responsibility was established through the Energy Policy Act of 2005. There are currently no

guidelines that have been accepted by the MMS or other U.S. agencies for the design of offshore wind power generators in U.S. waters. The codes and guidelines for offshore wind power development overseas have a limited history of use and have not yet been reviewed for their applicability to the conditions that exist on the U.S. OCS or for the levels of safety that would be required by the MMS and other U.S. agencies.

Substantial experience with land-based wind farms has provided the industry with the basis to understand complex wind loading and the associated design requirements for wind power generators, support structures, and foundations. The codes and guidelines that have been developed for the design of land-based wind turbine structures have been adapted to address issues associated with the marine environment. These additional requirements have focused primarily on the loads generated from waves and currents and the effect of these loads on the design of the support structure and its foundation.

The MMS has significant experience with the design, fabrication, and installation of offshore structures. As stated in the Code of Federal Regulations, the MMS utilizes the American Petroleum Institute (API) Recommended Practice for Planning, Designing, and Constructing Fixed Offshore Platforms (API RP-2A Working Stress Design [1]) as the basis for regulating the design and assessment of offshore structures in U.S. waters. This recommended practice is currently in its twenty-first edition, reflecting refinements based on the design of over 7,000 structures installed in the Gulf of Mexico, offshore Southern California, and in the Cook Inlet of Alaska. In addition to the application for oil and gas platforms located in U.S. federal waters, API RP-2A has been used for the design of numerous offshore platforms worldwide.

API RP-2A provides a basis for the design of offshore structures subject to wave, wind, current, and earthquake loading conditions; however, it does not address the scope and range of all conditions that are required for the design of wind turbine support structures. API RP-2A would have to be adapted or supplemented with other standards if it were to be used as the basis for wind turbine design.

Guidelines that have been developed for the design of offshore wind turbine generators, such as IEC 61400-3 [2], have utilized offshore guidelines similar to API RP-2A as the basis for the

development of their marine requirements. Therefore, guidelines such as IEC 61400-3 and API RP-2A may include similar design requirements for wave and current loading conditions. However, a direct comparison of the IEC and API requirements show that there are some specific differences. The IEC uses a 50-year return period for the definition of extreme environmental design conditions. API RP-2A uses a 100-year return period for the definition of design conditions for high consequence platforms. There are other differences in the guidelines, such as load factors and factors of safety that must also be evaluated to fully compare levels of structural reliability that are generated with the use of each of these guidelines. This complete assessment is the focus of this study.

1.4 OBJECTIVE

The objective of this study was to compare two different design guidelines with respect to their applicability to the design of offshore wind turbine support structures in U.S. waters. The study compared the IEC61400-3 and API RP-2A guidelines¹ and included a detailed assessment of the levels of structural reliability for extreme storm loading conditions that are achieved through the use of these guidelines.

The focus of this study was to specifically assess the difference in the 50- and 100-year storm conditions that are included in the IEC and API guidelines, respectively. This required an assessment of the design process and resulting structural requirements (e.g., member sizes) that are needed to meet the specific requirements of each guideline. Therefore, the comparative assessment of reliability has addressed the failure probabilities under strength requirements since these are affected by the aforementioned return periods. A comprehensive reliability assessment would also address other failure conditions including, for example, operational failures due to mechanical systems, overload of rotor blades, and fatigue. This study has specifically determined the reliability indices associated with the potential for the overload of the substructure under extreme loading conditions and does not specifically address any other failure condition.

¹ In this study, we use the word guideline(s) and standard(s) interchangeably as these refer to the set of rules or recommended practices provided by the respective organizations for OWTG.

2.0 METHODOLOGY

The API and IEC guidelines were compared to establish both their similarities and differences with respect to their applicability to offshore wind turbine support structures in U.S. OCS waters. The IEC guideline has been developed specifically for offshore wind turbine support structures and addresses many design requirements that are specific to these types of structures that are not addressed within API RP2A, given API's focus on offshore oil and gas platforms. The IEC guideline does not specifically address the requirements for offshore wind turbine support structures in regions subject to hurricanes. Also, the IEC guideline utilizes a 50-year storm condition to define the loads that are required to establish the minimum strength requirements for the support structure.

In contrast, given its focus on the design of offshore structures in the Gulf of Mexico, API RP2A specifically addresses the hazards associated with hurricanes. In contrast to the 50-year storm criteria used in IEC, API RP2A uses 100-year storm criteria for high consequence platforms. Therefore, while the IEC guidelines are more applicable to the specific requirements of offshore wind turbine support structures, it is not clear whether or not the application of the IEC guidelines would result in levels of structural safety that are consistent with the overall requirements of the Minerals Management Service, specifically with respect to regions subject to hurricanes.

The intent of this study has been to address these issues and to better understand how the guidelines compare in terms of the overall levels of safety for extreme storm loading conditions that are achieved through their application to offshore wind turbine support structures. Although the study has assessed the guidelines through various means, the fundamental methodology that has been used consists of a comparison of the reliability indices² that are computed for typical wind turbine support structures using the IEC and API guidelines in various conditions in U.S. OCS waters.

² The reliability index provides a measure of the structure's safety. Specifically, in this study, the reliability index measures safety against ultimate strength failure. This is assessed by developing an annual failure probability of the structure.

2.1 TYPES OF COMPARISONS

The study has compared the guidelines from two basic perspectives – direct comparison and comparative reliability.

2.1.1 Direct Comparison

A direct comparison of the IEC 61400-3 and API RP2A standards was performed to achieve a number of key project objectives. Firstly, the IEC and API standards are significantly different in terms of the definition of design environmental conditions and also with respect to the specific design procedures that are addressed within each specification. This first comparison provided a side-by-side examination of the standards through each step in the design process and addressed where the standards are similar or different. The definition of common elements within the codes helped form the basis for the comparison of reliability indices evaluated later in the study.

Secondly, this comparison also provided a “gap” assessment to establish design requirements that exist in one standard but not the other. As an example, the IEC provides a comprehensive definition of load cases including operating conditions (e.g., safe shutdown) that are not addressed within API RP2A. The use of API RP2A for the design of an OWTG would require supplemental guidelines to cover these other areas. Part of the objective of this task is to review each of the standards to identify these supplemental requirements. The results of the direct comparison are presented in Section 3 of this report.

2.1.2 Comparative Reliability

The second part of the comparison evaluated the guidelines based on performance requirements for extreme loading conditions, which were assessed in terms of system reliability. This comparison addressed directly the significance of the difference in the definition of extreme storm loading conditions – the 50-year storm for IEC and the 100-year storm for API.

2.1.2.1 *General Form of Reliability Assessment*

A standard will define, either directly or through reference to other standards, the environmental conditions (e.g., wind speed, wave height and current velocity), methods for the calculation of loads, methods for the calculation of resistance, load and resistance factors, and/or factors of safety that are required to form the basis of design. These requirements, along with design margin and the redundancy of the structure, will establish an overall level of safety or structural reliability. A typical design process does not address system reliability explicitly but incorporates an overall margin between demand and capacity through these various factors. An explicit analysis of structural reliability requires a probabilistic assessment of demand and capacity relative to each mode of failure, which would address the aforementioned factors as well as all sources of uncertainty in the process.

To assess the reliability of a system, such as an offshore wind turbine, against a performance metric, the likelihood of the system not performing is calculated giving regard to the uncertain nature of the parameters affecting the performance. The failure probability of a wind turbine system is calculated as

$$P_f = \text{Prob}[L > R] \quad (1)$$

Where,

- P_f is the annual failure probability
- L is the load (e.g., overturning moment experienced at mudline for the turbine)
- R is the resistance (e.g., moment resistance at the mudline cross section of the turbine)
- $\text{Prob}[\]$ is the annual probability of load exceeding the resistance of the turbine

The target annual failure probabilities for civil structures are typically in the order of 10^{-3} to 10^{-5} depending on the criticality of the system under consideration.³ In a reliability analysis, the failure probability can also be converted to a reliability index, β , defined as

$$\beta = \Phi^{-1} (1-P_f) \quad (2)$$

Where $\Phi^{-1}()$ is the inverse normal cumulative distribution function and β is the number of standard deviations away from zero at which the annual failure probability is equal to P_f . Another way of defining failure probability is the return period. The return period is the average number of years between two events that would induce “failure” in the structure. The return period is (approximately) the reciprocal of P_f . The exact value of the return period is $-1/\ln(1 - P_f)$, where “ln” is the natural logarithm, and this value is close to $1/P_f$ for small P_f values. Table 1 gives the value of annual failure probability for different β values.

Table 1: Relationship of reliability index with probability of failure and return period

β	P_f (per year)	Return Period (years)	P_f (per year)	Return Period (years)	β
2.5	6.21×10^{-3}	161	5.0×10^{-3}	200	2.576
2.75	2.98×10^{-3}	336	1.0×10^{-3}	1,000	3.090
3	1.35×10^{-3}	741	5.0×10^{-4}	2,000	3.291
3.25	5.77×10^{-4}	1,733	1.0×10^{-4}	10,000	3.719
3.5	2.33×10^{-4}	4,299	5.0×10^{-5}	20,000	3.891
3.75	8.84×10^{-5}	11,310	1.0×10^{-5}	100,000	4.265
4	3.17×10^{-5}	31,574	1.0×10^{-6}	1,000,000	4.753
5	2.87×10^{-7}	3,488,556	1.0×10^{-7}	10,000,000	5.199

Note that the calculation of P_f based on Equation 1, above, is for a system for which the loads and resistance are known. The loads and resistance are generally random variables with their annual probability distribution representing occurrence of a range of values per year. The figure

³ Recommending a specific target failure probability was not the intent of this study; however, the relationship between reliability index, failure probability, and typical values is provided here as background.

below presents these distributions and the shaded area provides an indication of P_f , the larger the shaded area the greater the probability of failure and vice versa.

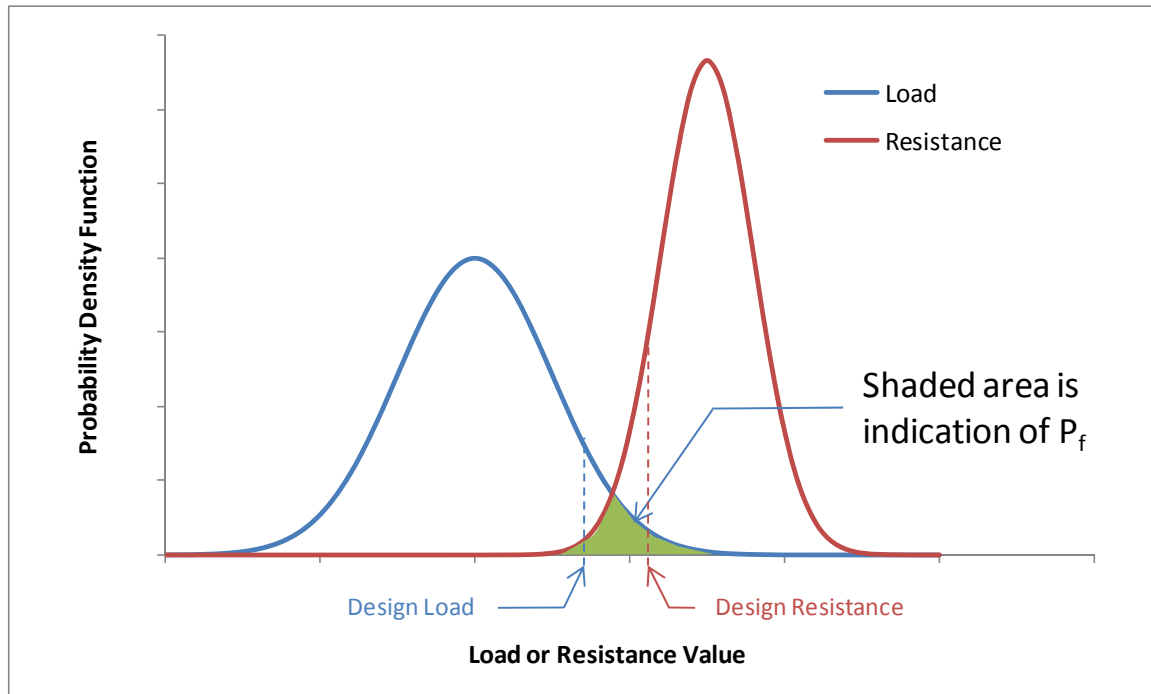


Figure 1: Indication of failure probability given load and resistance probability distributions

In a design guideline, a procedure or recipe is generally defined with a reference level design load and resistance to be used to confirm that the design resistance is greater than or equal to the design load. Once the designer achieves this condition, implicit target reliability is considered to have been met. The design load and design resistance are generally different in the API and IEC guidelines and could result in potentially different reliabilities for offshore wind turbines. The exploration of these differences is presented in the following sections. First a basic primer is presented below to describe how a design load and design resistance implies a target reliability or target failure probability. The main idea is to control or define the largest acceptable shaded area (or largest acceptable failure probability) in the figure above.

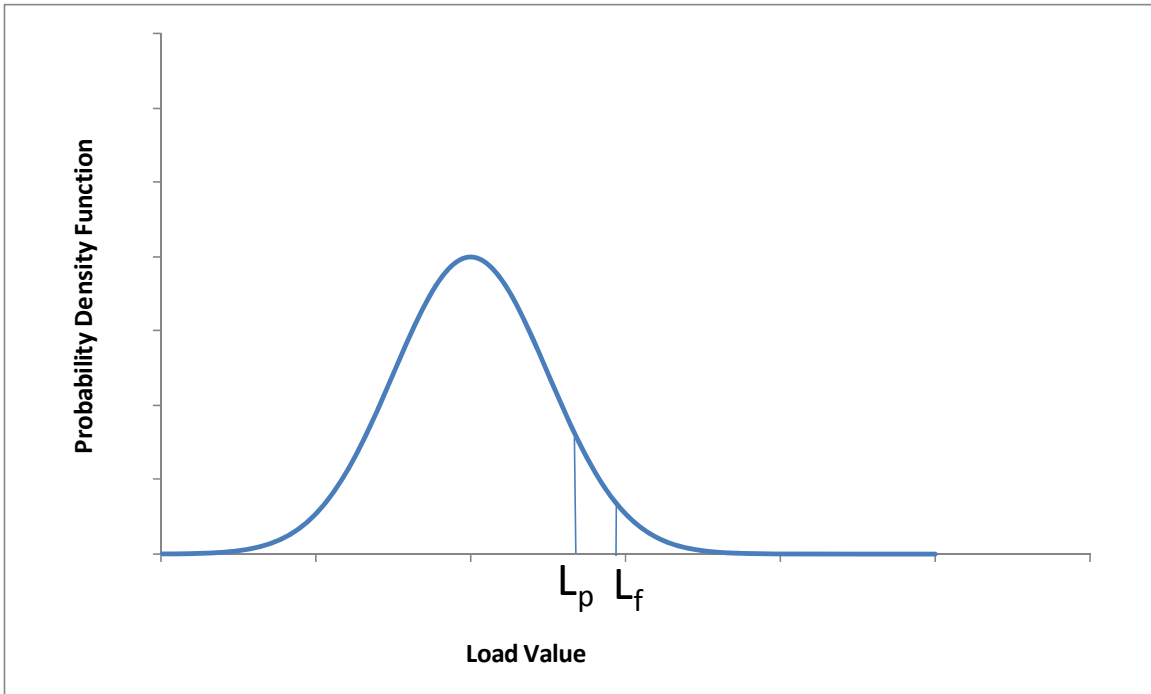


Figure 2: Specification of a factored load for design relative to a given load percentile

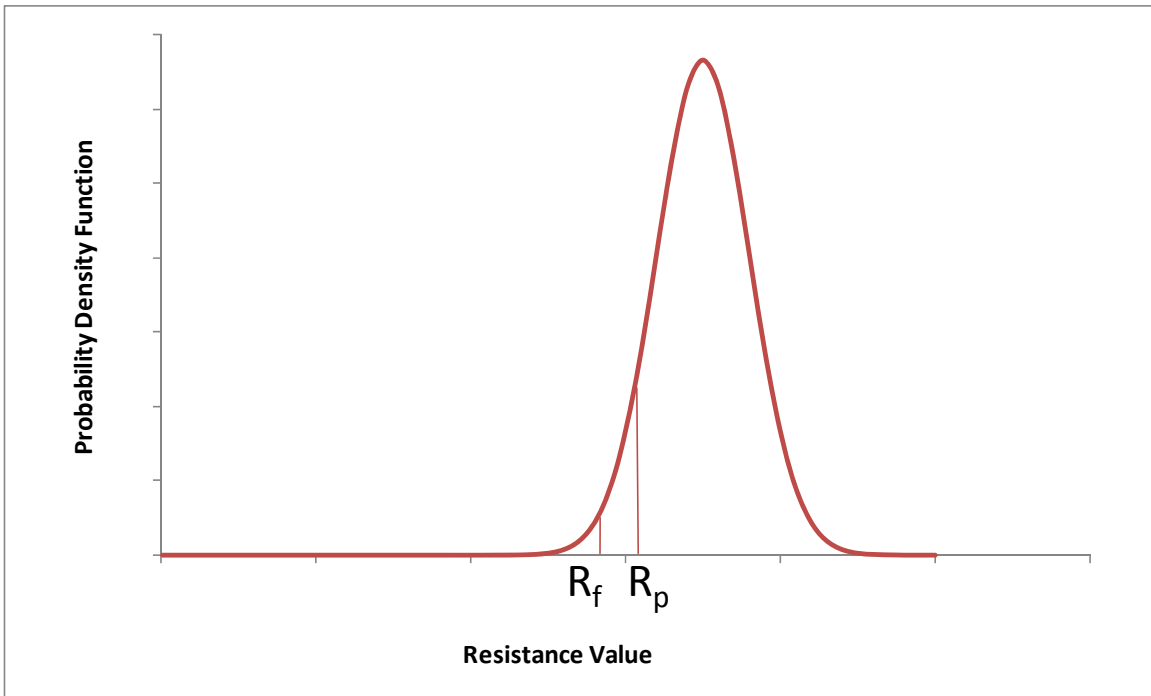


Figure 3: Specification of a factored resistance relative to a given resistance percentile

The concept in achieving a pre-specified safety level is that a designer must ensure that the design resistance R_f must be greater than or equal to the design load L_f . The subscript “f” denotes a factored load or resistance defined as a factor times load or resistance at a predefined percentile on the annual probability distribution. In other words, $R_f = \text{Resistance Factor} \times R_p$ and $L_f = \text{Load Factor} \times L_p$. Note that R_p is generally a 5-percentile value (or 1- or 3-percentile value, depending on the application and design code being used) for an ultimate strength assessment whether following the API or IEC standard. The 5-percentile value implies that only 5% of the time will a particular material actually have a lower strength than R_p . The resistance factor is generally less than one, i.e., a weaker strength (versus R_p) is assumed to ensure a stronger design, while the load factor is generally greater than one, i.e., a more severe load (versus L_p) is assumed to again ensure a stronger design. The net effect of a resistance factor that is less than one and a load factor of greater than one is to ensure that the “shaded area” in Figure 1 is no greater than a predefined acceptable limit. Note that API suggests a 99-percentile (or a 100-year return period) for L_p with a load factor of 1.0. IEC suggests a load factor greater than 1. For example, a factor of 1.35 for normal (for instance, no mechanical fault) extreme load cases for ultimate strength assessment with L_p being the 98-percentile value (or a 50-year return period value). In order to compare the inherent reliability within API and IEC, one must consider the net effect of the load and resistance factors along with the percentile values assumed in each code.

2.1.2.2 Inherent Reliability

The first part of the reliability assessment included a general comparison of the inherent levels of reliability that are achieved through the application of the guidelines without specific details regarding site conditions or structure type. The IEC guideline, and its complementary codes and standards such as ISO,⁴ use a Load and Resistance Factor Design (LRFD) approach. LRFD achieves the intended margin of safety with recognition of different levels of variability and uncertainty that are associated with different types of loading and component strength. API RP2A is available in both LRFD and Working Stress Design (WSD) formats. In contrast to

⁴ The IEC guideline focuses on the definition of all loading conditions for wind turbine support structure design and does not address specific component strength requirements (i.e., the resistance side of the equation). This part of the design process is covered by other codes and standards that are included by reference in IEC.

LRFD, the WSD method uses a single factor of safety that is included in calculating component strength. The loads are un-factored in WSD. The WSD format of API RP2A was used in the comparison due to its longer⁵ and more extensive application of fixed base offshore platforms in the Gulf of Mexico. The inherent reliability comparison was intended to address the basic differences in the guidelines that come from the different design methods, load factors, and factors of safety.

To determine the reliability indices for generic classes of OWT support structures, the criteria and design formulations in each standard were used. To characterize the extreme loading conditions in each standard (i.e., the 50- and 100-year storms for IEC and API, respectively) the assessment addressed the specific criteria and design formulas in each standard. This first assessment did not address sources of reserve strength that are design specific, such as those achieved through structural redundancy, actual material yield, design conservatism, or additional margin for extreme loading conditions that may be created through other loading conditions (e.g., fatigue). Thus, the results reflect higher reliability indices.

2.1.2.3 Regional Variations

The design guidelines that are adopted in the U.S. will have to address the hazards associated with tropical storms. The potential exposure to tropical storms can be addressed in any site specific design with the evaluation of historical wind and wave data that includes both tropical and non-tropical data. The inclusion of tropical storms may increase the severity of both wind and wave data depending upon the frequency and relative severity of tropical storms in the region. Tropical storms can occur in the Gulf of Mexico and along the entire east coast of the U.S.; however, historical data indicates that the frequency and severity of tropical storms is less severe for the northern latitudes. Therefore, while there is a threat of tropical storms along northeastern states, this may not control the design conditions when compared to the conditions associated with non-tropical storms in that region.

⁵ The WSD and LRFD versions of API RP2A are in their 21st and 1st editions, respectively.

In areas where tropical storms are more frequent, such as the Gulf of Mexico, the design level wind speeds and wave heights will reflect these potentially more severe conditions. The definitions of wind and wave conditions are defined with exceedance information that describe the likelihood that any given condition, such as a specific wave height or wind speed, will be exceeded in any reference period of time, which is normally one year. A steep exceedance curve indicates that larger events become much less probable. A less steep exceedance curve indicates that larger events are more probable. The reliability of a structure in such a region is affected by this potential.

The second part of the reliability assessment addressed regional variability by specifically investigating the difference in the characteristic wind and wave exceedance data for tropical and non-tropical areas.

2.1.2.4 Site Specific Assessments

The final part of the reliability comparison included two case studies to document the application of the IEC and API guideline for two representative sites and support structure configurations. The intent of this task was to introduce the actual aspects of the design process, to evaluate the specific differences that are achieved in the use of the IEC and API guidelines, and to assess the significance of these differences in terms of overall levels of reliability for extreme loading conditions.

The case studies included the development of site specific oceanographic and wind data to determine wind and wave loading. This data was provided by Oceanweather.⁶ Additional detail regarding the form of this data and how it was applied to the design process is provided in Section 6.2.3 of this report.

2.2 RANGE OF CASE STUDIES

There are numerous variables in a site specific design that can impact the comparison of reliability. These include, for example:

⁶ The data was provided by Oceanweather under the contract of this JIP project for two sites, the Massachusetts and Texas sites.

- Water Depth
- Wave load conditions
- Wind speed conditions
- Current velocity
- Surge depth
- Soil type and strength
- Turbine size
- Turbine operating conditions
- Structure type
- Structural response to wind, wave, and current in shallow waters

No existing information on the relative affects of these various parameters was available; therefore, it was not possible to select a specific set of variables that would clearly define the extent of variability in the reliability index for various site conditions. Also, given budget limitations, it was not possible to assess the sensitivity of the reliability index to each variable separately nor was it possible to assess a large number of combinations. Therefore, only variables that were deemed to have the greatest impact on the reliability index were included – structure type, water depth, and wind and wave condition.

2.2.1 Structure Type

There are a number of different types of support structures that may be used for offshore wind turbines. These include; monopiles, gravity base structures, tripods, jackets, and various floating concepts. Different design standards will very likely produce levels of reliability that vary for these different concept types. The study focused on the structure types that will most likely be used in the near term development of offshore wind farms in the U.S. This included a monopile and a tripod, as illustrated in Figure 4.

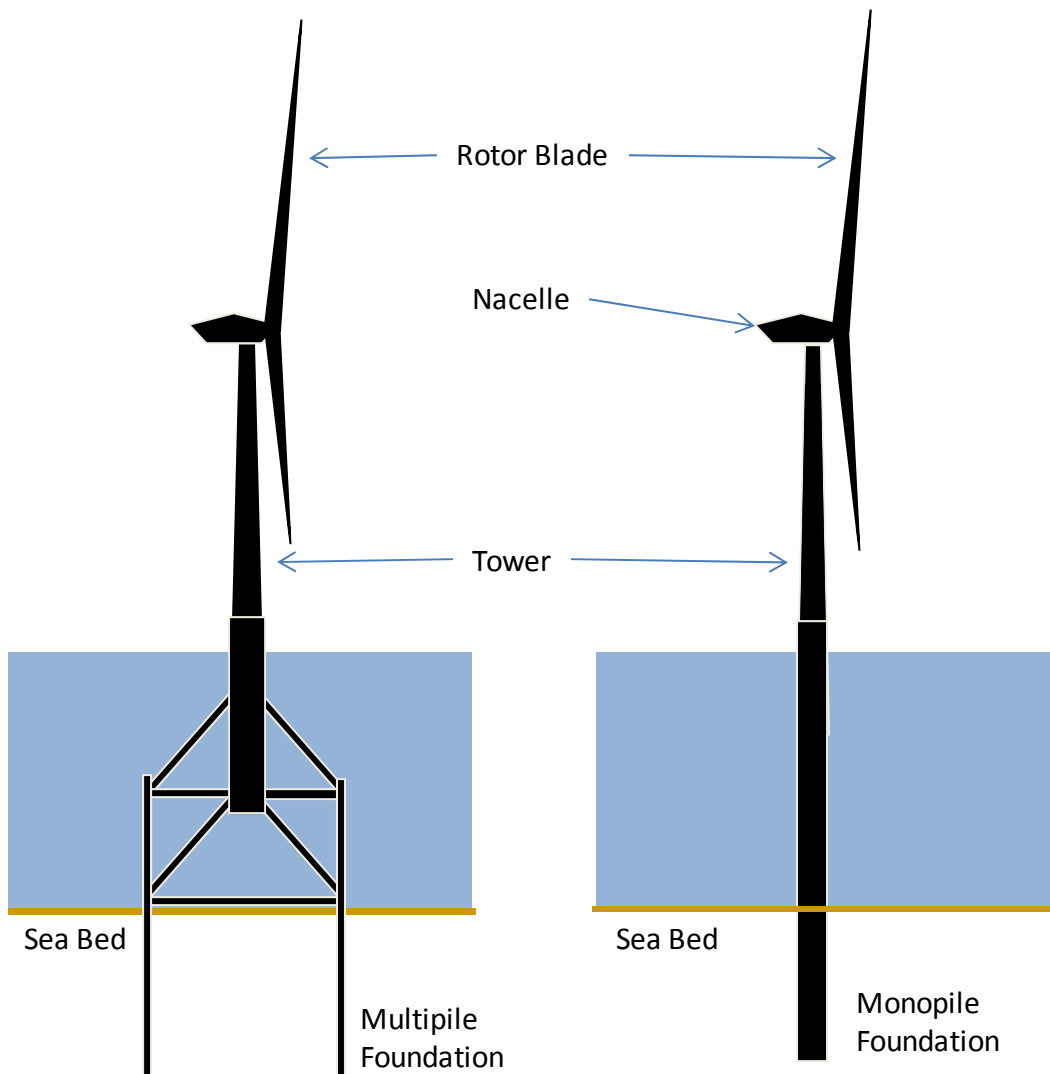


Figure 4: Types of support structures

2.2.2 Site Conditions

The levels of structural reliability will also vary as a function of site conditions that affect the specific attributes of a design. This includes water depth, soil conditions, design wind speeds, wave heights, etc. Again, a comprehensive evaluation of each of these parameters was beyond the scope of this study. Two sets of site conditions were selected to represent both mild and moderately severe combinations of conditions. The mild site conditions were represented with a shallow water depth, stiff soil, and moderate environmental conditions. The more severe site

condition was represented with intermediate water depth, stiff soil, and harsher environmental conditions.

2.2.3 Case Study Combinations

The combinations of structure type and site condition were selected on the basis that monopiles would be most applicable for shallow sites and that tripods would potentially be used at deeper water locations. Figure 5 illustrates this focused set of combinations.

		Structure Type	
		Monopile	Tripod
Site Condition	Site 1: Offshore Massachusetts (15m water depth)	Case 1	-
	Site 2: Offshore Texas (24m water depth)	-	Case 2

Figure 5: Case study combinations

2.3 STUDY TEAM

The organization of the study team is illustrated in Figure 6.

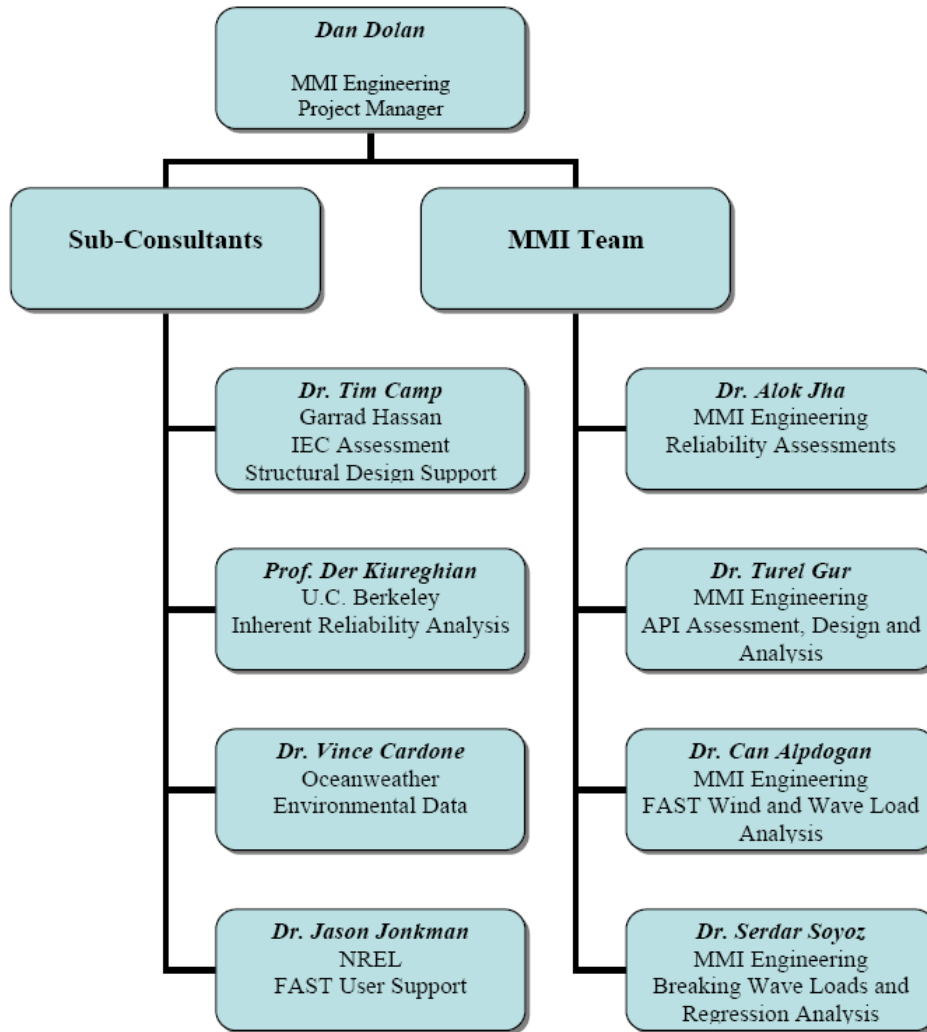


Figure 6: Project organization chart

The team includes organizations and individuals encompassing all aspects of the design, analysis, and assessment of comparative reliability of OWTG. The organizational responsibilities were allocated roughly as follows.

MMI Engineering was responsible for the overall management of the project, the assessment of the API guidelines, the statistical analysis of the raw metocean data provided by Oceanweather, all wind and wave load simulations, the structural response analysis, conceptual designs, the ultimate strength analysis, and the reliability analysis.

Garrad Hassan had lead responsibility for the direct comparisons of the IEC and API guidelines and was responsible for the assessment of the IEC guidelines. Garrad Hassan also provided support for the conceptual design for the case studies, provided input to the design process for the IEC portions of the case study work, and reviewed all structural design and analysis results.

Professor **Armen Der Kiureghian** of the University of California, Berkeley performed the initial comparison of the inherent reliability assessment.

Oceanweather provided all oceanographic data required for the site specific case studies.

The team would also like to acknowledge Dr. Jason Jonkman of NREL for his support during the project. Dr. Jonkman provided his services outside the subcontract from in-kind NREL funds. He provided valuable input and support on the use of the FAST simulation software used for the calculation of wind and wave forces for both of the case studies.

3.0 SUMMARY OF AVAILABLE GUIDELINES

3.1 BACKGROUND

The first edition of API RP-2A was published in 1969. It has undergone several changes as more data and experience became available on the performance of the platforms in hurricanes. Figure 7 shows the timeline for the development of the API RP-2A.

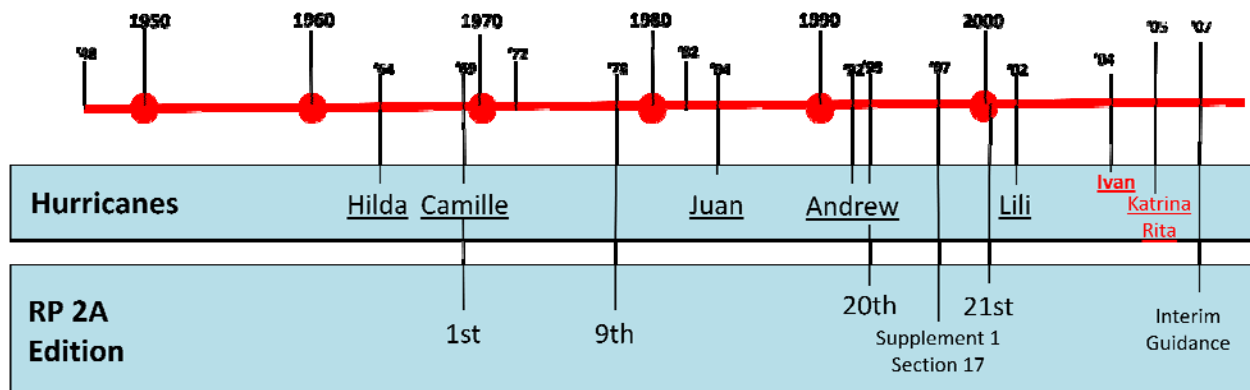


Figure 7: Timeline for the development of API RP-2A

API RP-2A provides design procedures for offshore oil and gas structures. It provides methods to calculate loads and structural capacity, and the environmental data for the continental U.S. The guideline is self sufficient and has few references to other standards. It does not provide guidelines on turbine specific load cases or wind induced fatigue.

API presents three categories for offshore structures in terms of life-safety or failure consequence. The failure consequence categorization includes various factors. Examples are: anticipated losses to owner, such as structure repair or replacement, lost production, or cleanup; anticipated losses to other entities; and anticipated losses to industry and government. The three categories are L-1 High Consequence, L-2 Medium Consequence, and L-3 Low Consequence. For the purposes of comparison of reliability of API to IEC, L-1 category was deemed to be of closest relevance to IEC's highest wind turbine classification, and was the category chosen for the remainder of this report to compare to IEC.

The API series of standards and recommended practices have been developed with support from industry. The API currently maintains over 500 standards and recommended practices covering all segments of the oil and gas industry, including the design and construction of fixed base and floating offshore platforms. The U.S. Federal Government provides specific regulations for the exploration and production of oil and gas resources in U.S. waters. The MMS refers to the API standards for the design of offshore platforms, as stated in the Code of Federal Regulations (CFR).

IEC 61400-3 is a standard issued by the International Electrotechnical Commission. The first committee was formed in 1987. There are 10 parts to IEC 61400 that specify design and assessment methods unique to wind turbines. In particular, IEC 61400-1 and IEC 61400-3 refer to design requirements for onshore and offshore wind turbines, respectively. A working group, WG3, was formed in 2000 to develop the offshore wind turbine design standard, which was at the voting stage of the publication procedure as of February 2009.

IEC 61400-3 provides a comprehensive set of design load cases for wind turbine support structures. It does not address structural capacity and values for environmental parameters are not provided. It refers to other standards/guidelines for turbine machinery and code checks, as illustrated in Figure 8.

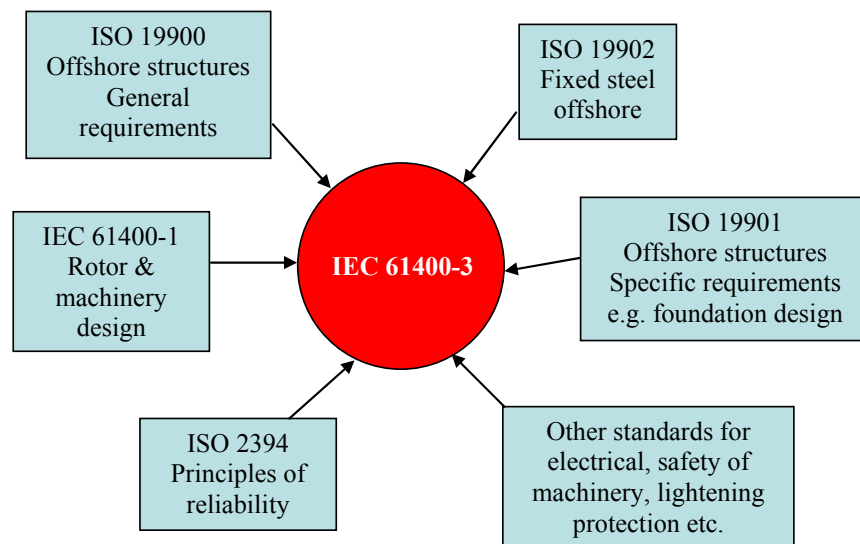


Figure 8: Reference guidelines/standards used by IEC 61400-3

Governmental initiatives include a series of publications by the Department of Energy/Health and Safety Executive in the United Kingdom, Norwegian Petroleum Directorate (NPD) standards in Norway, and the Danish Energy Authority (DEA) standards in Denmark. Germanischer Lloyd (GL) and Det Norske Veritas (DNV) are two classification societies that have been active in developing design guidelines specifically for offshore wind turbines.

3.2 API RP 2A

The API recommended practice for offshore platforms (API RP-2A Working Stress Design) was first compiled in 1969. Since its inception, RP-2A has undergone substantial expansion and refinement to meet the changing needs of industry and in response to “lessons learned.” The recommended practice is in its 21st edition. The types of structures that have been designed using RP-2A range from major multi-level platforms installed in very deep water to minimal structures located in shallow water for the development of marginal fields. Structures that have been designed using API RP-2A are located in areas that are dominated by extreme storms, hurricanes, earthquakes, and ice. API RP-2A provides a valuable experience base that can be used for the design of structures operating in harsh marine environments.

API RP-2A addresses all of the requirements for the design of offshore oil and gas platforms. It provides detailed guidance, good practices, design principles, and formulas for the development of member forces and the calculation of individual component capacity (e.g., individual member strength in bending, tension, compression, buckling, and fatigue).

API RP-2A is specifically applicable to the design of offshore oil and gas platforms, and as such, does not include provisions that have been developed specifically for offshore wind turbine support structures. RP-2A categorizes structures into three levels of exposure based on specific life safety and consequence of failure. These exposure categories may be used to define environmental design criteria.

While RP-2A does not include specific provisions for wind turbines, the guideline does include a wide array of technical information required for the design of offshore structures that are applicable to offshore wind turbine support structures. The guideline provides extensive

environmental information on wind, wave, and currents on the U.S. OCS. It also provides guidelines for pile and member design, analysis, fabrication, installation and inspection.

3.3 IEC 61400-3

Technical Committee TC-88 of the International Electrotechnical Commission has compiled the international guidelines for wind turbines since 1988. TC-88 has a number of working groups, project teams, and maintenance teams that produce and revise the guidelines, technical reports, and technical specifications.

TC-88 has developed IEC 61400, which is a series of standards specific to the design and assessment of wind turbines. IEC 61400 currently comprises ten standards, covering a range of topics from safety and design requirements to performance assessments of prototype turbines. Of these, 61400-1[3]: “Design Requirements” and 61400-3: “Design Requirements for Offshore Wind Turbines” contribute the most to the design process. IEC 61400-3 is currently in draft form, though at one of the final stages of the publication procedure.

IEC 61400-3 specifies the requirements for the definition of site conditions and, together with IEC 61400-1, provides essential design requirements for offshore wind turbines. The standard is intended to provide an appropriate level of protection against damage from all hazards during the planned lifetime of the structure. IEC 61400-3 is fully consistent with, but does not duplicate, the requirements of IEC 61400-1, which is the IEC standard for onshore wind turbine design. IEC specifies that these standards be used together.

IEC 61400-3 focuses on the engineering integrity of the structural components of an offshore wind turbine but also provides requirements for subsystems, such as control and protection mechanisms, internal electrical systems, and mechanical systems. One of the most valuable aspects of IEC 61400-3 is the rigorous specification of design load cases that address a range of design situations in combination with applicable external conditions.

IEC 61400-3 does not include component design requirements or a capacity formula. The guideline requires the use of other codes for these elements and refers to the ISO standards for component design as illustrated in Figure 8. The standard allows for the use of other industry

design guidelines, such as GL, DNV, and API. Nonetheless, IEC specifies that when partial safety factors from national or international design codes are used together with partial safety factors from IEC 61400-3, the reliability achieved should be equal to or greater than safety factors implied by ISO. For this study, ISO was the standard used for resistance (material) safety factors or resistance design examination.

3.4 ISO

Founded in 1947, the International Organization for Standardization (ISO) is a network of national standards organizations from 157 countries. ISO provides a worldwide framework for the development and international standardization of a wide range of standards, covering topics relevant to wide sectors of business, industry, and technology. As of August 2006, ISO had a portfolio of 16077 standards, ranging from standards for agriculture and construction, mechanical engineering, manufacturing and distribution, to transport, medical devices, information and communication technology, and services.

Offshore technologies standards are contained in the ISO 19900 – 19909 series. While these standards do not specifically address offshore wind turbines, considerable guidance is given for the design of offshore structures [6] in general, particularly with regard to structural integrity.

Relevant ISO standards for offshore wind turbines include:

- ISO 2394: General principles on reliability of structures
- ISO 4354: Wind actions on structures
- ISO 19900: General requirements for offshore structures
- ISO 19901: Specific requirements for offshore structures
- ISO 19902: Fixed steel offshore structures
- ISO 19903: Fixed concrete offshore structures

3.5 COMPARISON OF API AND IEC GUIDELINES

This section compares the design philosophies contained in the guidelines. A detailed comparison of the two guidelines can be found in Appendix D.

3.5.1 Wind Fatigue

The API guideline (focused on wave-driven structures) does not require inclusion of wind loads in fatigue analysis; however, for a wind turbine structure, this element of loading is critical. The IEC defines a collection of load cases that must be considered for fatigue, encompassing all the combinations of operating conditions and environmental conditions that contribute to the overall fatigue damage. For each of these cases full time domain simulations must be run including wave, wind, gravitational, and inertial loads.

The wind fatigue loading is sensitive to the wind spectrum that is used. The API standard provides a one-dimensional wind spectrum, which it says may be used; however, a more detailed three-component spectral model is required by the IEC.

3.5.2 Load Cases

The API standard categorizes four loading conditions:

1. Operating environmental conditions combined with dead loads and maximum live loads appropriate to normal operations of the platform.
2. Operating environmental conditions combined with dead loads and minimum live loads appropriate to the normal operations of the platform.
3. Design environmental conditions with dead loads and maximum live loads appropriate for combining with extreme conditions.
4. Design environmental conditions with dead loads and minimum live loads appropriate for combining with extreme conditions.

In the above, “design environment conditions” refer to the extreme conditions with a return period of 100 years.

However, wind turbines have a complex interrelation between operating loads and environmental conditions, and a central part of the IEC 61400-3 standard is the prescription of design load cases. They detail many different operating conditions that could be essential to engineering design, including electrical conditions and turbine faults. IEC 61400-3 also examines environmental conditions of appropriate severity to combine with each case.

3.5.3 Wake Induced Velocities

When wind turbines are operating in close proximity to each other, the wake of one can influence the wind loading on another downstream. The IEC gives guidance on how this should be taken into account.

3.5.4 Extrapolation of Stochastic Ultimate Loads

For time based simulations based on stochastic sea states and turbulent wind, and that consider a range of wind speeds, the IEC standard describes how characteristic load effects may be determined using extrapolation techniques.

3.5.5 Slam Loading

Both codes have formulation of estimating slam loads; however, the coefficients differ between the two codes and could result in different levels of slam loads. The maximum slam load based on API is half of that based on IEC. Also, there is no clear explanation to define the decay of maximum slam load with time in API. For this report, the intent was to utilize a formulation that would closely mimic the physical process for large diameter structures, such as a monopile, and so a formulation based on IEC was used.

3.5.6 Wave Kinematics Correction

Neither the API nor the IEC standard provides adequate guidance on how to develop wave kinematics for wave heights up to the breaking wave limit. Stream function wave theory is one of several options that are available to define wave the particle kinematics that are needed in the

definition of wave load.⁷ This process is required in both the API and IEC design methodologies. All wave theories are limited to some extent in that they can become numerically unstable for wave heights slightly less than that associated with the breaking wave limit. Therefore, the definition of the total wave load for a structure that is subject to breaking waves requires some additional calculation that is not addressed in either API or IEC.

⁷ Stream Wave theory is a nonlinear regular wave theory that offers a formulation of wave kinematics (wave particle velocity and acceleration) to calculate drag and inertia forces on a structure. This theory is limited in applicability up to a certain wave height to water depth ratio. At a given depth, wave breaking happens at a wave height that is greater than the wave height at which Stream theory is not applicable anymore and so the need to address this “gap” between the Stream theory wave height limit and the wave breaking wave height limit.

4.0 INHERENT RELIABILITY

4.1 ASSUMPTIONS AND PREMISE

A straightforward way to compare inherent reliabilities of IEC 61400-3 and API RP-2A is to generate separate designs of a structure using each guideline and then assess and compare the respective reliabilities of the two designs. To provide a broad comparison of the two guidelines, this exercise would need to be repeated for a large number of structural types and environmental/load conditions. A simpler approach is to compare the two guidelines without considering a specific structural design. This approach is possible by eliminating structure-dependent coefficients in the design or reliability formulations.

In general, performance criterion in design guidelines is defined in terms of load effects, e.g., stresses, internal forces, and deformations. However, statistical information is usually available in terms of loads applied, e.g., from wind and waves. The transformation from loads to load effects depends on the configuration and other properties of the structure. Limit state equations are developed that include the transformation from load to load effects and compare the inherent reliability in the two guidelines without resorting to a specific structure.

4.2 DEVELOPMENT OF LIMIT STATE EQUATION – API & IEC

4.2.1 Independent Wave and Wind Loads

To illustrate the process and to provide an initial comparison of inherent reliability, this framework was applied to a simple offshore wind turbine problem. The design of a typical monopile was the selected example. It was assumed that the monopile would be controlled by bending at the mudline. The performance criterion in the guideline can be written as:

$$R_{code} - S_{code} = R_{code} - c L_{code} \geq 0 \quad (3)$$

where R denotes capacity (or resistance), S denotes load effect, L denotes load, and c denotes an influence coefficient, which converts the load to the appropriate load effect. The subscript

“code” is used to indicate that the capacity and load values are determined in accordance with the rules specified in the guideline. Assuming the performance criterion is satisfied at the limit, the inequality sign in the above expression is replaced with an equality sign, from which one can solve for the influence coefficient:

$$c = \frac{R_{code}}{L_{code}} \quad (4)$$

As an example, for bending stress at the mudline resulting from overturning moment imposed on this mudline section, the bending stress is M/Z (i.e., overturning moment divided by the section modulus), so the influence coefficient c in this case is $1/Z$.

For reliability analysis, a limit-state function $g(\mathbf{x})$ must be formulated so that $\{g(\mathbf{x}) \leq 0\}$ defines the failure event, with \mathbf{x} denoting the random variables of the problem. In the present case, the limit state function can be written as:

$$\begin{aligned} g(R, L) &= R - cL \\ &= R_{code} \left(\frac{R}{R_{code}} - \frac{L}{L_{code}} \right) \end{aligned} \quad (5)$$

where R and L now define the random capacity and load values. For any specifications of the distributions of R and L , and the code values R_{code} and L_{code} , the reliability of the design can be evaluated without resorting to a particular structure. Furthermore, since any positive scaling of the limit-state function does not alter reliability, the above limit-state function can be simplified to read

$$g(R, L) = \frac{R}{R_{code}} - \frac{L}{L_{code}} \quad (6)$$

This formulation is convenient as the random variables are normalized by their respective code values.

The API RP-2A (WSD) and IEC 61400-3 guidelines have two fundamental differences in specifying the code capacity and load values:

- a) **Formats:** API specifies $R_{code} = SF \cdot R_n$ and $L_{code} = L_n$, where SF is an “allowable stress reduction factor” and R_n and L_n are nominal capacity and load values, whereas IEC specifies $R_{code} = R_c / \gamma_m$ and $L_{code} = \gamma_f L_c$, where γ_m is a “material factor,” γ_f is a “partial load factor” and R_c and L_c are “characteristic” capacity and load values. For failure in bending of a section, the allowable stress reduction factor SF in API and the material factor γ_m in IEC depend on the outer diameter (D) to wall thickness (t) ratio of the section being analyzed for bending strength failure. In general, the ultimate strength to yield strength capacity ratio reduces with increasing D/t ratio. Both API and ISO provide detailed formulations of this variation for a range of D/t ratios. It is not clear, however, why ISO D/t ratios go up only to 120 while API D/t ratios go up to 300 to provide the variation of material (allowable) safety factors.
- b) **Nominal and Characteristic Values:** In particular, for wind and wave loads, API specifies L_n as the 100-year value, whereas IEC specifies L_c as the 50-year value. R_n and R_c are the 5-percentile resistance value for ultimate strength assessment.

Another note on the limit state formulation is that IEC (actually the material strength formulation in ISO) and API have slightly different approaches in setting up the limit state equations for bending. ISO utilizes the ratio of the plastic to elastic section modulus in the design strength check equation using factored loads. The ISO formulation (as is the API formulation) can be written in a much simpler form by assuming a given D/t ratio; in the discussions below, a specific D/t ratio is assumed and enables a direct comparison of safety factors between API and ISO. This is consistent with the core intent of the formulation of limit states in both codes – to permit the section to go up to initiation of yield at the outer fibers of the section under bending. In both codes, empirical data is used to define a conservative estimate of when yield begins in the outer fibers.

Using Equation (6), the limit-state functions for determining the inherent reliabilities of the two guidelines can be written as:

$$\text{API: } g(R, L) = \frac{R}{SF \cdot R_n} - \frac{L}{L_n} \quad (7a)$$

$$\text{IEC } g(R, L) = \frac{\gamma_m R}{R_c} - \frac{L}{\gamma_f L_c} \quad (7b)$$

The “net” safety factor for both API and IEC can be developed to directly compare how the two guidelines fare in terms of inherent safety. These equations can be rewritten with implicit percentile values for nominal (characteristic) values in terms of design check equations:

API: Must ensure: $SF \cdot R_{5\%} > L_{100\text{yr}}$ which can be rewritten as $R_{5\%} > (1/SF) L_{100\text{yr}}$

IEC: Must ensure: $R_{5\%} / \gamma_m > \gamma_f L_{50\text{yr}}$ which can be rewritten as $R_{5\%} > \gamma_m \gamma_f L_{50\text{yr}}$

To compare IEC directly to API, one can rewrite IEC design check as

$$\text{IEC: } R_{5\%} > \gamma_m \gamma_f (L_{50\text{yr}} / L_{100\text{yr}}) L_{100\text{yr}}$$

The net safety factor for API is $F_{\text{API}} = 1/SF$ and for IEC is $F_{\text{IEC}} = \gamma_m \gamma_f (L_{50\text{yr}} / L_{100\text{yr}})$. When F_{API} equals F_{IEC} the resulting reliability in both codes is exactly the same. Similarly, when F_{API} is greater than F_{IEC} , API would result in a higher reliability and vice versa. Note that the ratio $(L_{50\text{yr}} / L_{100\text{yr}})$ depends on the metocean condition and the response of the structure to the metocean condition, while the remaining factors ($SF, \gamma_m \gamma_f$) do not depend on the metocean condition.

Table 2 compares these net safety factors for an offshore wind turbine with bending stress at the mudline as the key criterion for failure. The comparison is performed for a tubular section with two different D/t ratios, i.e. outer diameter to wall thickness ratio. As mentioned earlier, equations in both codes provide the actual material or allowable safety factors to use for a given D/t ratio.

Table 2: Net safety factors for API and IEC

	API		IEC				
D/t	SF	F _{API}	γ _m	γ _f	L ₁₀₀ / L ₅₀	F _{IEC}	Conclusion for L ₁₀₀ /L ₅₀ = 1.2
Small	1	1	1.05	1.35	1.2	1.181	API Safety < IEC Safety
100	0.864	1.157	0.9654	1.35	1.2	1.086	API Safety > IEC Safety

For a given D/t, say 100, one can now easily find the threshold L_{100yr} / L_{50yr} that would make API and IEC generate equally reliable designs. This threshold is 1.126 ($= 0.9654 \times 1.35 \times 0.864$), so:

Table 3: 100-year to 50-year load ratio threshold to compare API to IEC

L ₁₀₀ / L ₅₀	Conclusion for D/t=100
< 1.126	API Safety < IEC Safety
= 1.126	API Safety = IEC Safety
> 1.126	API Safety > IEC Safety

In summary, if the 100-year load is more than 1.126 times the 50-year load, the API will result in a higher reliability compared to an IEC (for D/t of 100).

Next is an investigation of the actual reliability indices that result from each of the design guidelines as assessed for a “perfectly designed” structure for each code. The offshore wind turbine is analyzed for the ultimate strength failure and is assumed to occur in a severe environment much greater than the cut out wind speed of the turbines, and so the turbine is assumed to be in an idle state. The detailed formulations presented by [7, 8, 13] were used to account for errors in modeling the capacity and load values. This report adapts the reliability formulation with some modifications relevant to this study.

Accordingly, the normalized capacity (R / R_n or R / R_c) in Equations 7(a) and (b) are replaced by $\tilde{F}_y X_m$, where \tilde{F}_y is the ultimate bending capacity normalized by its nominal or characteristic value (here assumed to be the 5-percentile value for API and IEC) and X_m is a random variable representing the uncertainty in the capacity model. For extreme wind loading the normalized

load is replaced with $\tilde{L}_a X_a (1 + X_{dyn} T) / 2$, where \tilde{L}_a is the normalized annual maximum 1-hour mean wind load, X_a and X_{dyn} are model error terms and T is a random variable representing the turbulence effect. For drag-dominated wave loading, the normalized load is replaced with $\tilde{L}_w X_h$ where \tilde{L}_w is the normalized annual maximum hydrodynamic load (based on a significant wave height determined for a 1-hour reference period) and X_h is a model error. Note that the exact time durations of averaging for wind speed and significant wave height are not critical for this report, as the key interest is in comparative assessment of API and IEC, and we use the same temporal averaging for both codes. Also, note that for ultimate strength assessment the underlying data ultimately being used is for tropical storms whose temporal durations are greater than 1 hour or 3 hour periods, i.e., a single large annual storm (with a 50- or 100-year return period) lasts much longer than a 3 hour period, and so for this comparative study in this section, we assume the scaling factor for temporal effects is not of significance at this point.

API specifies a variable allowable stress reduction (ASR) factor between 0.75 and 0.60 in bending for members with high D/t ratios. However, for the extreme load condition, API allows an increase of one-third in the ASR factor. Assuming a D/t of 100, the ASR is 0.648, and the result is a net allowable bending stress of 0.864 F_y , where F_y is the 5-percentile bending strength value. The IEC guideline specifies the partial material factor $\gamma_m = 1.05$ for small D/t ratios; for D/t=100, $\gamma_m = 0.9654$ and, for the extreme load condition, the partial load factor $\gamma_f = 1.35$. The limit state equations are given below,

Wind

$$\text{API: } g(\mathbf{x}) = \frac{\tilde{F}_y}{SF} X_m - \tilde{L}_a X_a \frac{1 + X_{dyn} T}{2} \quad (8a)$$

$$\text{IEC: } g(\mathbf{x}) = \gamma_m \tilde{F}_y X_m - \frac{\tilde{L}_a}{\gamma_f} X_a \frac{1 + X_{dyn} T}{2} \quad (8b)$$

Wave

$$\text{API: } g(\mathbf{x}) = \frac{\tilde{F}_y}{SF} X_m - \tilde{L}_w X_h \quad (9a)$$

$$\text{IEC: } g(\mathbf{x}) = \gamma_m \tilde{F}_y X_m - \frac{\tilde{L}_w}{\gamma_f} X_h \quad (9b)$$

The above formulation applies when a single load is acting on the monopile. The formulation needs to be expanded if additional loads, e.g., dead and live loads, are to be included. In the present case, these loads are expected to have negligible contributions and are not considered.

4.2.2 Wave and Wind Loads

Of course wind and wave loads never act alone. Therefore, we need to consider their combined effect. Article 2.2.2 in API RP 2A (WSD) states “Environmental loads ... should be combined in a manner consistent with the probability of their simultaneous occurrence during the loading condition considered.” IEC provides specific load combination cases to be considered. Here, we consider the design load case 6.2a in Table 1 of IEC-61400-3, which combines the extreme wind condition with the extreme sea state. Since the extreme wind and extreme wave are defined for different reference periods, the code recommends converting both values to a 1-hour reference period. Note that the offshore wind turbines are a very dynamic system and the combined wind and wave dynamic coupling may have a material impact on the structural response to a combined wind and wave loading. A detailed assessment of this combined loading on specific structures is presented later in the report. However, for the purposes of this section, a notional combination of wind and wave loads is performed by simply assuming that the combined wind and wave load is a square root of the sum of the squares of the individual wind and wave loads with a combination factor for wave loads. This portion of the wind and wave combination is also a simpler adaptation of References 7 and 8.

The combined wind and wave limit state is then (note that below formulation also assumes bending ultimate strength, now for the combined wind and wave load):

$$API: g(\mathbf{x}) = \frac{\tilde{F}_y X_m}{SF} - \frac{\sqrt{[\tilde{L}_a X_a (1 + X_{dyn} T)]^2 + \alpha^2 (\tilde{L}_w X_h)^2}}{2 + \alpha} \quad (10a)$$

$$IEC: g = \gamma_m \tilde{F}_y X_m - \frac{\sqrt{[\tilde{L}_a X_a (1 + X_{dyn} T)]^2 + \alpha^2 (\tilde{L}_w X_h)^2}}{\gamma_f (2 + \alpha)} \quad (10b)$$

Here α represents the ratio of wave-induced stress to wind-induced stress and is assumed to be smaller than 1 for wind-driven systems. In this report, an arbitrary α value of 0.25 is assumed. Later in the report, a fully coupled wind and wave analysis is performed, and for this section only a notional combination of wind and wave loads is assumed for comparison of API to IEC safety factors.

4.3 LOAD AND RESISTANCE VARIABLES

A brief description of the variables [7, 8] used in the analysis is given below:

\tilde{F}_y - lognormal distribution with 5% coefficient of variation (CoV) and 1.13 as its 5-percentile value,

X_m - lognormal distribution with mean of 1.11 and CoV of 8.5% (0.085).

X_a and X_{dyn} - lognormal distribution with both means equal to 1 and CoVs equal to 0.10 and 0.05, respectively;

T - Gumbel distribution with mean equal to 1 and CoV equal to 0.1;

\tilde{L}_a - is the square of a random variable with Gumbel distribution with CoV equal to 0.53 and a characteristic value equal to 1 (i.e., for API, value is 1 at 99-percentile, and for IEC, value is 1 at 98-percentile). Note here that wind load here is implicitly assumed to vary as wind speed squared.

X_h - lognormal distribution with mean equal to 1 and CoV equal to 0.10,

\tilde{L}_w - is the square of a random variable with Gumbel distribution with a CoV of 0.47 and a characteristic value equal to 1; that is, for API, value is 1 at 99-percentile, and for IEC, value is 1 at 98-percentile. Wave load is, similarly, assumed to vary as wave height squared.

The CoVs assumed here for \tilde{L}_a and \tilde{L}_w reflect the much larger uncertainty (compared to References 7 and 8) for the site-specific wind speed and significant wave height data used later in this report. Note that the CoVs assumed for the different random variables above and in References 7 and 8 are originally from Reference 13. Most of these CoVs are applicable to the current study as well, except for the metocean CoV, where the study in this report adopted values applicable for the sites and regions of interest in this report.

4.4 PRELIMINARY RELIABILITY INDICES

Reliability analyses were carried out with the above formulations of the limit-state function and assumed distributions. Table 4 lists the computed reliability indices for designs based on API and IEC guidelines under wind load and wave load alone, and the combined effect of wind and wave loads. The computed reliability indices are based on the second-order reliability method (SORM) and are computed by use of the *Relacs* software. This software has been used in the U.S. oil and gas industry for several joint industry projects funded by the MMS and provides for robust calculation of small failure probabilities by different reliability techniques, e.g. First Order Reliability Method and Second-Order Reliability Method, and offers a library of widely used probability distribution types to model the random variables within a limit state formulation.

Table 4: Reliability indices for wind and wave loads

Set	Code	Wind	Wave	Wind+Wave $\alpha=0.25$	MetOcean CoV
1	API	2.69	2.71	2.84	CoV _{Ws} =0.53, CoV _{Hs} =0.47
2	IEC	2.56	2.58	2.70	

Some observations on this table:

- The CoVs for Hs and Ws are high (vs. other regional statistics, discussed later) and are based on the site-specific data used later in this study. For purposes of this analysis, both CoVs are similar, implying the difference in 0.53 vs. 0.47 is nominal and so the difference in the reliability index for wind-only vs. wave-only case is “numerical noise” and are essentially the same.
- For a given code, for example, API, the resulting reliability of the wind plus wave data results in a nominally higher reliability. Again, this is an artifact of the procedure adopted for combining wind and wave loads. In reality, the wind and wave loads show a high correlation and so reliability for the combined load case may not necessarily be higher than for individual load cases.
- For the CoVs considered here, the IEC results in nominally lower reliability indices compared to API. As discussed earlier in the report, the key parameter that gives an indication of the relative reliabilities from API vs. IEC is the ratio of 100-year load to the 50-year load. Given the large CoVs studied here, the ratio is likely large enough to result in API achieving higher reliability than IEC for the ultimate strength assessment performed. In the following sections, the report compares reliabilities for different metocean CoVs, to convey the impact on API vs. IEC reliabilities.

5.0 REGIONAL COMPARISON OF RELIABILITY INDICES

This section builds upon the inherent reliability within API and IEC guidelines as applied to a regional metocean data. In the previous analysis, a generic structure and a generic metocean condition was analyzed to compare API and IEC. Now, we compare inherent reliability when performing a consistent analysis using API and IEC with regional data. Note that the two regions assumed in the analysis are offshore Massachusetts and offshore Texas. The specific locations for these sites are mentioned later and the exact locations for these sites are not needed for this section. Note that both these sites are subject to three types of storms:

- Tropical: Storms that generate in the tropics (less frequent, more severe)
- Extratropical: Storms that generate outside the tropical latitude (less frequent, more severe)
- Continuous: Storms representing less severe but more frequent storm conditions

The Texas and Massachusetts sites are both subject to all three storms at different frequency and severity combinations. While Massachusetts may have less frequent tropical storms (these cause the most severe metocean conditions at both sites), the long fetch length (open sea) generates larger waves compared to that of a more protected site.

The metocean data of these two sites reflect the local climate conditions expressed via the 1 hour average wind speed ($W_s, 1hr$) and significant wave height (H_s) for the annual maximum storm condition. Figure 9 and Figure 10 present the exceedance probability for the annual maximum W_s and H_s parameters. There are two types of storms included in this data. The “Continuous” storm data is for the past 20+ years of data representing continuous storm data (inclusive of those tropical or extratropical storms that happened in the last 20+ years). The “Tropical” storm data set represents the past 50 to 100 years of tropical storm-only data. The tropical storm data set is a better representation of the 50 to 100 year likely storms at these sites. Note that the Texas (TX) site indicates much more severe wind speeds for a given return period versus the Massachusetts (MA) site. On the other hand, the continuous storms in TX are milder than MA site.

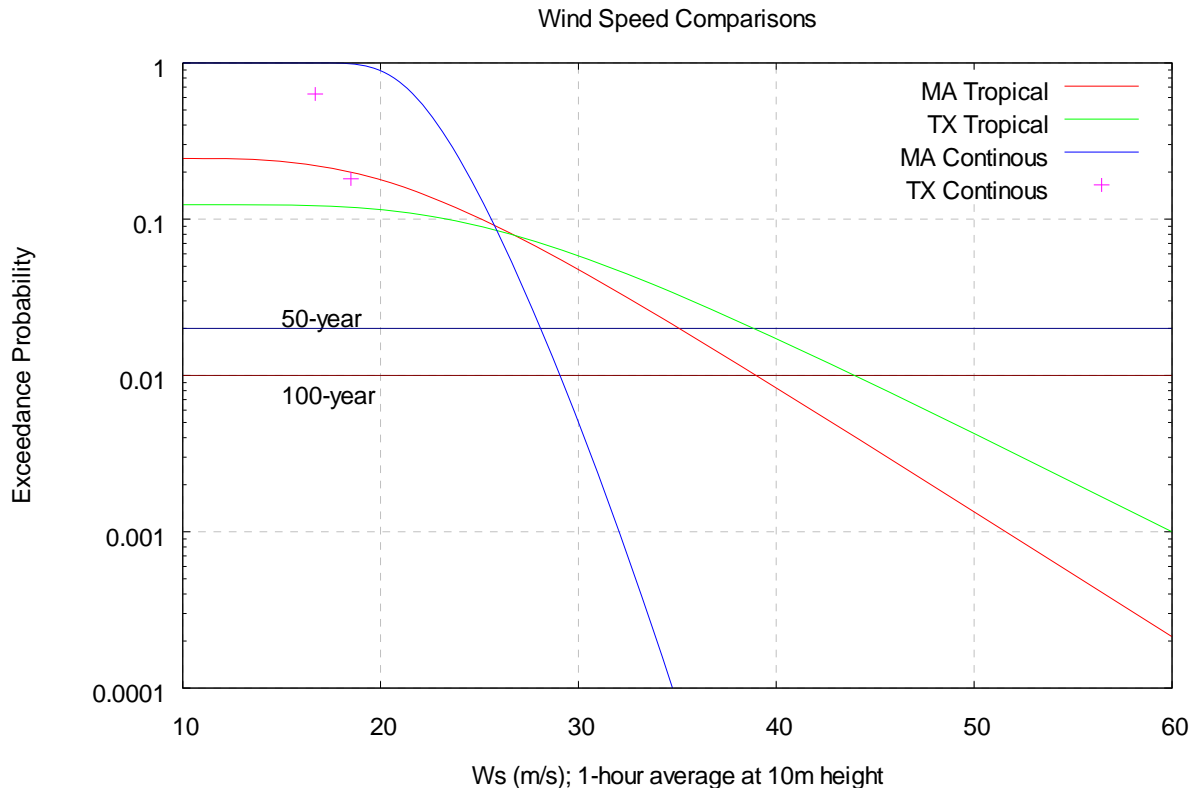


Figure 9: Wind speed comparison for MA and TX sites

Figure 10 provides the annual maximum significant wave height (H_s) for these sites. The distribution of H_s is very similar for a range return periods across both the TX and MA sites. The minor difference seen is within the margin of error or “noise” considering the limited data set used in formulating the probability distribution fits for H_s .

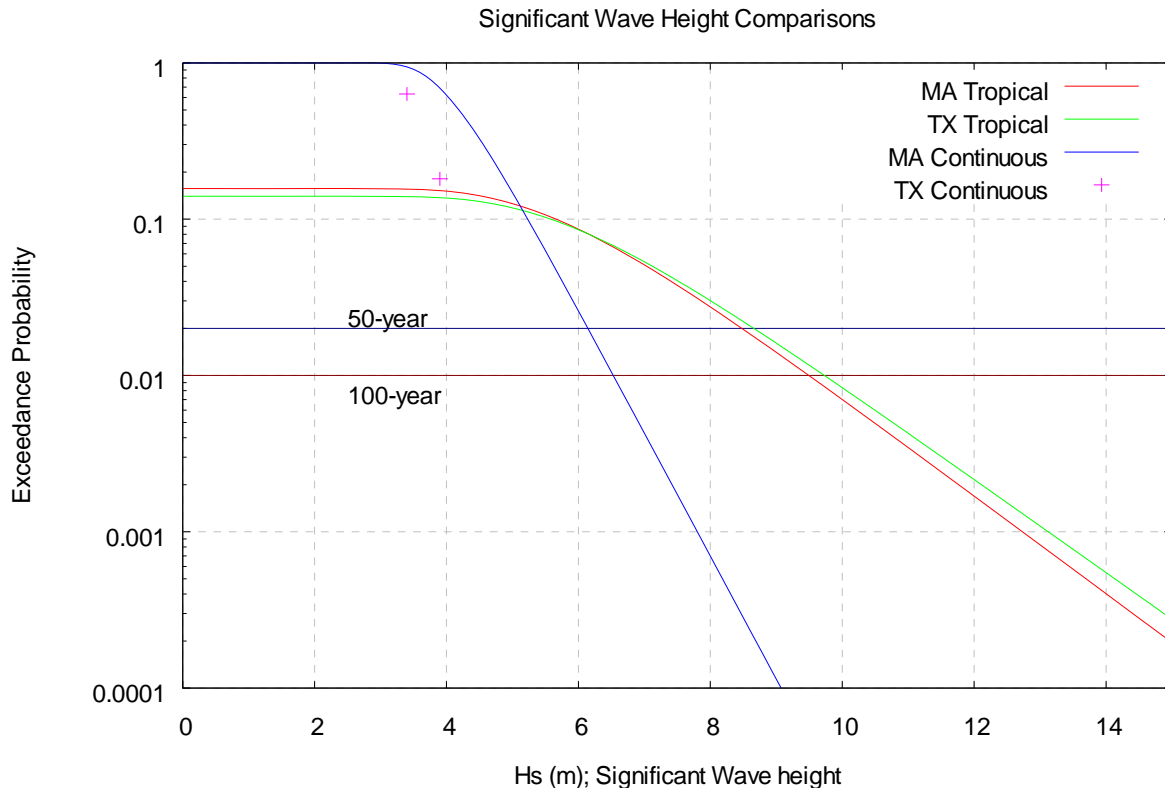


Figure 10: Wave height comparison for MA and TX sites

The key parameter of interest for the regional reliability comparison of a generic structure is the uncertainty in the metocean condition. Note that the CoV is not a measure of the severity of storms; it is a measure of variability in the storm severity. In other words, a small CoV does not necessarily imply a small severity; a small CoV implies a smaller scatter around a given storm severity.

For a perfectly designed structure (i.e., one where factored strength is exactly equal to the factored load for a given design recipe), the coefficient of variation (CoV) in the metocean parameter is the key parameter of interest to gage the resulting reliability across regions with different metocean severity. A larger CoV results in a lower reliability. Table 5 provides the CoV for the site-specific data for the MA and TX sites and also provides the CoV for other regions of interest in this comparison.

Table 5: Coefficient of variation across regions and for specific site data for MA and TX sites

	Ws	Hs
MA	0.40	0.45
TX	0.53	0.47
West GoM	0.25	0.25
Central GoM	0.25	0.25
North Sea	0.12	*
Philippines	0.25 to 0.35	*

*CoVs for Hs were not available for these regions, and were assumed to be the same as wind speed CoV, where needed

The CoVs for Hs are not provided in this table for the North Sea and for the Philippines, as this data was not readily available. The MA and TX CoVs are similar and are roughly twice the regional CoV for West and Central GoM metocean data provided in API 2INT-MET.⁸ In turn, the regional West and Central CoVs are twice the North Sea CoV; implying that the CoV for the site-specific data is about four times the North Sea CoV. The regional CoVs for GoM come close to the lower bound of CoV for the Philippines. From these CoV comparisons one can infer the following:

- The regional reliability of a perfectly designed structure for the MA and TX sites would be quite similar for a given design recipe.
- Given a perfectly designed structure using the same recipe across regions, the North Sea would result in the highest reliability, due to its least uncertain metocean condition (note least uncertain does not necessarily imply less severe, only that the severity is less uncertain).

In a separate study, a larger safety factor of approximately 1.7 on a 50-year load was recommended for the Philippines region to achieve the same level of reliability for the North Sea [see Clausen, 2007]. Given that GoM and site-specific MA data also show much larger CoV compared to the North Sea (as do the Philippines), a load safety factor larger than 1.35 would be

⁸ The CoV for the data provided in API 2INT-MET were calculated by fitting a Gumbel distribution to the return period curves for wind speed and significant wave height values for the referenced regions in the Gulf of Mexico.

required to achieve the reliability level implicit in the IEC recipe. Similarly, for the API based design, a larger material safety factor would be required to achieve the same reliability level implicit in the API.

Another observation that can be made is the comparison of the ratio of 100-year wind speed (or significant wave height) to the 50-year wind speed (or significant wave height). The ratio is slightly higher for the TX site wind speed compared to the MA site wind speeds; this is consistent with the higher CoV for TX vs. MA. Recall that the ratio of the 100-year to the 50-year wind load (which is approximately the square of the 100-year to the 50-year wind speed) for a given D/t ratio is an indication of whether an API design will be more or less reliable than one developed using IEC. The threshold of 1.126 (as mentioned earlier in the report defining the 100- to 50-year ratios where API and IEC reliabilities are equal) may not apply given the uncertainties in other random variables.

Table 6 presents the resulting reliability indices for an ultimate strength assessment for the Northeast site (labeled MA, for Massachusetts), and the Gulf of Mexico site (labeled TX, for Texas). Given the significance of the metocean variability (CoV), the table also presents results two additional regions: the Central Gulf of Mexico and the North Sea. The CoV for these regions are taken from prior studies on these regions, e.g. the Central GoM CoV were inferred from the metocean return period severities stated in API 2INT-MET. The key observations on these results are discussed right after the table.

Table 6: Reliability index comparison across MA and TX Sites, along with other regions with different Metocean CoV

Site	Code	Wind	Wave	Wind + Wave	WS CoV	Hs CoV
MA	API	2.89	2.87	3.05	0.4	0.45
	IEC	2.76	2.74	2.92		
TX	API	2.89	2.86	3.05	0.53	0.47
	IEC	2.76	2.71	2.92		
Central GoM	API	3.01	3.02	3.2	0.25	0.25
	IEC	2.94	2.95	3.13		
North Sea	API	3.27	3.3	3.55	0.12	0.12
	IEC	3.32	3.35	3.6		

The regional reliability analysis indicates the following:

- The beta values for a given code and safety factor are similar for the TX and MA sites. This indicates that for a “tuned” structure, whether using API or IEC, results in a similar beta value, although API generates marginally higher beta values (about 5%) compared to IEC in the simple case studied here.
- A third site was arbitrarily selected to demonstrate the effect of metocean CoV on beta values. This third site is the Central Gulf of Mexico with a lower CoV for both Wind and Wave tropical conditions. This lower CoV is partly due to a regional representation of the metocean data versus the site-specific data used for the MA and TX sites (there is more scatter in the lesser data available at a specific site vs. a regional data set). For Central GoM, the beta values increase by about 5% for both API and IEC, and API still generates slightly higher (about 2%) beta than IEC values; however, the difference (2% versus 5%) between the API and IEC values is less for the smaller CoV case. This reduction in difference can be understood again using the ratio of the 100-year to 50-year load as an indicator of the API to IEC reliability difference. When the CoV is smaller, the L_{100} to L_{50} is lower and so the API and IEC reliabilities converge.
- For the fourth site, the North Sea case, the CoV of 0.12 for Ws and Hs are the smallest and, as expected, the IEC generates a higher reliability than API.

The above observations reaffirm the earlier view that the ratio of the 100-year load to the 50-year load (which in turn depends on metocean variability) provides a key indication of how the API-based reliability would compare to the IEC-based reliability. A higher ratio of load will result in the reliability of the API design being higher than the reliability of the IEC design.

6.0 SITE SPECIFIC COMPARISONS

This section presents the results of the case study work described in Sections 2.1.2.4 and 2.2. The objective of the case studies was to provide a reliability comparison that addressed site specific conditions (e.g., wave height and wind speed) and specific substructure characteristics (e.g., redundancy and dynamic behavior). The case studies also introduced the effects of other design factors, such as fatigue and operating conditions that are not directly tied to the issue of design storm return period.

The case studies focused on the primary drivers that affect the design of the substructure components and the subsequent reliability comparison. The designs presented herein are representative of monopile and multi-piled support structure alternatives and should not be considered as complete or optimized. Another key assumption is that wind turbine is an upwind rotor or a horizontal axis turbine with blade turned towards the incoming winds. The results herein may not directly apply to other turbine configurations such as a downwind rotor or a vertical axis wind turbine.

6.1 TURBINE SPECIFICATIONS

6.1.1 Turbine Size

The size of the wind turbine (i.e., the megawatt rating of the turbine system) is predominant on both the magnitude of the wind load and the elevation of the centroid of effective wind pressure. Together, these two factors have a significant effect on the base overturning moment, which may control the design of many of the components of any support structure configuration. The demand (predominantly the wind load) on the support structure increases with increasing turbine size; however, it is not clear what effect turbine size may have on the relative levels of reliability that are achieved with API and IEC. The reason for this relates to the relative significance of wind and wave loading and how these forces vary for both operating and extreme loading conditions. It is intuitive, however, to assume that the 100-year wind and wave load would generally be higher than the 50-year wind and wave load for the same operating structure

configuration. The specific loads and resulting reliability are discussed in more detail in the subsequent sections of this report.

A 5-megawatt turbine was used as the basis of the study since input from the sponsors suggested this would be most representative of developments to be undertaken in the U.S. in the near future. At the beginning of the study, it was also thought that the larger turbine would trigger greater differences in the comparative reliability assessment; however, as mentioned above, this may not necessarily be the case.

The most significant factor in selecting the 5 MW turbine was the availability of models that were needed to define wind and wave loads for all of the conditions required during the case study analysis. Wind and wave force simulations were performed using the FAST⁹ software provided by NREL. NREL also provided the model data for their reference level turbine and this became the basis for all wind and wave force calculations performed during the study.

The properties of the turbine and blades used in the analysis are summarized in Table 7 and Table 8. These specifications are obtained from the NREL Offshore 5-MW baseline wind turbine as described in NREL/TP-500-41958 technical report [10].

⁹ Fatigue, Aerodynamics, Structures, and Turbulence. An Aeroelastic Design Code for Horizontal Axis Wind Turbines. Jason Jonkman, National Wind Technology Center. <http://wind.nrel.gov/designcodes/simulators/fast/>

Table 7: Properties of the NREL 5-MW baseline wind turbine

Rating	5 MW
Rotor Orientation, Configuration	Upwind, 3 Blades
Control	Variable Speed, Collective Pitch
Drivetrain	High Speed, Multiple-Stage Gearbox
Rotor, Hub Diameter	126 m, 3 m
Hub Height	90 m
Cut-In, Rated, Cut-Out Wind Speed	3 m/s, 11.4 m/s, 25 m/s (10-minute average, at hub height)
Cut-In, Rated Rotor Speed	6.9 rpm, 12.1 rpm
Rated Tip Speed	80 m/s
Overhang, Shaft Tilt, Precone	5 m, 5°, 2.5°
Rotor Mass	110,000 kg
Nacelle Mass	240,000 kg
Tower Mass	347,460 kg
Coordinate Location of Overall CM	(-0.2 m, 0.0 m, 64.0 m)

Table 8: Undistributed blade structural properties

Length (w.r.t Root Along Preconed Axis)	61.5 m
Overall (Integrated) Mass	17,740 kg
Second Mass Moment of Inertia (w.r.t. Root)	11,776,047 kg-m ²
First Mass Moment of Inertia (w.r.t. Root)	363,231 kg-m
CM Location (w.r.t. Root along Preconed Axis)	20.475 m
Structural Damping Ratio (All Modes)	0.477465 %

6.1.2 Tower Properties

The tower, which is the column that spans the height from the top of the support structure to the nacelle, is excluded as a design element for purposes of this study. The tower was included in all of the wind and wave load response analyses; however, the design of the tower was not varied for the IEC and API design conditions. The tower used in this study is identical with the one used by NREL for the analyses of 5MW Baseline Wind Turbine [10]. Some of the key dimensions of the tower are provided in Table 9:

Table 9: Tower dimensions [10]

Tower base outer diameter (m)	6.0
Tower base wall thickness (m)	0.03
Tower top outer diameter (m)	3.87
Tower top wall thickness (m)	0.02
Tower length (from tower base to yaw bearing) (m)	77.6

6.1.3 Turbine Operating Requirements

The support structure must be designed to avoid resonant response with the rotor. If such a condition were to exist, the amplification of motion would cause significant damage to the rotor and rotor blades and would also lead to premature fatigue distress in the support structure.

Turbine manufactures provide criteria for their specific turbines that are based on the operating speed of the rotor and number of blades. This data is typically represented in a Campbell diagram, such as that shown in Figure 11 for the reference 5 MW turbine. The Campbell diagram defines both the basic rotor and blade passing frequencies (i.e., the frequency with which any of the three blades pass the central support column) for a range of rotor speeds up to the operating speed of the turbine (i.e., the range between the two vertical lines). The normal range of rotor operating speeds can thus be used to establish a range of structure frequencies that will avoid resonant behavior for either of these two inputs. As seen in the diagram, resonance conditions would occur for structural frequencies of 0.20 and 0.34 Hz, corresponding to vibration periods of 5 and 3 seconds, respectively. The lower portion of this frequency range is most important for the substructure design since it is impractical to achieve the higher frequencies for the turbine size, water depths, and rotor heights considered as the basis of the study. A frequency of 0.25 Hz (4 second period) was defined as the minimum allowable for the first structural mode frequency for all support structure configurations at both sites.

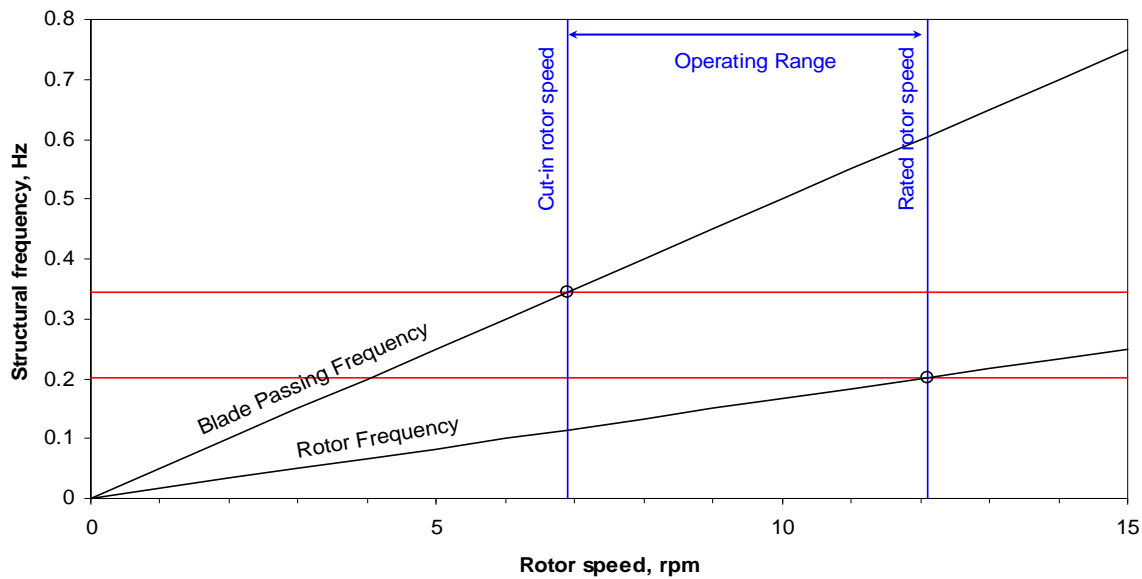


Figure 11: Campbell diagram

6.2 SITE CONDITIONS

Following the methodology described in Section 2.2, an assessment of candidate sites was completed based on current regional developments, wind power resource maps, the application of the various types of support structures, and the availability of wind and wave data that is required to define the necessary site specific design criteria. The evaluation criteria were reviewed with representatives from NREL and two sites were selected. These locations were submitted to the sponsors for review and comment prior to starting the case study analysis. There were no comments received regarding the selected sites.

6.2.1 Location and Water Depth

6.2.1.1 Site 1

The location of the site used for the first case study is shown in Figure 12.¹⁰ Site 1 is located south of Massachusetts and Rhode Island between Martha's Vineyard and Block Island. The site

¹⁰ Note these maps are publicly available on the Internet and were simply annotated with the site labels to indicate approximate location
http://www.windpoweringamerica.gov/wind_maps.asp

is located at 41°15' N 71°15' W. The water depth at Site 1 is approximately 15 meters. There are several other sites in this region that have been proposed for offshore wind power development. Therefore, this location was considered to be very applicable to current industry applications.

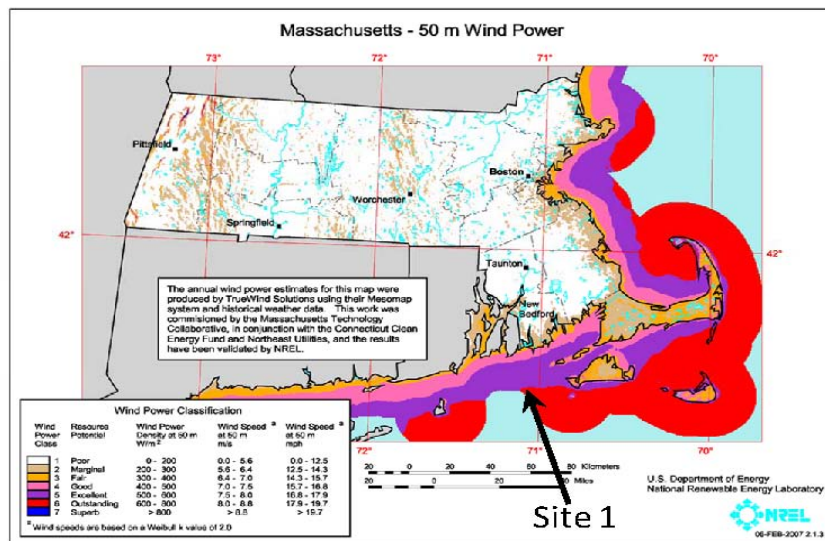


Figure 12: Location of MA site

6.2.1.2 Site 2

The location of the site used for the second case study is shown in Figure 13. Site 2 is located southeast of Corpus Christi, Texas. The site is located at 27°15' N 97°7' W. The water depth at

Site 2 is approximately 24 meters. This site was selected on the basis of good wind power density, availability of wind and wave data, and potential for tropical storm loading. Unlike the situation at the Site 1 location, Site 2 was selected without any consideration of the location of other developments in the Gulf of Mexico.

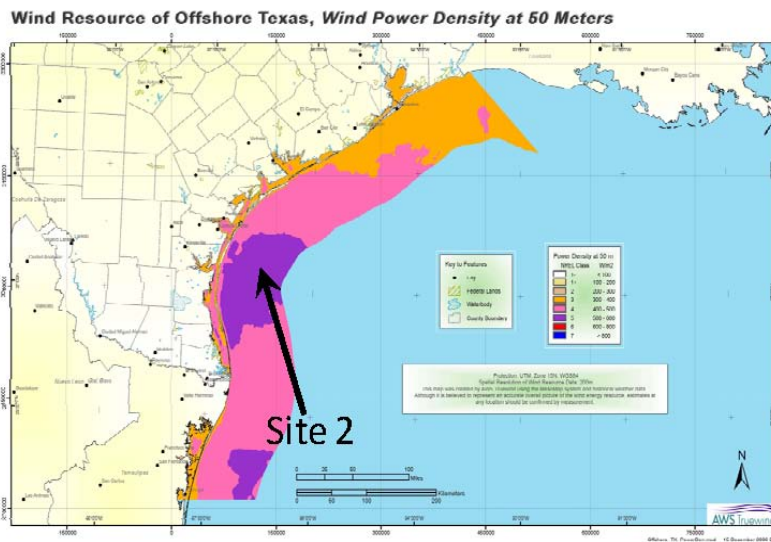


Figure 13: Location of TX site

The variation of tropical storm frequency and severity in the Gulf of Mexico was discussed previously in the report. Site 2 was selected with consideration of the wind resource map and did not specifically address a coastal area in the Gulf that would be subject to more frequent and

severe tropical storms. The results of the Site 2 case studies would change significantly if the site were located in the Central Gulf region instead of the Western Gulf region, which is defined by the API as less severe in terms of 100-year wind speeds and wave heights.

6.2.2 Support Structure Configuration

6.2.2.1 Site 1 Monopile

A monopile configuration was used for the Site 1 case study. The monopile is the most basic of configurations. It includes a large single pile that is driven to a penetration depth that provides the necessary mudline fixity to resist the large overturning moments caused by wind and wave loads. The monopile is assumed to extend to a distance of 10 meters above water line. At this point, there is a transition to the tower, which is connected to the monopile either by a bolted flange or with a grouted sleeve connection. It is assumed that the tower tapers in diameter from the transition to the upper flange that supports the nacelle. The yaw bearing that provides support to the nacelle is supported on the tower and located 87.6 meters above water line.

In order to establish an initial definition of the gross properties of the monopile, a parametric study was performed to evaluate the sensitivity of structural period to monopile diameter and soil condition. The results of this sensitivity are summarized in Figure 14. In this analysis, the monopile was assumed to have a constant D/t ratio. Given this assumption, all of the key properties of the monopile could be defined as a function of varying D . This includes the variables that control pile structural mass and stiffness and soil-pile interaction.

During the analyses, the monopile diameter was increased from 4 to 8 meters in 1 meter increments. The other dimensions of the structure increased proportionally. Note that the nacelle mass remains constant. Five different soil shear strength profiles were used to assess the sensitivity to soil strength. The selected soil profiles cover a wide range of soil conditions. For each monopile diameter and soil profile pair, an Eigenvalue analysis was performed to estimate the structure modes of vibration. Soil-pile interaction was represented explicitly using soil springs to model the lateral bearing ($p-y$), shaft friction ($t-z$) and end bearing ($q-z$) reaction of the soil. The soil spring properties were developed based on the formulations recommended by API RP2A.

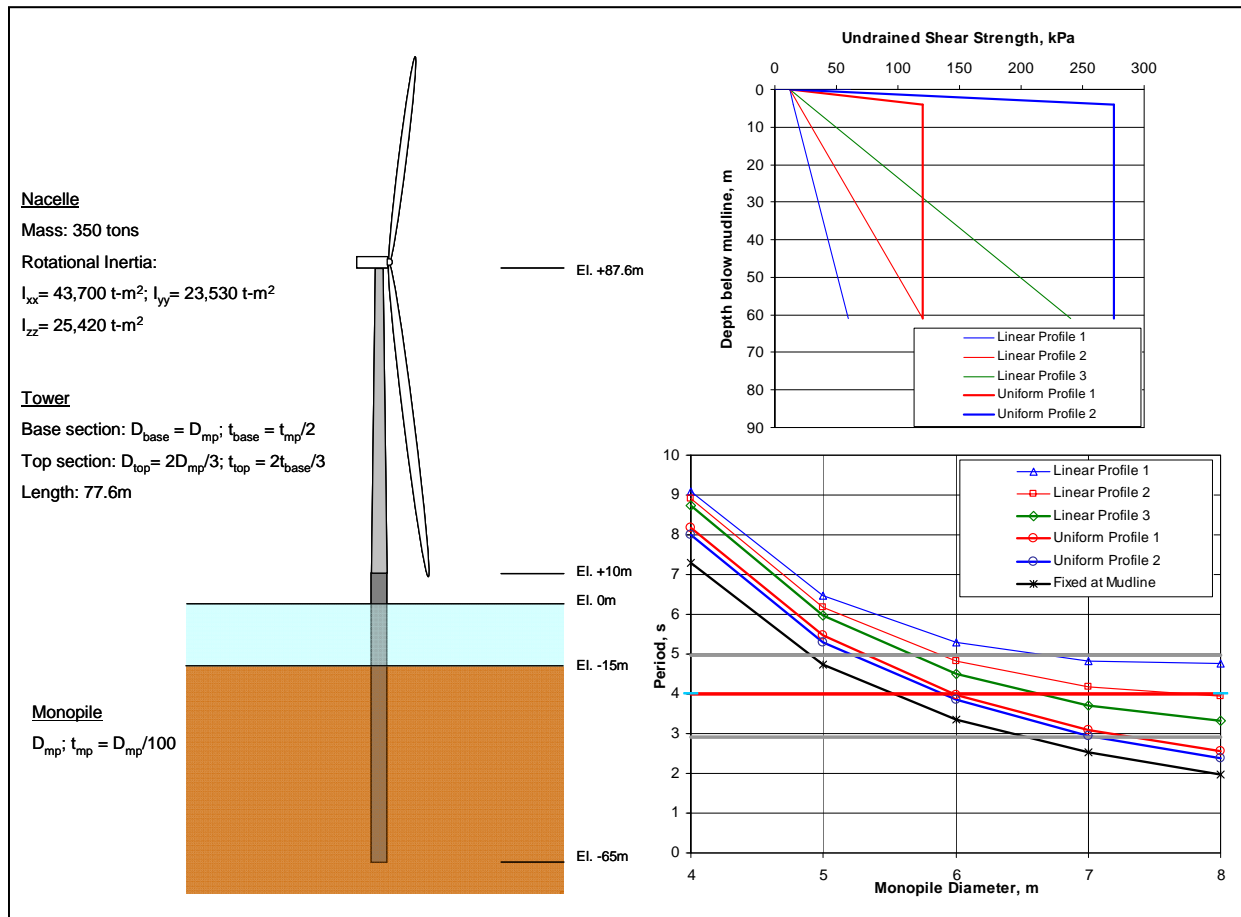


Figure 14: Parametric study for determining monopile dimensions

The bottom right graph of Figure 14 summarizes the results of the Eigenvalue analyses. The first mode period of the structure is inversely proportional to the monopile diameter. The period of the structure falls above the maximum allowable value of 4 seconds for all diameters less than 5.5 meters. A monopile diameter D_{mp} of 6 meters was selected as this generated the 4 second target maximum period for the stiff clay profile used as the basis for the study. The corresponding wall thickness is 60 mm.

The Eigenvalue analysis results show that the soil profile has a strong influence on the structural period. At D_{mp} of 6 meters, the period is slightly below 4 seconds for the stiff clay soil profiles. However, the periods ranged between 3.9 to 5.4 seconds for the 6 meter monopile for the soil profiles included in the sensitivity study. The variation in the period resulting from the changes

in the soil stiffness becomes even more significant as the monopile becomes stiffer (i.e. larger diameter monopile).

The basic properties of the monopile are illustrated in Figure 15. The fixed attributes of the monopile configuration included the flange elevation, nacelle height, and tower top diameter. The attributes of the monopile that were considered to be primary variables include its diameter, wall thickness, and penetration depth. Note that the pile wall thickness was assumed to be uniform through the depth of the pile for simplicity.

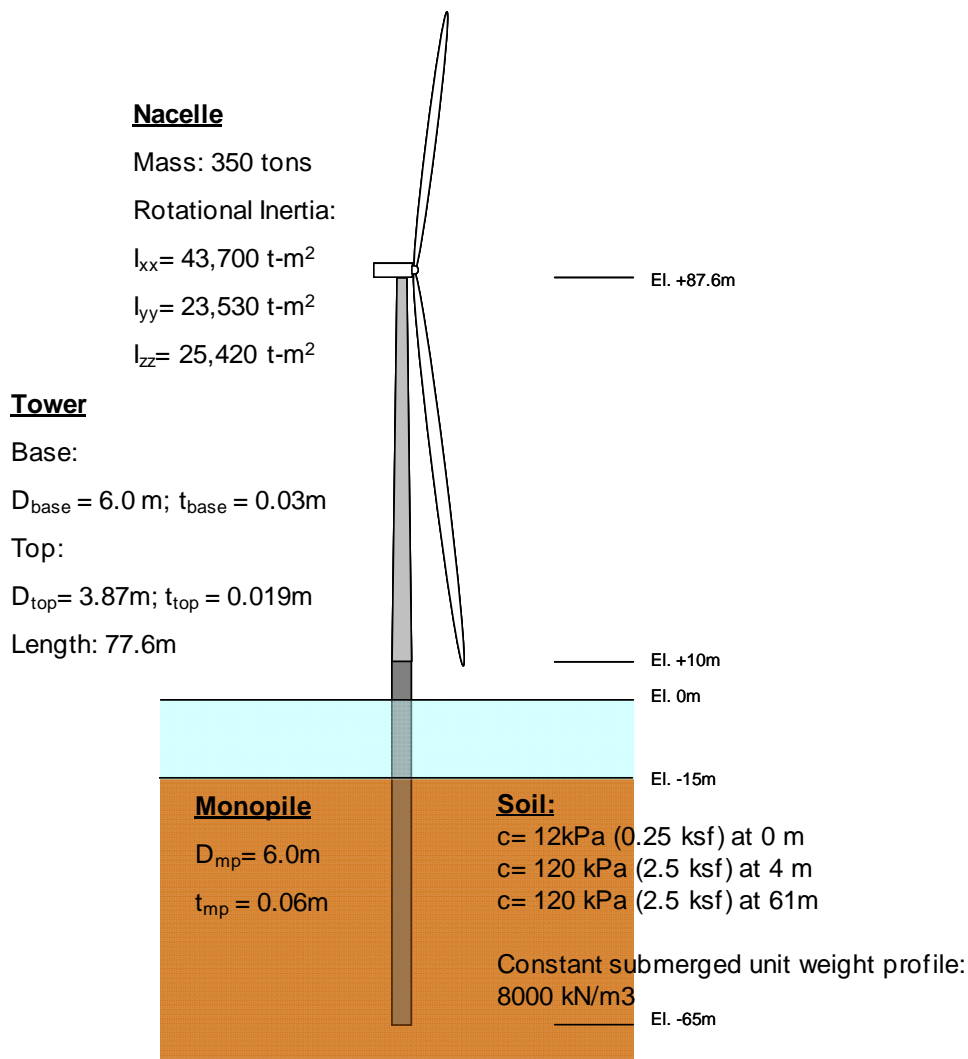


Figure 15: Monopile with a 4s period

6.2.2.2 Site 2 Tripod

A tripod configuration was used for the Site 2 case study. The tripod concept is one of several multi-piled configurations. The basic difference between the multi-pile concepts and the monopile is in their ability to resist overturning forces through the couple of pile axial tension and compression forces rather than bending, as in the case of the monopile. These configurations can provide greater strength and stiffness for systems in deeper water where the large monopile diameter may become prohibitive both in terms of material and installation costs.

The basic properties of the tripod are illustrated in the following figure. The tripod is configured to look identical to the monopile above water, so all of the parameters that were identified in that zone for the monopile apply to the tripod as well. The attributes of the tripod configuration that were considered fixed included the flange elevation, nacelle height, and tower top diameter. The attributes of the tripod that were considered to be primary design variables included base dimension, pile size, pile penetration, tripod leg length and diameter, elevation of brace to column connection, diagonal brace configuration size and thickness, central column diameter and bottom taper, and horizontal bracing configuration size and thickness. Unlike the monopile where the design variables are limited, there are numerous variables included in a tripod configuration. It was not the intent of this study to optimize the design of either of the site concepts; rather, the intent was to assess the difference in these concepts relative to their comparative levels of reliability.

A series of analyses were performed to assess the sensitivity of the first mode period to various design variables. The key variables included base dimension, pile size, number, size and orientation of the diagonal braces. These analyses established a reasonable range of these design variables that could be used to achieve the same period of vibration goal. Once the gross dimensions of the tripod were defined, a similar sensitivity analysis was performed to assess the significance of secondary design variables. The design was not optimized to minimize weight or assess any other performance factor (i.e., reserve strength).

In general, the level of optimization performed on a design would affect the structural parameters, such as weight and section dimensions. The level of optimization could also affect

the overall structural reliability for ultimate strength. The intent of the design codes is to achieve an optimized structure (i.e., a “perfect” design) that provides the reliability level implicit in a code via the safety factors. The use of higher safety factors will generate a reliability level greater than that implicit in the codes. This would be referred to as a conservative or “unoptimized” design. The designer or owner generally decides how much more reliability (i.e. more than suggested in design codes) to design for depending on factors such as cost investment and risk tolerance.

4s Period
Tripod Design

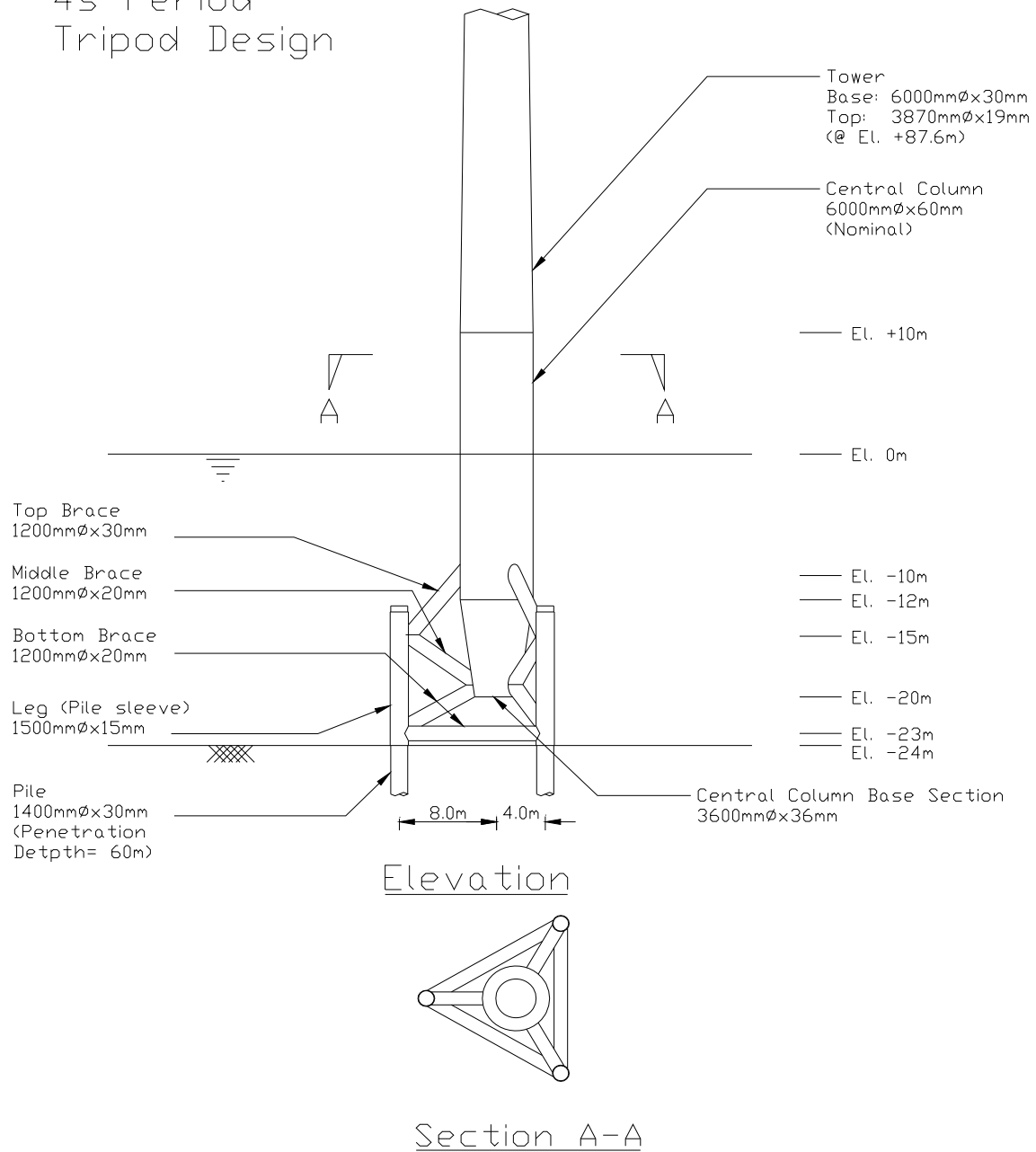


Figure 16: Tripod with 4s period

6.2.3 Oceanographic Data

Site specific wind, wave, and current data were developed for the two selected locations by Oceanweather. This data is referred to as hindcast data and similar data is also used by the oil and gas industry for much of the reliability work for offshore structures in the Gulf of Mexico. The hindcast data is generated by metocean models that have been calibrated to observed data from past storms.

The metocean data included the following:

- Wind speed for 1 hour average duration
- Significant wave height H_s
- Average zero-crossing wave period
- Current velocity
- Surge height

The data that was available to define the Site 2 (TX) metocean conditions are as follows:

- Tropical: covering tropical storms from 1900 to 2005
- Extratropical and Continuous storms: metocean statistics provided from analysis of Extratropical storms from 1957-2000 and Continuous storms from 1990 to 2005.

The above data sets were analyzed to extract the storm statistics for the metocean parameters of interest in this project (i.e., wind speed, H_s , current, and surge). These storm parameters were fitted with analytical probability distributions (i.e., Gumbel or Weibull) resulting in the most robust fit to the annual storm statistics. These annual analytical fitted distributions were used in the reliability calculations. For the two sites analyzed, the tropical storm data is the basis for the extreme storm parameters (e.g., for the 50 year and the 100 year storms), while the Continuous storm data set is the basis for the operating storm case (e.g., for storms with return period less than 1 to 5 years).

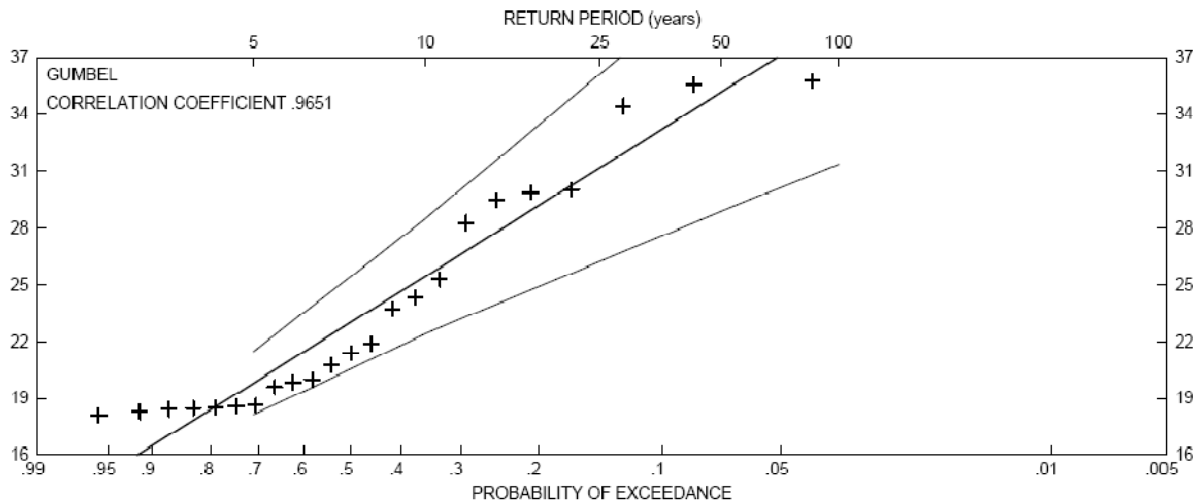


Figure 17: Gumbel Fit to Site-Specific Wind Speed Data for MA Site (Y-Axis is Wind Speed). The Upper and Lower Bounds Around the Gumbel Fit Represent the 95% Confidence Bounds on the Fitted Data.

Figure 17 shows the fitted Gumbel distribution plotted with the hindcast data for 1 hour wind speeds (in meters per second) at 10m reference height. The hindcast data includes all tropical storm data available for this site from Oceanweather. The tropical storm data is a good basis for extreme storm parameters and is not likely to give a good estimate for operating storms (for operating storms the continuous storm data was used). The tropical storm (hindcast) data is filtered to select the greatest wind speeds in 48 hour durations to avoid double counting of wind speed peaks from the same storm. Half of the greatest wind speed peaks are then selected and used to determine a probability distribution function for the data. The probability distribution function with the highest correlation is generally selected to represent the most robust solution. In almost all the cases analyzed, the Gumbel probability distribution generated the best correlation with underlying hindcast data.

In order to get the extreme wind speed and significant wave height values for extreme storms independently, the storm data is filtered to extract separately wind speed and significant wave height peaks. Figure 18 provides the fitted distribution for H_s for the MA site.

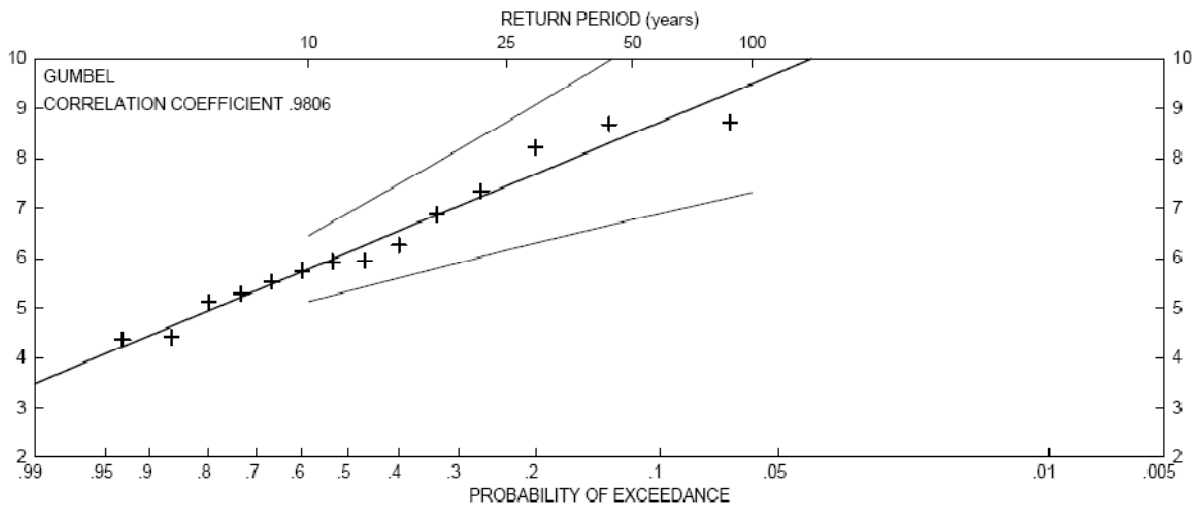


Figure 18: Fitted Gumbel to significant wave height tropical storm data (y-axis is Hs in meters). The upper and lower bounds around the Gumbel fit, represent the 95% confidence bounds on the fitted data.

The key metocean parameters for offshore wind turbines are wind speed and significant wave height. The remaining parameters are defined based on Hs. For example, given a storm with a specific Hs value, the data regression provides the associated wave period, maximum wave height, current velocity, and surge height. Given an Hs value, the remaining ocean parameters are modeled as deterministic with the value obtained through regression functions that define the parameter as a function of Hs.

Figure 19 conveys the level of correlation seen in wind speed and Hs values. The correlation for this data was about 85%. This correlation is included¹¹ in the reliability analysis to calculate the reliability index.

¹¹ The annual maximum wind speed (1 hour average at 10m reference height) and the annual maximum significant wave height are each specified by a Gumbel probability distribution and a correlation coefficient of 0.85 is additionally specified to model the observed correlation in the hindcast data. For the design storms (i.e., 50-year storm for the IEC and 100-year storm for the API), the independent 50-year and 100-year estimates are used to define the storm. This is a simplification versus analyzing two 100-year storms defined as 100-year Hs with associated wind speed and a second 100-year storm defined as 100-year wind speed with associated Hs. The simplification is reasonable and conservative given the high correlation between wind speed and wave heights, and alleviates the need to analyze two storms.

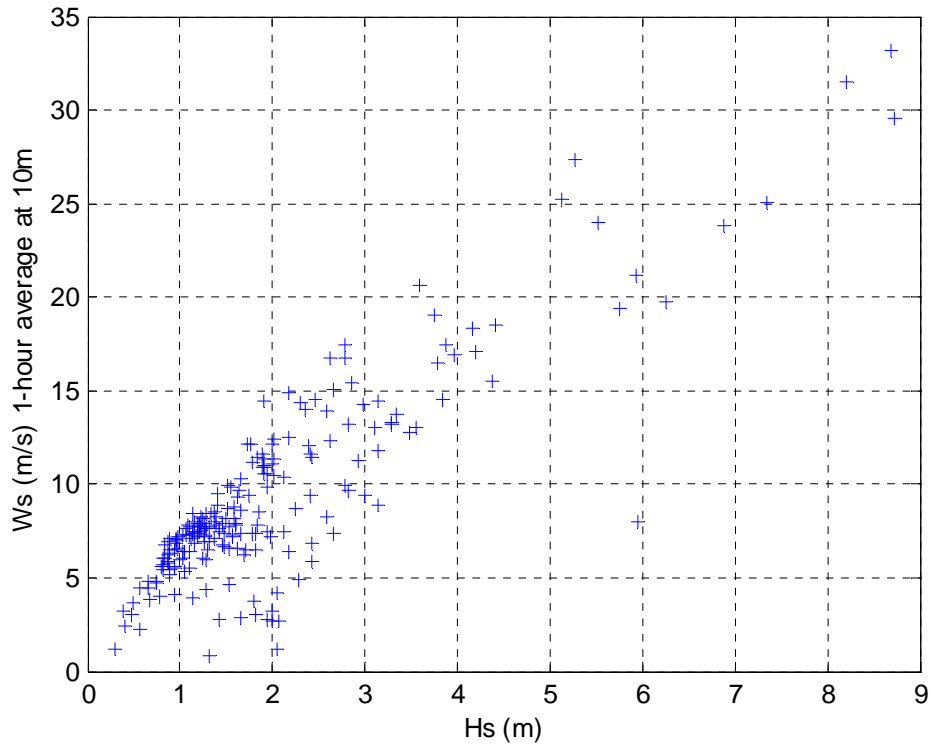


Figure 19: Correlation of wind speed and Hs for tropical storms

The next few figures convey the deterministic regression functions used to relate the associated ocean parameters to Hs. Although not relevant, in these figures, the GP number refers to the grid point used in the hindcast models to generate the metocean parameters. The Massachusetts site is referred to as GP 3468 and the Texas site is GP 7091.

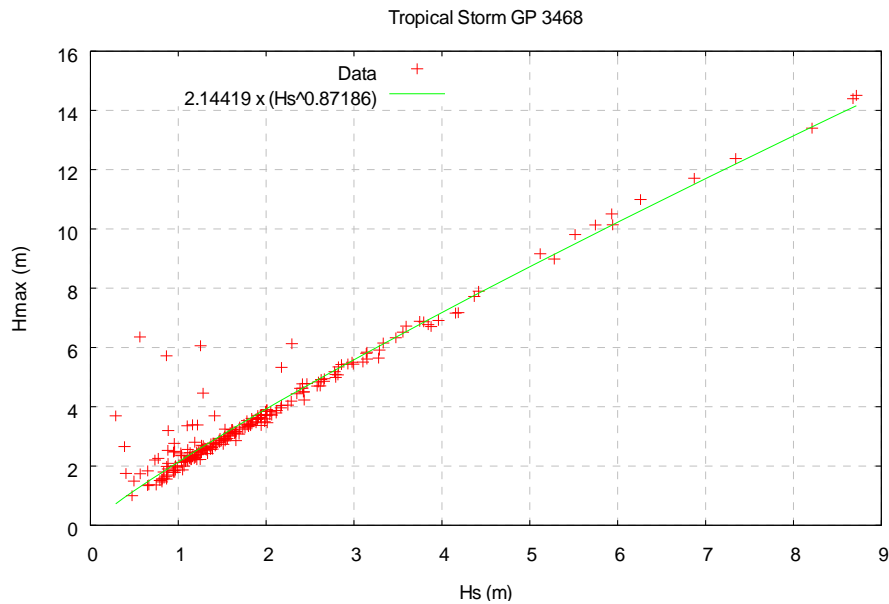


Figure 20: MA site relation of maximum wave height in a tropical storm with the Hs value of that storm

The hindcast data from Oceanweather does not account for breaking wave consideration. The large Hmax values represent “unbroken” waves. Later we discuss the breaking wave limit and how the wave heights were reduced to account for this effect.

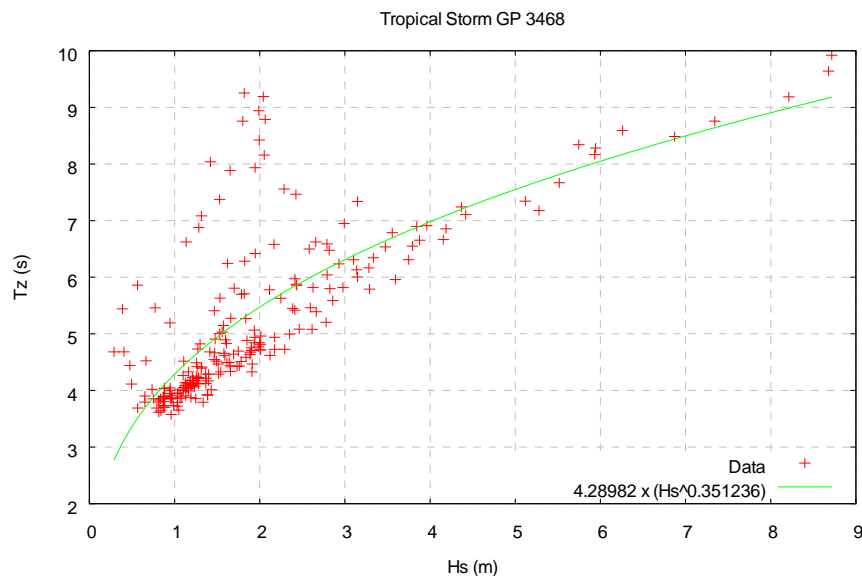


Figure 21: The average zero-crossing period in a storm related to Hs, the wave period for the maximum wave height is assumed to be 1.2 x Tz

The scatter observed in Tz values for small Hs values causes only a nominal change in the wave load on the offshore wind turbine structure. The load also generally decreases as the wave period increases. Therefore, a conservative simplification was adopted where the median Tz value was used as the associated Tz (and hence the associated Tmax) for small values of Hs. Small wave heights do not generally cause ultimate strength failure so this assumption was considered reasonable. The data for large Hs values is limited and does not show a large scatter around the median Tz value.

Figure 22 shows the relationship of surge height to significant wave height. The hindcast data indicates scatter in the surge height; however, as the regression line indicates, the surge height generally increases with Hs. This regression line was used to calculate the surge height to be used for storms with different Hs values.

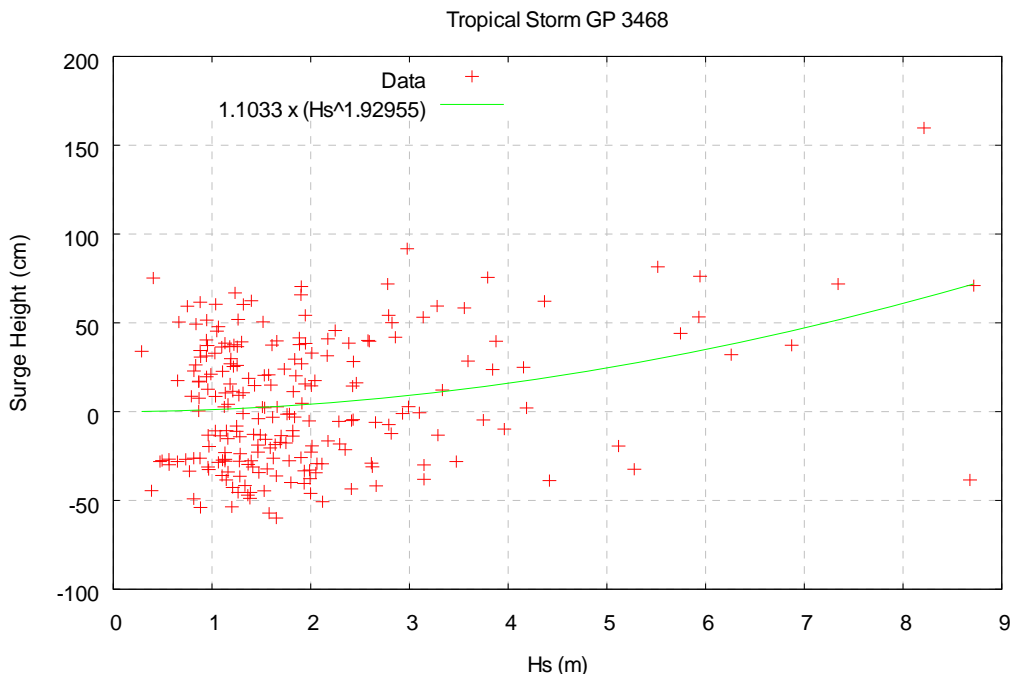


Figure 22: Surge height as a function of significant wave height for MA site

Similarly, the next several figures are for TX site.

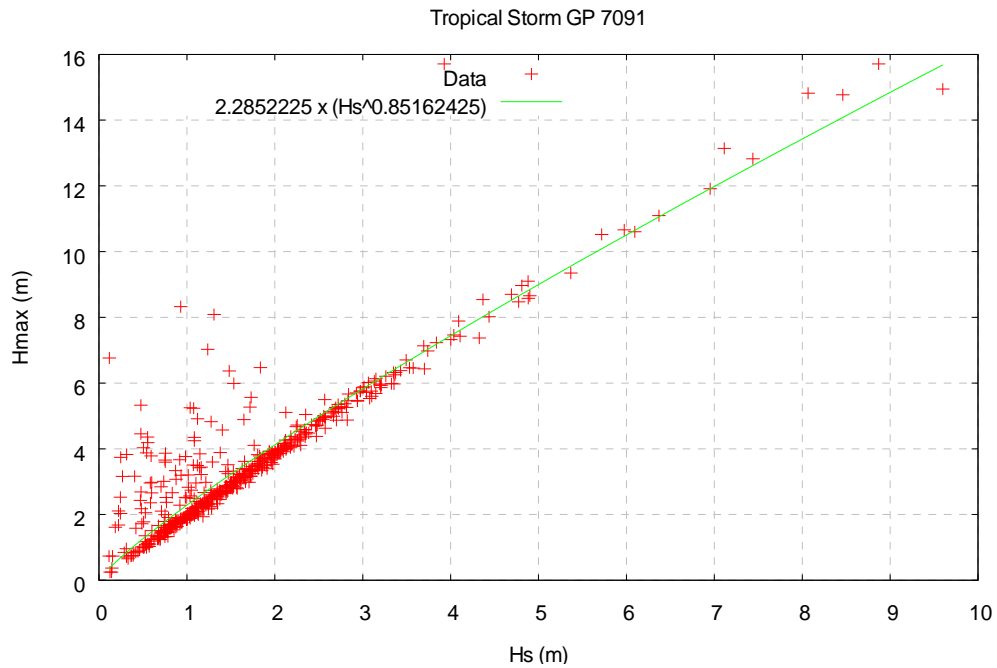


Figure 23: Maximum wave height related to Hs for tropical storms for TX site

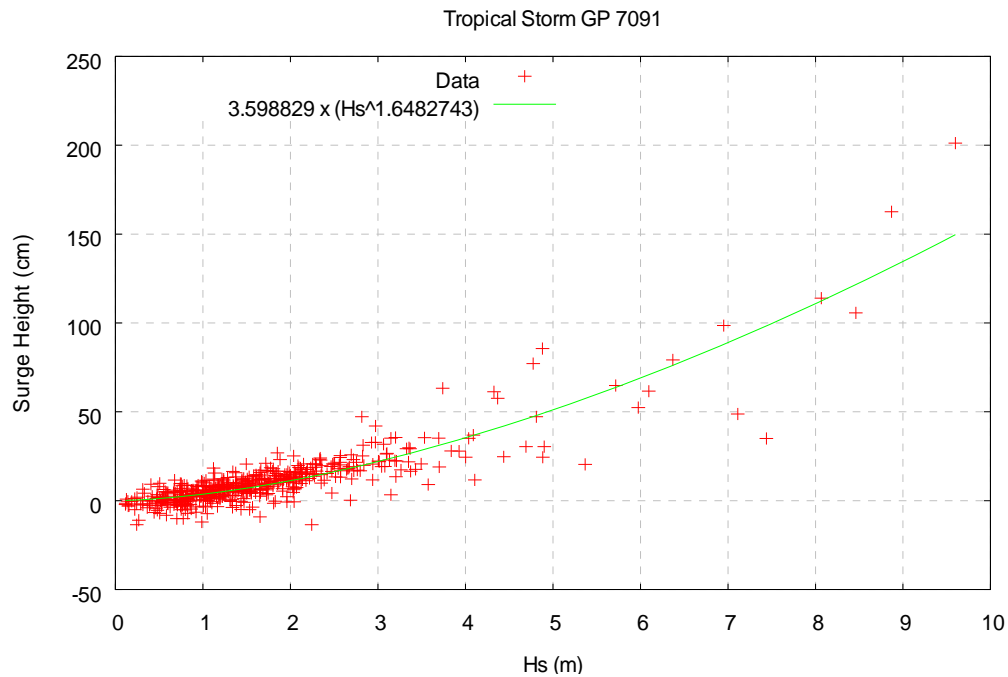


Figure 24: Surge height related to Hs for tropical storms for TX site

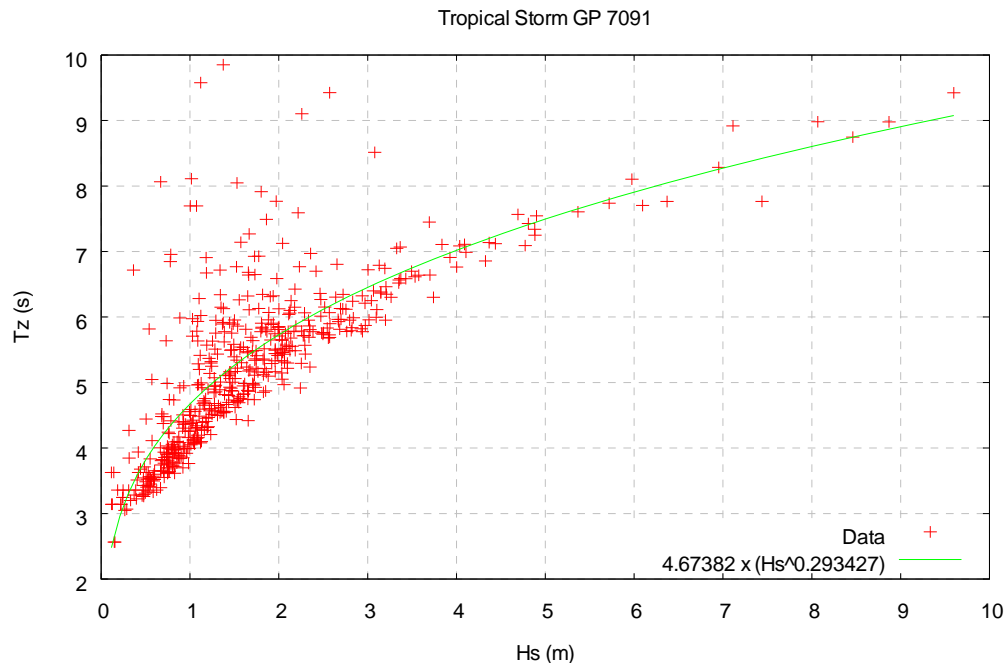


Figure 25: The average zero-crossing wave period ($T_{max} = 1.2 \times T_z$) related to H_s in tropical storms for TX site

6.2.3.1 *Breaking Waves*

The wave data provided by Oceanweather is based on a hindcast model that applies various wind and wave measurement to define criteria at specific grid points. This model does not specifically address breaking waves; therefore, wave heights defined using this model for shallow water conditions may be significantly greater than the breaking wave limits. To address this limitation in the data, wave heights were reduced when required to equal the associated breaking wave limit corresponding to the specific water depth. This correction also required special attention to the wave slam forces associated with breaking waves. Additional detail on this issue is presented in Section 6.3.4.

6.2.3.2 *Site 1 Wind and Wave Data*

The wave and wind data that was developed for Site 1 is summarized in Table 10. This summary includes the conditions used for the Power Generation (Operating), 50-year, and 100-year storm conditions. At the water depth of 15m, the wave heights defined using the hindcast model for both the 50- and 100-year storms exceed the breaking wave limit. The wave height for the 50-

year storm was reduced from 13.85 m to 10.67 m. The wave height for the 100-year storm was reduced from 15.27 m to 10.78 m. *The application of the breaking wave limit is a key factor in the comparative reliability assessment as it equalizes the design conditions that are applied for 50- and 100 year waves. The difference in the storm loading conditions is therefore limited to wind speed in these conditions.*

Table 10: Metrocean criteria for MA site

Storm Type	Ws 10m,1hr (m/s)	Hs (m)	Tz (sec)	Hmax (m)	Tmax (sec)	Hmax_ broken (m)	Tmax_ broken (sec)	Surge (m)	Current (m/sec)
Operating Condition	9.20	3.99	6.97	7.17	8.37	NA	NA	0.159	0.146
50 year Storm	35.15	8.50	9.10	13.85	10.92	10.67	9.82	0.686	0.180
100 year Storm	39.02	9.50	9.46	15.27	11.35	10.78	9.87	0.850	0.185

Operating Condition: H_{RP}=1 & W_{RP}<1

50 year Storm: H_{RP}=50 & W_{RP}=50

100 year Storm: H_{RP}=100 & W_{RP}=100

6.2.3.3 Site 2 Wind and Wave Data

The wave and wind data that was developed for Site 2 is summarized in Table 11. At the Site 2 water depth of 24m, the wave heights indicated using the hindcast model for both the 50- and 100-year storms are less than the breaking wave limit and therefore no adjustment of this data was required.

Table 11: Metrocean criteria for TX site

Storm Type	Ws 10m,1hr (m/s)	Hs (m)	Tz (sec)	Hmax (m)	Tmax (sec)	Hmax_ broken (m)	Tmax_ broken (sec)	Surge (m)	Current (m/sec)
Operating Condition	12.95	3.4	6.69	6.48	8.03	NA	NA	0.27	0.35
50 year Storm	38.96	8.68	8.81	14.39	10.57	NA	NA	1.27	0.88
100 year Storm	43.99	9.74	9.11	15.88	10.94	NA	NA	1.53	0.98

Operating Condition: H_{RP}=1 & W_{RP}<1

50 year Storm: H_{RP}=50 & W_{RP}=50

100 year Storm: H_{RP}=100 & W_{RP}=100

The comparison of the operating, 50-, and 100-year conditions for the Site 1 and 2 locations reveals some interesting trends. As expected, the wind speeds associated with the Gulf of Mexico

site are consistently greater than those for the Massachusetts site. However, the wave heights for the Gulf of Mexico site are greater than those for the Massachusetts site for the extreme conditions only. The operating wave height is less severe at the Gulf of Mexico site. This follows the discussion presented in Section 2.1.2.3.

6.2.4 Other Site Assumptions

To permit easier comparison of results, a stiff clay profile was selected to represent both sites. Variability in soil strength was not included in the reliability assessment; however, sensitivity analyses were performed to assess the change in structure vibration frequency for reasonable variation in soil stiffness. The shear strength profile selected for the analyses (Uniform profile 1) is shown in Figure 14.

No special site conditions were included in the study. This includes seafloor slope, seafloor irregularity, and scour.

6.3 ANALYSIS METHODOLOGY

The methodology adopted for the analyses in this study is summarized in Figure 26. Due to the complexity of the formulation of steep and breaking wave forces and some limitations of the FAST simulation software in this regard, a sequential process was developed to determine loads and structural response. The gross dimensions of each structure were developed based on the dynamic performance considerations described in Section 6.2.2. Using FAST to define the wind and wave force time histories and to specifically represent the change in blade wind forces caused by motions in the system generated by wave loading, a coupled model of the turbine, tower, and support structure was developed. The FAST analysis does not determine the impulsive forces caused by breaking wave slam on the tower. The FAST analysis is also restricted to some extent by the limits in particle kinematic theories that are used to define wave drag and inertia forces. Lastly, FAST does not determine the wind force applied directly to the tower shaft through drag. These additional forces were estimated using CAP and other calculations and added to the FAST results to define the complete set of physical loads.

Once the total wind and wave forces were defined, a second model was developed and used for both the structural design calculations (e.g., member utilization checks) and nonlinear capacity analysis. Member sizes were evaluated and modified as required to meet the minimum IEC or API requirements for each case study.

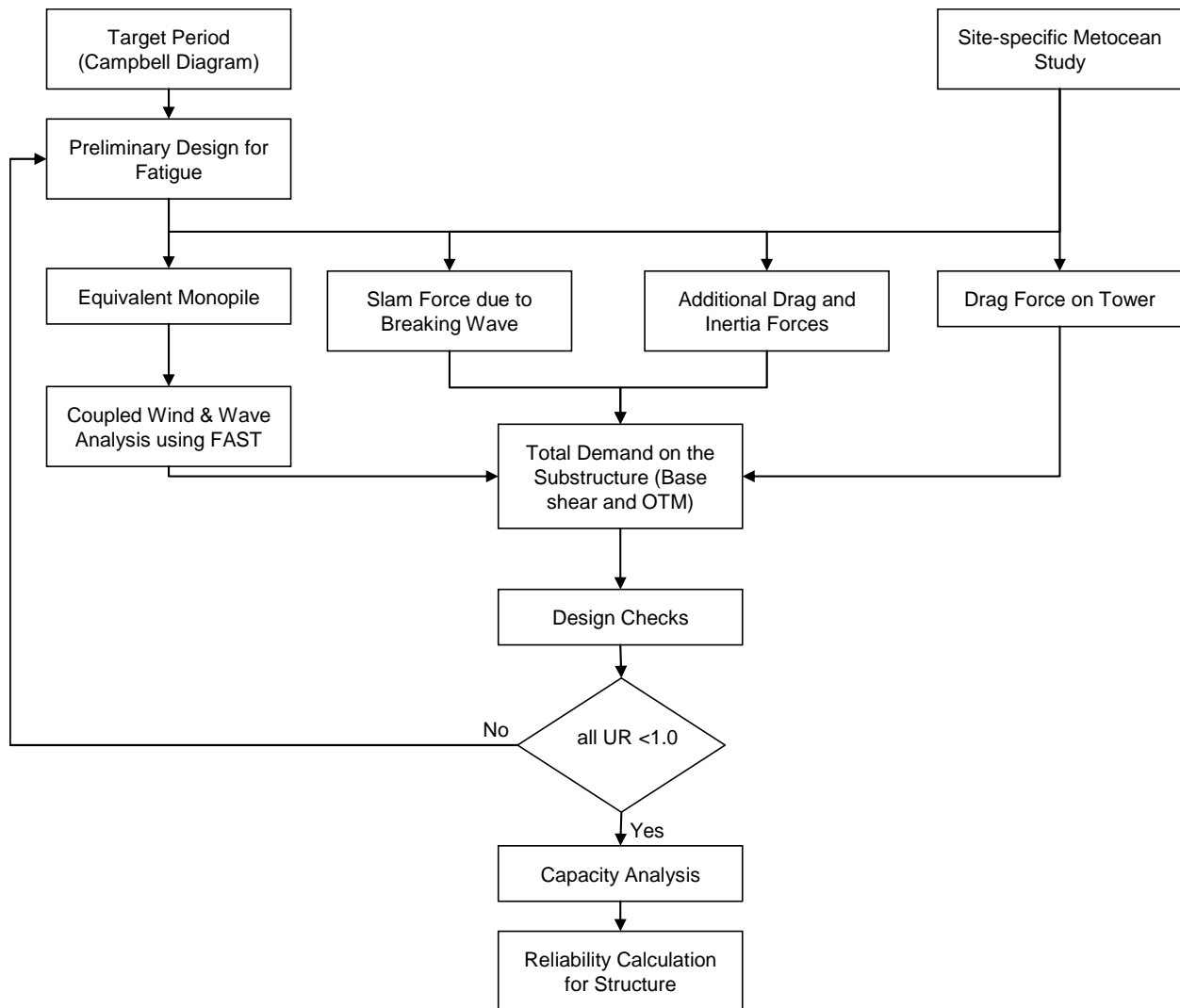


Figure 26: Methodology flowchart

6.3.1 Coupled Wave and Wind Load Analyses

In order to evaluate the demand for a range of site specific environmental conditions, a series of dynamic, coupled wind and wave analyses were performed. The FAST code developed by the National Renewable Energy Laboratory (NREL) was used for the analysis. FAST is a comprehensive aerodynamic/hydrodynamic simulator capable of calculating the response of an onshore or offshore wind turbine under operational and extreme metocean conditions.

The initial intention was to perform an uncoupled analysis of dynamic wind and wave loads. However, a series of initial simulations were performed that showed that there was a notable difference in the response of the structure when modeled using uncoupled and coupled analyses. Similar studies performed by Argyriadis *et.al.*[11] reveals that for a 5MW wind turbine the uncoupled wind and wave analysis overestimates the base shear force and overturning moment by 9% and 15%, respectively.

Each load case was defined with a combination of wave height and wind speed. Each case was examined with a number of different wind/wave simulations to assess the effect of variation of wind turbulence and to provide a bound to maximum structural response. A separate study was performed to assess the number of simulations that are necessary to obtain a reasonable estimate of the maximum demand for different turbulent wind flow models (Appendix C). Each analysis that was performed included 10-minute time history simulations for ten different stochastic simulations of turbulent wind flow.

The following subsections categorize the wind turbine loads and describe how each are modeled and analyzed.

6.3.1.1 Wind Load on Blades

The calculation of blade wind load requires the definition of full-field wind flow time histories defined at grid points that cover the vertical plane of turbine blades (Figure 27). TurbSim¹² was used to develop wind turbulence time histories. A stochastic turbulence model (extreme

¹² A stochastic, full-field, turbulent-wind simulator for use with the AeroDyn-based design codes (YawDyn, FAST, and MSC.ADAMS®)
<http://wind.nrel.gov/designcodes/preprocessors/turbsim/>

turbulence model for wind-turbine class 1, according to IEC 61400-1 Edition 3 standard) was applied for a given mean wind velocity at hub-height. Due to the stochastic nature of the turbulence model, ten different simulations were performed for a single mean wind velocity specified at hub-height. The vertical mean wind profile was obtained by applying a power law over the rotor disk and a logarithmic profile below the disk. The power law exponent as stated in IEC is 0.14 for normal wind conditions and 0.11 for extreme winds. Below the rotor disk, API suggests use of a logarithmic vertical wind profile consistent with IEC.

The aerodynamics calculations were based on two-dimensional airfoil-data coefficients (pitch, drag, and pitching moment coefficients), with corrections for three-dimensional behavior. These calculations were performed within the AeroDyn module of FAST software. The structural (summarized in Table 7) and aerodynamic properties of blades were obtained from Jason M. Jonkman (NREL).

In the aerodynamic load calculation for extreme storms, it is assumed that the blades are able to yaw into the incoming winds. This is referred to as the “normal” condition in IEC. An “abnormal” condition would be one where the yaw mechanism is ineffective during severe weather, leaving the blades in some other orientation. This abnormal condition would result in potentially greater loads than when the blades are facing the incoming winds. The IEC permits use of a lower safety factor (of 1.1) for the 50-year load in an abnormal extreme load condition. A safety factor of 1.35 is used for normal extreme condition.

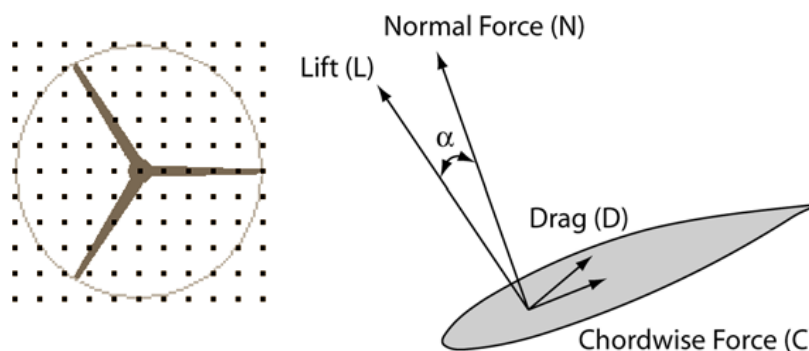


Figure 27: Grid points for the wind velocity data and force components acting on a blade¹³

¹³ References: The figure showing the grid points is from *Turbsim User's Guide for version 1.40*, NREL, September 12, 2008
 The figure showing the forces on the blade is from *AeroDyn Theory Manual*, NREL/EL-500-36881, Dec. 2005

6.3.1.2 Wave Load on Monopile

A coupled dynamic wave and wind analysis requires the time-history of wave forces applied along the depth of the structure. Incident wave kinematics were modeled with Stream function wave theory. To calculate the drag and inertia forces on the monopile, the relative velocity form of Morison's equation (Eq. 11) was used:

$$F = -C_A \rho V \ddot{q} + (1 + C_A) \rho V \frac{\delta u}{\delta t} + \frac{1}{2} C_D \rho A (u - \dot{q}) |u - \dot{q}| \quad (11)$$

where A is the projected area, V is the displaced volume of the cylinder per unit length, q is the displacement degree of freedom of tower/monopile node, u is the water particle velocity, C_A and C_D are the normalized hydrodynamic-added-mass and viscous drag coefficients respectively. \dot{q} is the velocity and \ddot{q} is the particle acceleration. In this representation, the inertia coefficient C_M is $1+C_A$. The drag and inertia coefficients used for each type of substructure are listed in Table 12 and Table 17, and the calculation of these coefficients is provided in Appendix B.

Morison's equation becomes less accurate for member diameters that are large relative to the length of the wave. A typical wave length of the incident storm waves used in the analysis is about 100 meters. For the monopile diameter of 6 meters, the ratio of wave length to the member diameter is well above the limiting value of 5 as suggested by API RP2A for Morison's equation applicability.¹⁴

The relative magnitudes of the wave drag and inertia forces are provided for one wave height in Figure 28. This plot shows that the magnitude of the inertia term (generated by wave particle acceleration) is generally equivalent to the drag term (generated by wave particle velocity) for this condition. This relationship was important to define the equivalent wave force coefficients used in FAST. Also, the inertia term will become more predominant for smaller wave and/or larger monopile diameters.

¹⁴ This limitation will be more important for the smaller waves that contribute to fatigue.

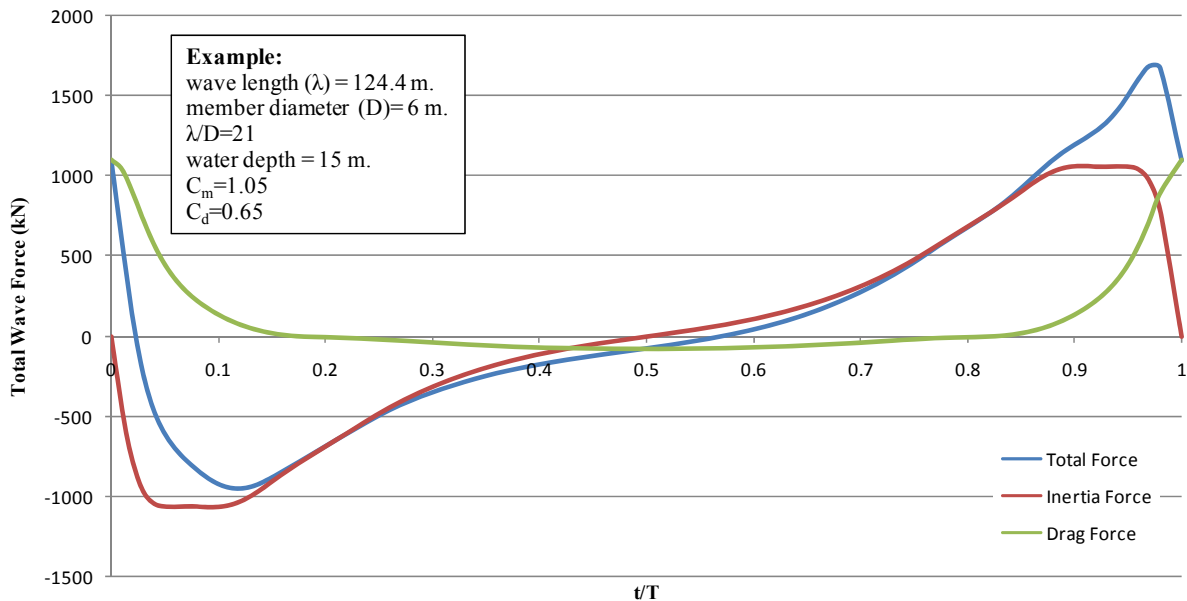


Figure 28: Plot showing the contributions of drag and inertia forces separately to the total time history of wave force for one wave cycle (t/T is the time expressed as a fraction of the wave period T)

A series of analyses were performed to verify the wave force formulation included in FAST. Various comparisons were completed to assess time-histories of monopile base shear and overturning to those generated with CAP and through other independent wave force calculations.

6.3.1.3 Wind Load on Tower

The FAST program does not represent the drag load on the tower due to wind. This drag force was calculated independently following Eq. (2.3.2-8) in API RP-2A (see also the Eq. 12 below), using a logarithmic vertical wind profile and mean wind speed at hub-height. This static force was then superimposed with the aerodynamic loads obtained by FAST.

$$F = (\rho/2)u^2C_S A \quad (12)$$

where u is wind velocity and C_S is shape coefficient (0.5 for cylindrical sections) and A is the projected area of the tower facing the incoming wind. Note that both API and IEC suggest modeling all physical loads, the API formulation was used only as a matter of convenience.

6.3.2 Equivalent Monopile Properties for FAST Analyses

The FAST program is limited to the extent that it presumes a fixed monopile support structure configuration. The program represents the supporting structure both in terms of applied wind and wave load but also, and more importantly, in terms of the structural vibration characteristics that affect the resulting turbine wind loads. Any support structure other than a fixed monopile requires an equivalent representation to capture the first mode of vibration, wave drag, and inertial loading. An equivalent fixed base monopile was “tailored” to match the desired structural period for each case study by changing the Young’s modulus of the tower and monopile material. The target structural period for both sites was selected to avoid resonance due to the turbine rotor rotation and the aerodynamic effect of the blade passing in close proximity to the support tower. This concept is explained in detail in Section 6.1.3 with the use of a Campbell diagram. The equivalent representation of the monopile is illustrated in Figure 29.

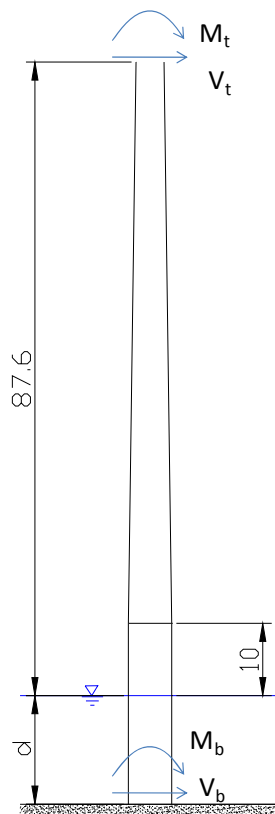


Figure 29: Tower and monopile model properties

6.3.3 FAST Wave and Wind Load Analyses

The numerical results for the load analysis are presented in Sections 6.4.1 and 6.5.2. This section provides a general description of the analysis method.

A range of wave and wind conditions were specified for both sites. Ten simulations were performed for each case using a combination of wind and wave conditions. For each simulation, a different turbulent field was specified for the mean wind speed. It was determined through an additional set of parametric analysis that ten simulations provide a stable representation of the wind force, specifically the mean value of the maximum wind force.

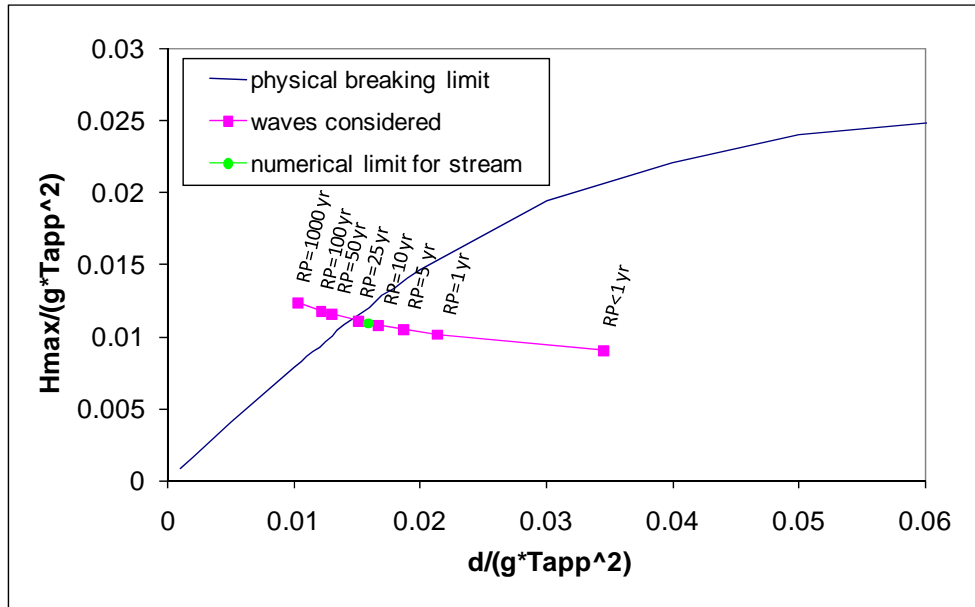
The FAST program can model both the operating (rotating blades) and parked (stationary blades) conditions. During extreme wind conditions (for mean hub-height wind speeds above 25m/s) the turbine is positioned as parked. 25m/s is the cut-out wind speed specified in NREL's 5-MW Baseline Wind Turbine.

Four internal force and moment components were obtained for each analysis (or case) in the form of a time-history; namely, tower top shear and over-turning moment (V_t and M_t in Figure 29), monopile base shear and over-turning moment (V_b and M_b). The maximum of these components were recorded for each simulation. The mean of these maxima were calculated over the 10 simulations. The mean of these maximum force components were then used for the reliability assessment of each structure.

6.3.4 Breaking Wave Forces

The breaking wave limit identifies the combination of wave height, wave period, water depth, and seafloor slope that causes instability in the wave form that leads to the breaking wave condition. For this study, a flat sea bed is assumed. A zero seafloor slope produces a spilling breaking wave condition. Impact forces were calculated in cases where wave instability was indicated. Using Stream function particle kinematic theory, additional drag-inertia forces were also calculated if the wave was found to be numerically unstable prior to wave breaking. To obtain the total base shear and overturning moment, these forces were added to what was calculated by the FAST analysis and with the wind forces on the tower.

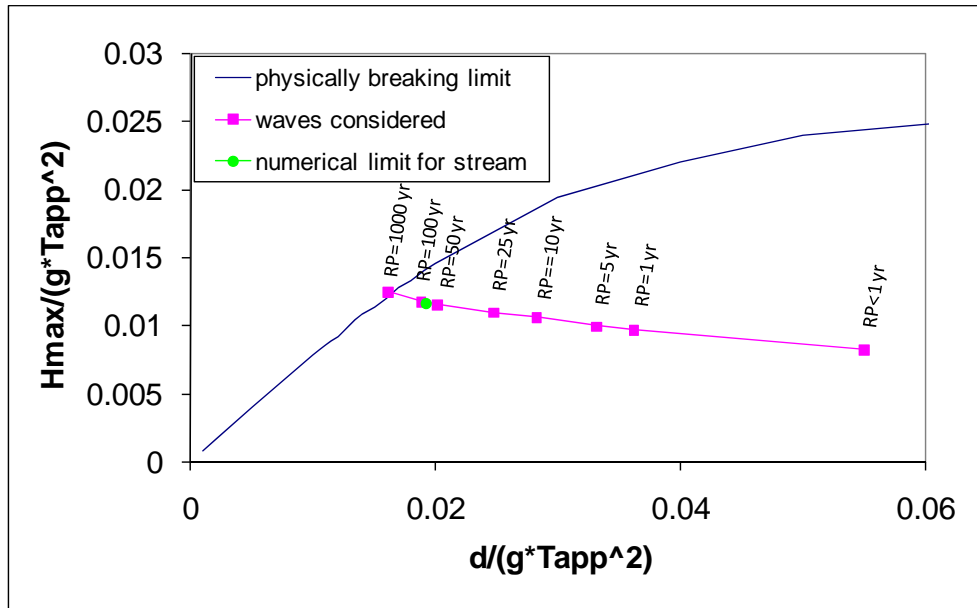
Figure 30 shows the wave conditions for Site 1 (Massachusetts) along with the breaking wave limit. It also shows the numerical limit to the range of applicability for Stream function.



Hmax (m)	Tmax (sec)	Physically Stable	Numerically Stable	Return Period (years)
3.92	6.6	Yes	Yes	<1
7.17	8.37	Yes	Yes	1
8.54	8.98	Yes	Yes	5
9.91	9.54	Yes	Yes	10
11.24	10.03	Yes	No	25
15.27	11.35	No	No	100
19.72	12.58	No	No	1000

Figure 30: Breaking waves at MA site. (Tapp is the apparent wave period.)

Figure 31 shows the wave conditions for Site 2 (Texas). It also shows the Stream function limitation for this condition. The issue of breaking waves was not a contributing factor for Site 2 up to the 100-year return period due to the deeper water depth at this site.



Hmax (m)	Tmax (sec)	Physically Stable	Numerically Stable	Return Period (years)
3.59	6.55	Yes	Yes	1<
6.48	8.03	Yes	Yes	1
7.28	8.36	Yes	Yes	5
9.15	9.05	Yes	Yes	10
10.94	9.62	Yes	Yes	25
14.39	10.57	Yes	Yes	50
15.88	10.94	Yes	No	100
20.48	11.94	No	No	1000

Figure 31: Breaking waves at TX site

Below is the procedure that was used to calculate impact forces due to wave breaking. A conceptual illustration of the problem is provided in Figure 32. The breaking wave impact force was calculated based on the guidelines provided in IEC [2] using Equation 13.

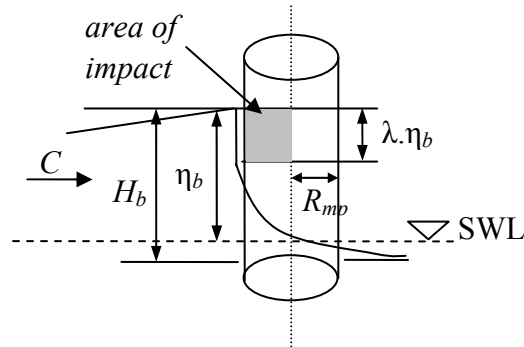


Figure 32: Concept of breaking wave

Where:

C: wave celerity

H_b: wave height at the breaking location

η_b: maximum elevation of the free water surface above the still water level

R_{mp}: radius of the cylinder

λ: curling factor ~ 0.5

ρ: water density

$$F = \lambda \eta_b \cdot \rho \cdot R \cdot C^2 \cdot \left(2 \cdot \pi - 2 \cdot \sqrt{\frac{C}{R}} \cdot t \cdot \text{Arc tan} \sqrt{1 - \frac{1}{4} \cdot \frac{C}{R}} \cdot t \right) \quad (13a)$$

for $0 \leq t \leq \frac{1}{8} \cdot \frac{R}{C}$

The first term in the equation is the maximum value; the second term is the decay of force with time. The maximum value is twice that given in API.

$$F = \lambda \eta_b \cdot \rho \cdot R \cdot C^2 \cdot \left(\pi \cdot \frac{\sqrt{\frac{1}{6} \cdot \frac{1}{\frac{C}{R}} \cdot t'}}{\sqrt{\frac{1}{6} \cdot \frac{1}{\frac{C}{R}} \cdot t'}} - 4 \sqrt{\frac{8}{3} \cdot \frac{C}{R}} \cdot t' \cdot \text{Arc tan} \sqrt{1 - \frac{1}{4} \cdot \frac{C}{R}} \cdot t' \cdot \sqrt{6 \cdot \frac{C}{R}} \cdot t' \right) \quad (13b)$$

for $\frac{3}{32} \cdot \frac{R}{C} \leq t' \leq \frac{12}{32} \cdot \frac{R}{C}$ with $t' = t - \frac{1}{32} \cdot \frac{R}{C}$

A representative impact force time history is provided in Figure 33 for Site 1 with a maximum wave height of 10.78 meters.

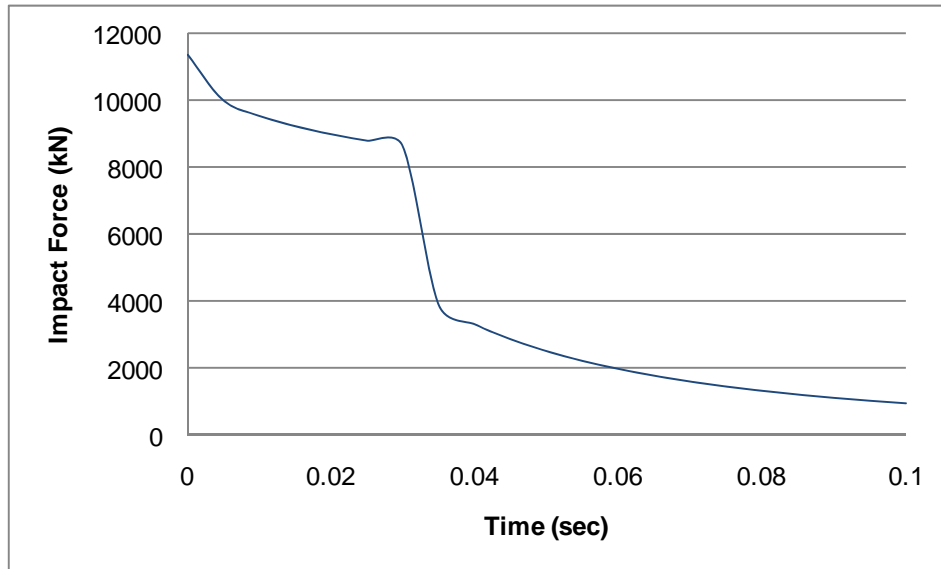


Figure 33: Impulse input force

A CAP analysis was performed to calculate the dynamic response of the monopile to this impulse loading. The mudline overturning moment time history is provided from this analysis in Figure 34. This response shows significant transient behavior in the monopile. This is due to the instantaneous nature of the loading. The peak of 43.6 M-m is the representative OTM due to impulse loading.

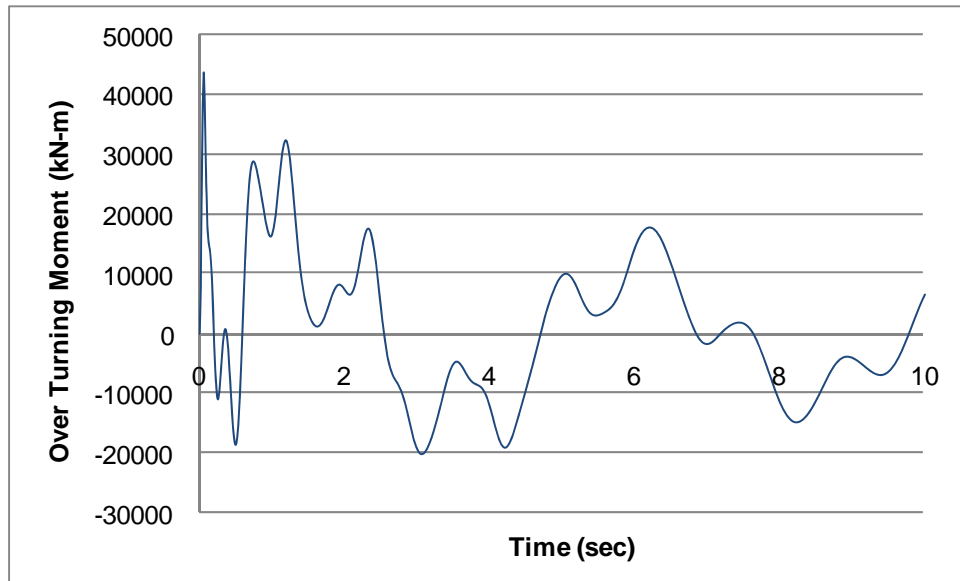


Figure 34: Impulse input force

6.3.5 Additional Drag and Inertia

Figure 30 and Figure 31 illustrate the difference in maximum wave heights as defined by the limit to Stream function and the physical breaking wave. An additional drag and inertia force component was calculated to address this issue. Figure 35 shows the concept of how this force is treated.

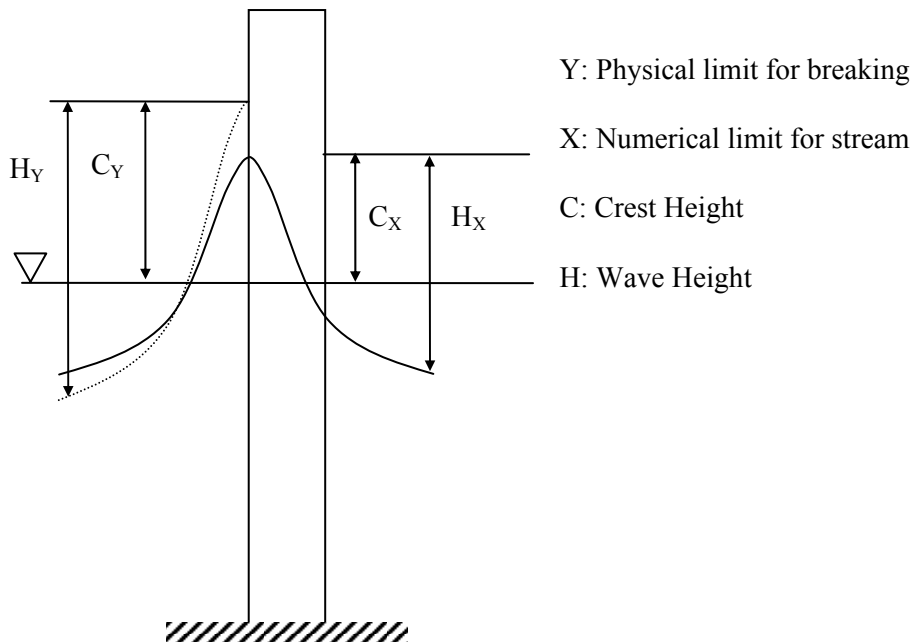


Figure 35: Additional drag and inertia forces

We assume that $C_X/H_X = C_Y/H_Y$ and the velocity profile stays constant above C_X

The formulation is provided for the Site 1 with a maximum wave height of 10.78 meters and the corresponding surge of 0.85 meters. Utilizing Stream function, we calculate C_X as 8.44 meters, maximum horizontal velocity as 10.92 m/sec, and maximum horizontal acceleration as 6.00 m/sec². The equivalent drag and inertia coefficients of 1.05 and 1.43 were used for this analysis. The maximum stable wave height H_Y is 76.31% of the water depth.

$$H_y = 0.763 \times 15.85 = 12.10m$$

$$\Rightarrow C_y = 12.10 \times 8.44 / 10.78 = 9.47m$$

The base shear due additional drag and inertia is:

$$\text{Additional Base Shear} = F_D + F_I$$

$$F_D = C_D \frac{\rho}{2g} Au |u|$$

$$F_I = C_m \frac{\rho}{g} V \frac{\delta u}{\delta t}$$

$$F_D = C_D \frac{\rho}{2g} \times 6 \times (9.47 - 8.44) \times 10.92^2 = 387kN$$

$$F_I = C_m \frac{\rho}{g} \times \pi \times 9 \times (9.47 - 8.44) \times 6.00 = 250kN$$

$$\Rightarrow \text{Additional Base Shear} = 637kN$$

$$\text{Additional OTM} = 637 \times (24.29 + \frac{(9.47 - 8.44)}{2}) = 15800kNm$$

6.4 MASSACHUSETTS CASE

A series of wave and wind load analyses were performed at the start of the development of the monopile concept to assess the variation in load as a function of projected area of the monopile, its stiffness, and the corresponding first mode of vibration. These analyses indicated clearly that the basic properties of a monopile (i.e., base diameter and thickness) at its critical section (i.e., the location of maximum bending moment immediately below mudline) would be controlled by the allowable range in the first mode period that was established to avoid accelerated fatigue.

This assessment was applicable for both the IEC and API conditions as it was found that the required minimum section properties to provide adequate strength for the 50 or 100-year design conditions was significantly less than that required to achieve a maximum first mode vibration period of 4 seconds.

There are a number of combinations of monopile diameter and wall thicknesses that can be used to achieve the required maximum 4 second vibration period. Generally speaking, in terms of stiffness, greater overall efficiency is achieved with larger diameter and smaller wall thickness. Other factors that must be considered include the feasibility and cost of driving large diameter piles, the larger drag and inertia wave forces, local buckling, soil-pile interaction, and foundation stiffness. A monopile diameter of 6 meters with a mudline wall thickness of 60 mm was found to provide a reasonable balance of all design parameters. Additional detail on this design is provided in Figure 15. This configuration was used for the remainder of the calculations for the Site 1 case study.

6.4.1 Wind and Wave Load Analyses with FAST

A monopile model was developed for input into FAST for wind and wave load analysis. FAST is configured to model monopile support structures; therefore, most of the properties of the structure were represented directly. FAST does not model soil-pile interaction and the additional flexibility that occurs due to lateral soil strain. This was represented in the model by reducing the steel modulus of elasticity (both for the tower and the monopile). FAST is not capable of formulating variable drag and inertia coefficients that would be appropriate for conditions where marine fouling would occur underwater. An equivalent set of drag and inertia coefficients were determined through a separate set of wave load time history analyses using the Capacity Analysis Program (CAP) software, which does address variable drag and inertia coefficients (Appendix B). The resulting equivalent monopile properties that were used for the FAST analyses are summarized in Table 12.

Table 12: FAST input data for MA site

Monopile thickness (m)	0.06
Tower base outer diameter (m)	6
Tower base wall thickness (m)	0.03
Tower top outer diameter (m)	3.87
Tower top wall thickness (m)	0.02
Steel density (effective) (kg/m ³)	8,500.00
Steel Young's modulus (E) (MPa)	1.537E+5
Steel shear modulus (G) (MPa)	5.913E+4
Water Depth, d (m)	15
Height monopile extends above MSL (m)	10
Length of Tower + Monopile (m)	102.6
C_d	1.05
C_m	1.43
Structural fore-aft period (s)	4.0

6.4.2 Total Wind and Wave Load Demand

As described in Section 6.3.3, the results of the FAST analyses had to be modified to include the elements of the wave and wind load that were not explicitly represented in FAST. This included wave slam, tower wind forces, and an additional component of wave drag and inertia force that was not properly represented for very steep waves prior to breaking. Table 13 provides the result of the FAST analysis including these additional components of force. These are nominal loads and do not include any load factors.

Table 13: Structural loads at MA site

Storm Type	Brace Shear (kN)				
	FAST (Wind & Wave)	Tower Wind	Slam	Addition	Total
Operating Storm	2,450	7	0	0	2,450
50-year Storm	3,350	112	2,650	625	6,740
100-year Storm	3,450	139	2,680	637	6,910
Storm Type	Mudline Overturning Moment (MN-m)				
	FAST (Wind & Wave)	Tower Wind	Slam	Addition	Total
Operating Storm	113	0.43	0	0	113
50-year Storm	76	7.26	43.1	15.3	142
100-year Storm	84	9.11	43.6	15.8	153

H: Max Wave Height

W: Wind Speed

RP: Return Period

FAST: Aerodynamic + Hydrodynamic Drag + Inertia

Addition: Additional Drag & Inertia which was not calculated in Stream theory due to numerical issues

This table should be viewed with the perspective that the monopile design will be most sensitive to overturning moment (OTM) at the mudline. A review of this data provides some key insights that are summarized as follows:

- The difference between the loading associated with the 50- and 100-year condition is not significant. This is partly due to the breaking wave limitation, which equalizes the wave heights for these conditions.
- The wave slam force represents a substantial portion of the total load on the system for the storm loading conditions. If the wave slam forces were reduced significantly, the Power Production (operational) loading condition, which is based on 1-year wave criteria and the rated wind speed, would likely control the monopile design.
- The slam load calculations for the 50- and 100- year conditions are very sensitive to surge. The slam loads are calculated using the maximum elevation of the free water surface which includes storm surge (the surge height is calculated from H_s using regression on hindcast data; see Figure 22). In shallow water, the crest kinematics can vary dramatically for small changes in water depth. This is shown in Appendix H.

- Superimposing the four components of load (aerodynamic and hydrodynamic loads from FAST, tower wind, slam, and stream correction) is conservative. The intent is to estimate the annual maximum load in a storm; more specifically, the maximum combined wind and maximum wave load in a storm with a given frequency (return period). The conservatism comes from algebraically adding peak value of each component, which assumes these peaks occur at the same time. In reality, there is a lag between the different component peaks depending on whether a component is drag dominated or inertia dominated. The drag components are driven by wind or wave velocity, while the inertia components are dominated by wind or wave acceleration. The velocity and accelerations achieve their maximum values at different times. The FAST analysis includes this effect for the wind and wave force components that are modeled explicitly (i.e., rotor wind and normal substructure wave), but the maximum values for remaining components are simply added. It is reasonable to make this conservative assumption for the objectives of this study since it has a consistent effect for both the API and IEC analyses).

6.4.3 Strength Checks

Structural response was assessed for each load condition (i.e., unfactored mudline base shear and overturning moment) using the CAP model. CAP includes a pile-soil interaction capability (Figure 36) and thus properly represents the effect of soil bearing on both pile fixity and bending moment. Table 14 lists the unfactored design loads used in the CAP analyses. API RP2A utilizes these unfactored loads whereas IEC/ ISO requires the application of load factors (1.1 for gravity loads, and 1.35 for extreme environmental loads) prior to the structural response analysis.

A material strength of 250MPa (36 ksi) was assumed for the initial utilization ratio check for the monopile. The analyses indicate that higher strength steel is not needed for this case.

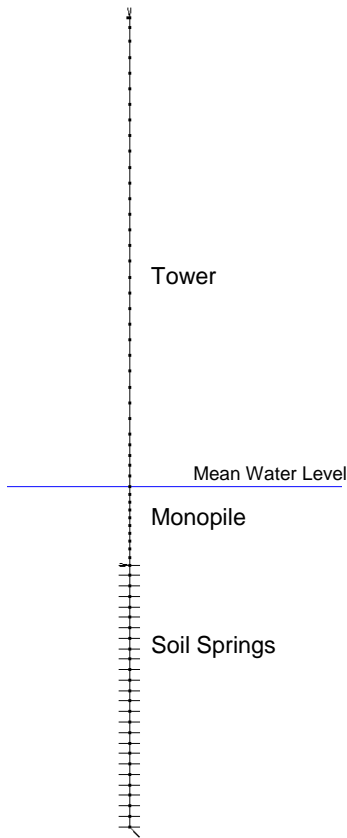


Figure 36: Monopile model in CAP

Table 14: Monopile design loads for MA site

Load Case	Unfactored Loads			Design Loads per API (no load factors)			Design Loads per IEC/ISO (1.1 Gravity + 1.35 Environmental)		
	Gravity Analysis	Wind/Wave Analysis					Axial Load (kN)	Shear (kN)	Moment (MN-m)
	Axial Load (kN)	Shear (kN)	Moment (MN-m)	Axial Load (kN)	Shear (kN)	Moment (MN-m)	Axial Load (kN)	Shear (kN)	Moment (MN-m)
Power Production	8,486	2,454	124	8,486	2,454	124	9,335	3,313	167
Parked (50-yr Metocean Criteria)	8,486	6,744	175				9,335	9,104	236
Parked (100-yr Metocean Criteria)	8,486	6,907	186	8,486	6,907	186			

The monopile cross-section was evaluated using both the API and IEC design formulations. The maximum utilization ratios (i.e., ratio of stress demand by external loads to allowable stress per API; ratio of the stress demand by factored external loads to factored strength per IEC/ISO) for the monopile are summarized in Table 15.

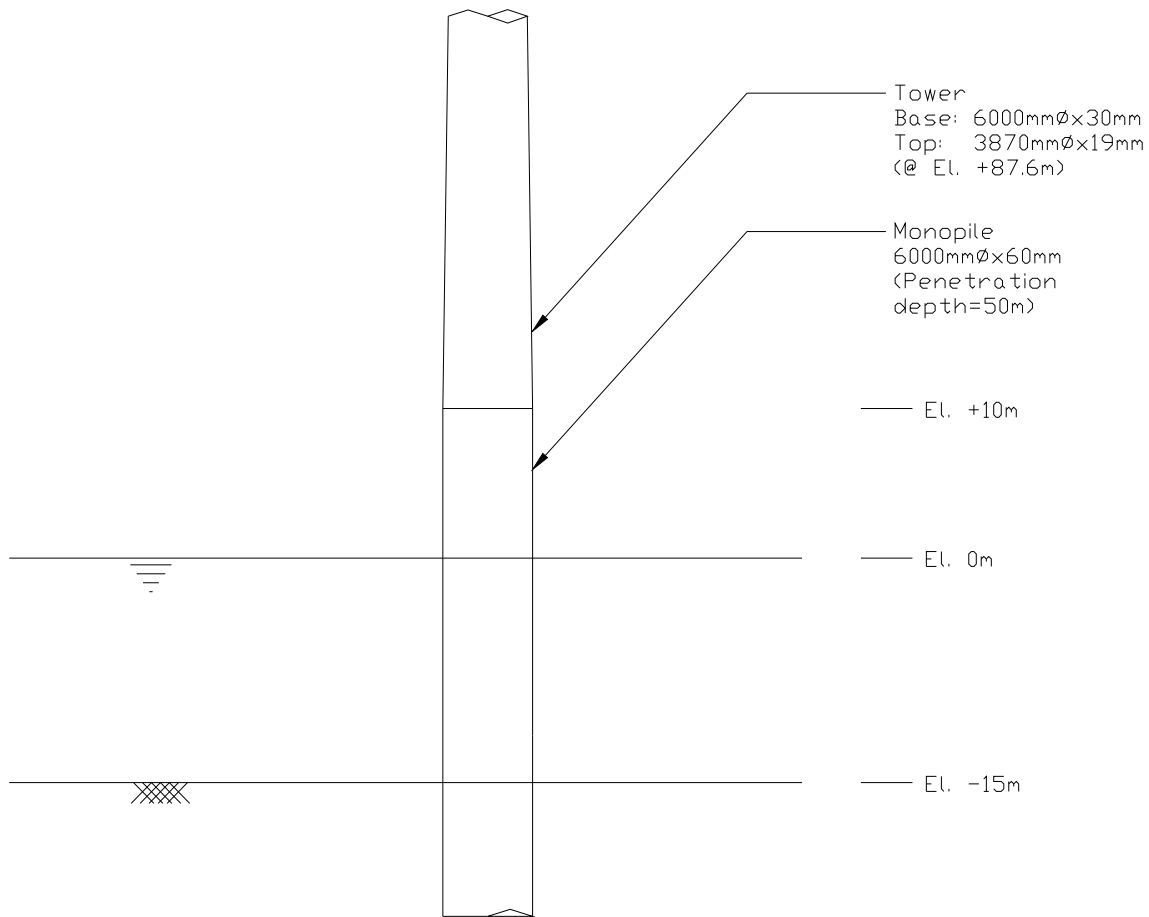
Table 15: Member utilization ratio

	Based on API RP2A		Based on IEC / ISO 19902	
	Power Production ^a	Parked/Idling	Power Production ^b	Parked/Idling
Combined Axial Load and Bending	0.570	0.605	0.433	0.595
Shear	0.044	0.093	0.043	0.118

^a without one-third allowable stresses increase factor

^b with the same load and material factors from parked/idling condition

The results shown above indicate that the design is well within the acceptable limits for both API and IEC. There were no changes. Therefore, the final design (both per API RP2A and per IEC) for the monopile at Site 1 (MA site) is as shown below:



Elevation

Figure 37: Monopile details (final design)

These results confirm that the design of the monopile is predominantly controlled by the maximum first mode period of vibration. In addition, the utilization ratios for API and IEC are essentially identical for this case.

A perfectly tuned design would achieve utilization ratios of 1.0 for all components of the structure using factored loads and factored strength. Such a design would achieve the reliability implicit in a given design code. The utilization ratios for this design are significantly less than 1.0 (the largest utilization is 0.6). Therefore, this structure will generate a very high level of reliability (or very high beta values, presented later).

These results indicated very clearly that the basic properties of the monopile (i.e., base diameter and thickness) at its critical section (i.e., the location of maximum bending moment immediately below mudline) would be controlled by the allowable range in first mode period established to avoid accelerated fatigue. The minimum section properties required to provide adequate strength for the 50 or 100-year design conditions was significantly less than those required to achieve a maximum first mode vibration period of 4 seconds. Thus, this assessment was applicable for both the IEC and API conditions. *The dependency of the monopile design on resonance avoidance for the site 1 (offshore Massachusetts) conditions is a key factor in the comparative reliability assessment since it makes any difference in the extreme loading condition inconsequential. The 50-year IEC and 100-year API monopile designs are therefore identical for the site 1 conditions.*

6.4.4 Capacity Analysis

It is clear by inspection that the reliability indices for the API and IEC solutions would be identical for the site 1 monopile. Nevertheless, the reliability analysis was completed to define the resulting indices and to provide a base of comparison for the Site 2 analysis.

A series of structural capacity analyses were performed to determine the total capacity of the monopile design. These capacities were then used as input to the reliability analysis. The capacity analyses were completed using CAP software. CAP includes an explicit representation of both material and geometric nonlinear behavior. The monopile was modeled in CAP first to establish the effect of the soil-pile response and to determine the location of maximum pile bending below mudline. Figure 38 shows the results from the capacity analysis with the API extreme load case as an example.

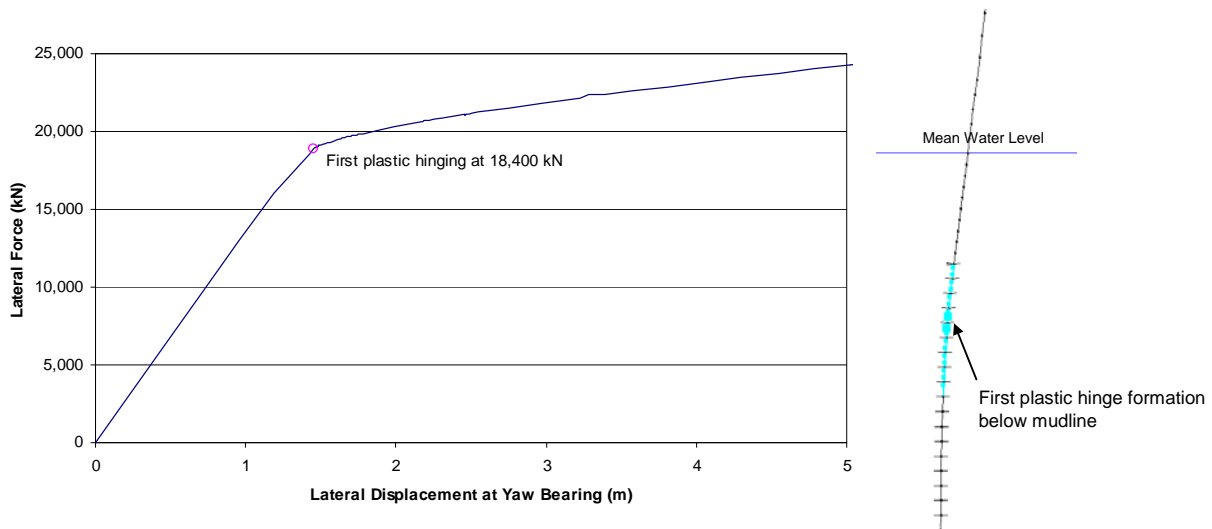


Figure 38: Results of a typical capacity analysis.
 (Left: Load-displacement curve; Right: deflected shape with nonlinear events.)

In the analyses, the monopile lateral capacity was assumed to be reached when the first full plastic hinge developed in the monopile below mudline. Table 16 presents the monopile capacity for each load case.

Table 16: Lateral load and overturning capacity for the monopile

Load Case	Capacity		Capacity/Demand Ratio	
	Base Shear (kN)	Base OTM (MN-m)	Base Shear	Base OTM
Power Production (Operating Storm)	9,930	459	4.05	4.05
Parked/Idling (50-yr Storm)	19,100	401	2.83	2.83
Parked/Idling (100-yr Storm)	18,400	406	2.66	2.66

The CAP model was used for a series of lateral “pushover” analyses to assess the ultimate strength of the monopile for each of the design loading conditions. While the variability in capacity for the monopile is somewhat academic, these analyses confirm the substantial amount of reserve capacity for the monopile.

The ratio of the capacity to design load provides a clear indication of the reliability implicit in the design. If the ratio of the capacity to design load is greater than the “net” safety factor, then

the design would result in a higher safety than suggested by the design guide. The ratio of capacity to design load is about 4.3 for the operating case and about 2.7 for the 50-year and 100-year cases. These factors are far greater than the net safety factors mentioned in Table 3.

Therefore, the resulting reliability indices for this structure would be far greater than that which is implicit in both design codes.

6.4.5 Reliability Analysis

To calculate the reliability of the monopile, the following simple limit state function was used:

$$G() = R/L - 1 \quad (15)$$

When $G()$ is less than zero, failure is assumed to happen in the ultimate strength. The resistance or capacity is modeled as a lognormal random variable with a CoV of 15%, and 5-percentile value equal to C (=460MNm)

The load L is modeled as $L=L_{BW} X_{BW} + L_{tower} X_{Tower} + L_{Slam} X_{Slam} + L_{Corr} X_{Corr}$

Where,

- L_{BW} is the aerodynamic blade load and the hydrodynamic wave load calculated using FAST and is a function of wind speed and wave height.
- X_{BW} is the model uncertainty and variability for aerodynamic load on blade and hydrodynamic load from drag and inertia from wave particle kinematics acting on the foundation. This is assumed to have a lognormal probability distribution with mean value of 1 and CoV of 7% (7% CoV was obtained from the FAST analysis of L_{BW}).
- L_{tower} is the wind load on the tower, and is a function of wind speed.
- X_{Tower} is the model uncertainty on tower wind load and is assumed to be Lognormally distributed with mean of 1 and CoV of 5%.
- L_{Slam} is the wave slam load, if any, on the structure portion below water, is a function of wave height and total water depth (i.e., surge height plus water depth).

- X_{Slam} is the model uncertainty for slam loads and is assumed to be lognormally distributed with mean of 1 and CoV of 20%. Note this CoV is relatively large to represent the uncertainty associated with the breaking wave forces on large diameter structures.
- L_{Corr} is the additional load associated with the Stream function correction and is a function of wave height and total water depth.
- X_{Corr} is the model uncertainty for the load correction L_{Corr} . This is assumed to be lognormally distributed with mean of 1 and CoV of 5%

In this formulation, the metocean parameters that drive the load calculations are the wind speed and significant wave height for the annual maximum storm condition. The significant wave height implicitly defines the zero-crossing wave period, current velocity, and the surge height experienced for different storm severities (return periods). The wind speed and significant wave height are in turn correlated for the MA site. The metocean data at the MA site indicates that the wind speed (W_s) and significant wave height (H_s) have a correlation coefficient of 84%. In the reliability analysis, W_s and H_s are each modeled using the Gumbel distribution for tropical storms as found from the site-specific data for this site, and the correlation between W_s and H_s is modeled as 84%. The alternate approach would be to model either W_s or H_s as an independent distribution and the second parameter as conditional on the first distribution of the wave. This approach was not used due to limitations on the probability distribution of the conditioned parameter. Also, generally for fixed offshore platforms, H_s is selected as the independent variable and W_s is chosen as the conditioned variable. However, for offshore wind turbines, W_s may be far more critical and thus should be used as the independent variable, while H_s may be critical when slam loads come into effect for extreme storms. Therefore, the correlation coefficient approach was adopted to give equal weight to W_s and H_s in the reliability calculation.

The variation of OTM with W_s and H_s is shown in the figures below. In all figures below, the aerodynamic load on the blade and the hydrodynamic load on the monopile are analyzed in FAST using simulated wind time histories and a Stream nonlinear wave elevation profile. The data provide average values of the maximum load (mudline overturning moment) for each simulated case. The load that is most relevant to the reliability analysis is the annual mean maximum overturning moment.

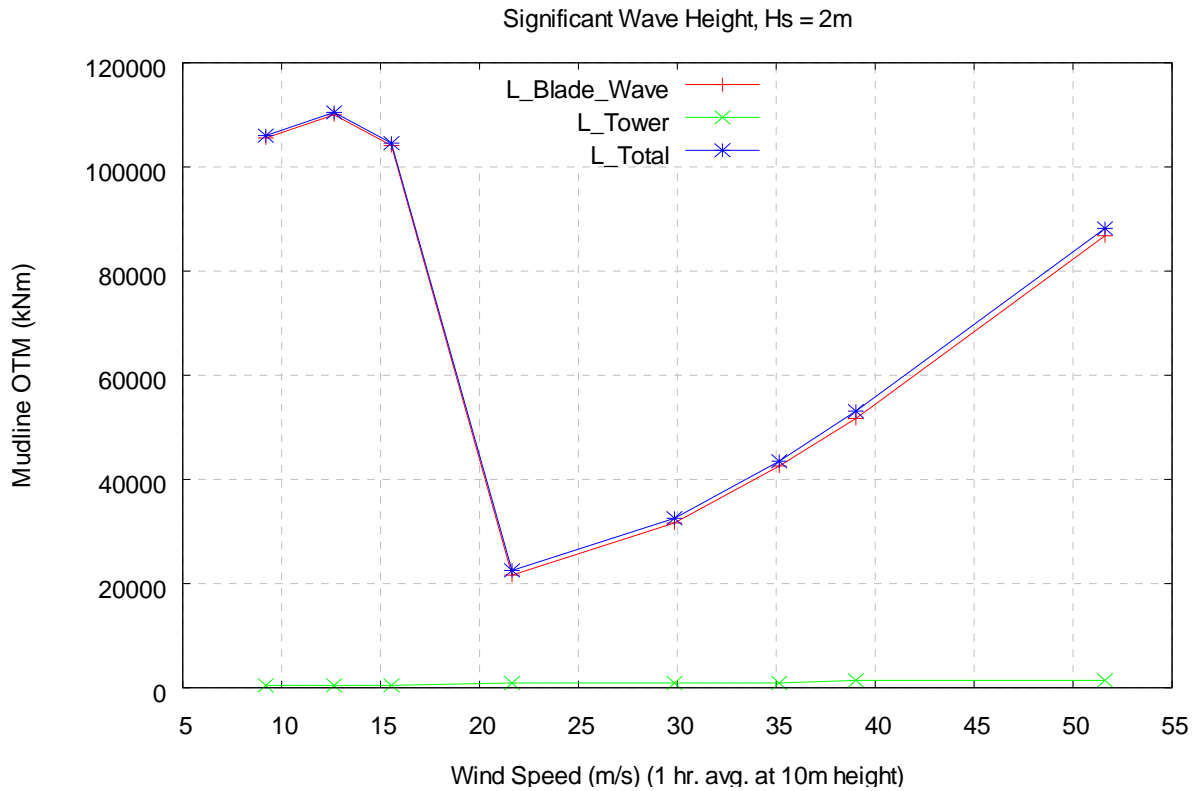


Figure 39: Mudline overturning moment (OTM) versus wind speed for the smallest storm analyzed. (There is no breaking wave phenomenon for this small storm.)

For wind speeds less than about 19m/s at 10m height (i.e., cut out wind speed of 25m/s at hub height of 90m) the turbine is operating and so the aerodynamic loads are high. As the wind speed goes past 19m/s, the turbine is assumed to be in parked mode, where the blades are “feathered” into the wind to reduce wind forces on blades. The wind load drops considerably as wind speed goes from an operating range (< 25 m/s at 90m height) to a parked range (> 25m/s at 90m height). Beyond wind speeds of 25 m/s, the load gradually increases with increasing wind speed.

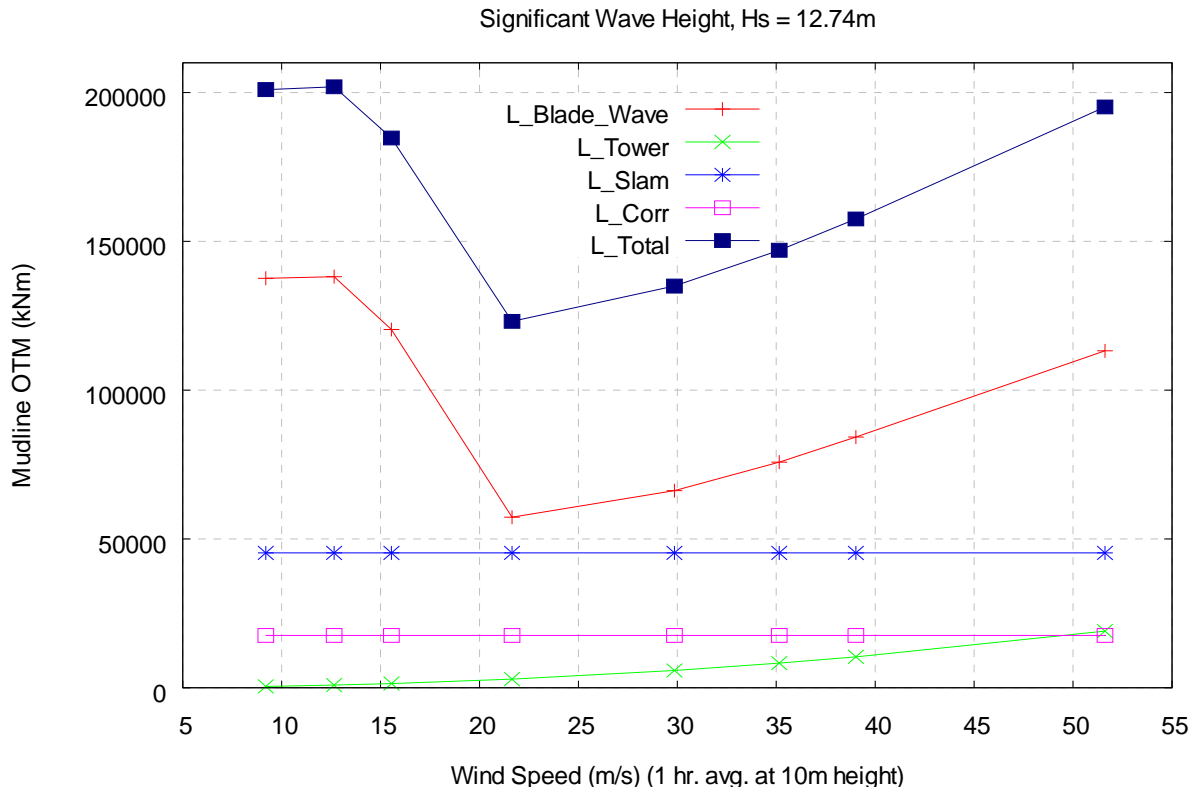


Figure 40: Mudline OTM vs wind speed for the largest storm analyzed. (Includes breaking wave effect.)

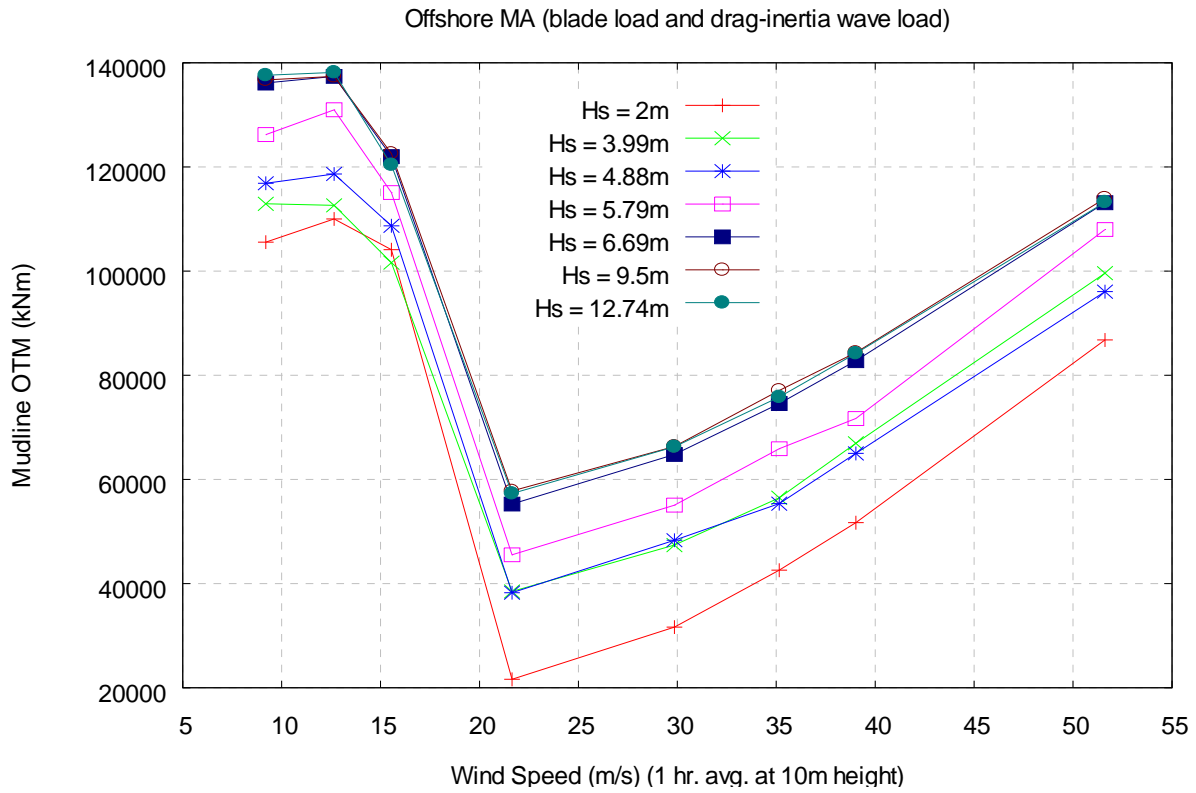


Figure 41: Loads on blade and wave loads only as a function of Ws, shown for all Hs values analyzed

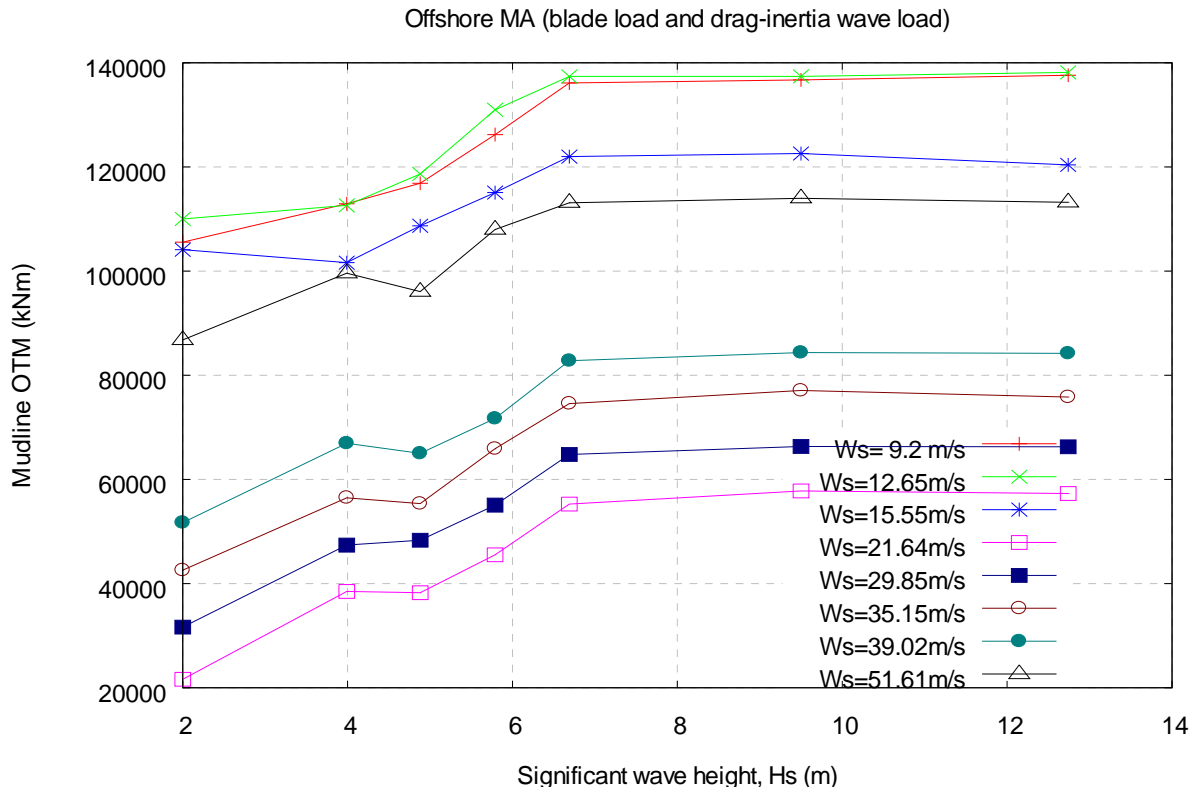


Figure 42: Loads on blade and wave load as a function of Hs

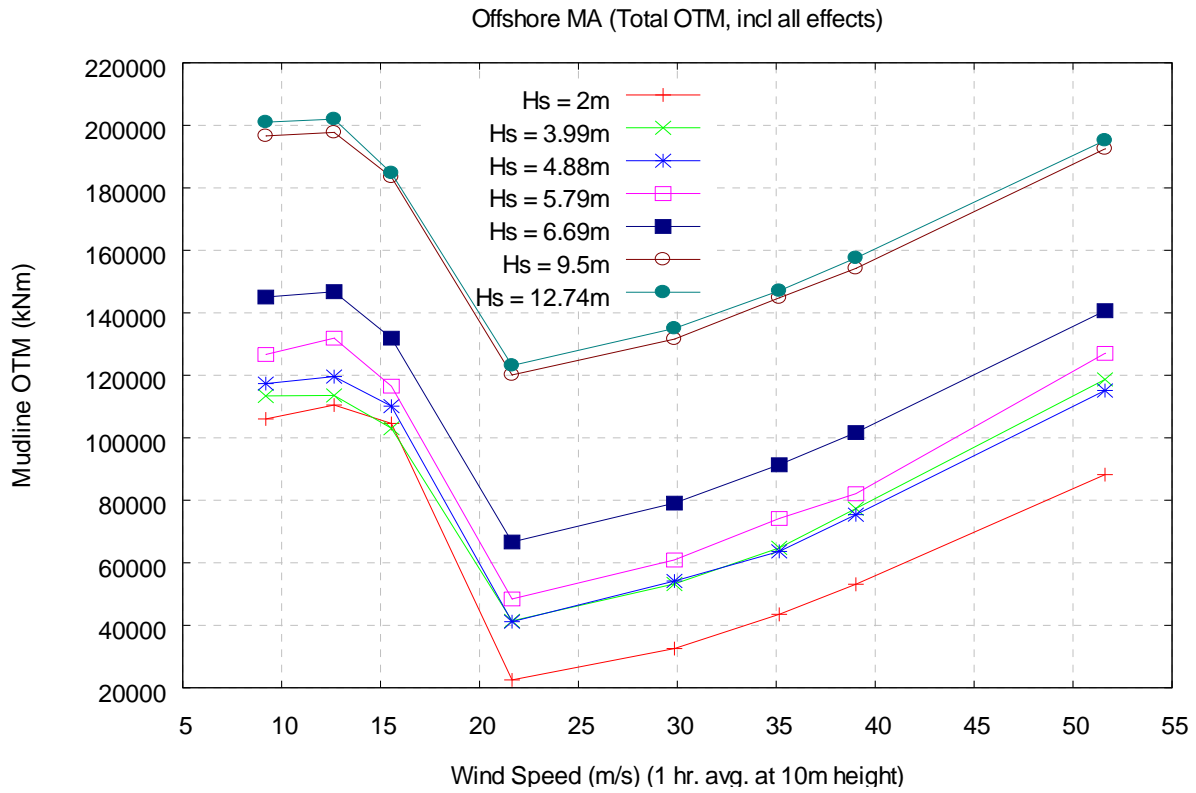


Figure 43: Total loads (including all applicable components) vs. wind speed. (1 hour average, at 10m reference height.)

The upper set of Hs values result in much higher loads than the smaller Hs set, which is primarily due to the occurrence of breaking waves for storms with Hs > 6.69m.

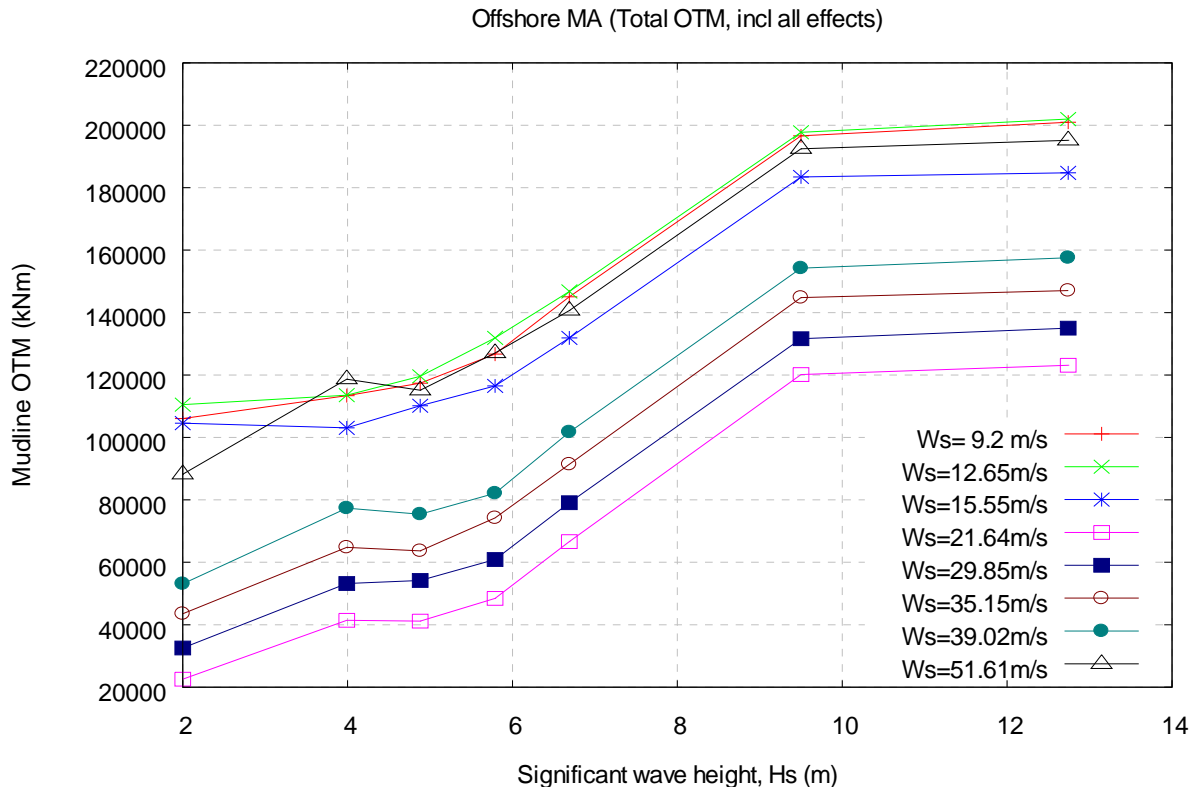


Figure 44: All components included as a function of Hs

Once the breaking wave height ($H_s \geq 9.5\text{m}$) has been reached, the loads do not increase significantly due to the similarity of slam loads.

Figure 45 and Figure 46 present the capacity and total load, in terms of mudline overturning moment. The first figure shows how these values vary with annual maximum 1 hour average wind speed. The second figure provides variation with annual maximum significant wave height. The capacity of the system is different for the operating and parked conditions due to the different proportions of wave and wind load. This causes the plastic hinge to form (see Figure 38) at different elevations along the pile. The capacity is substantially greater than the load even at the 1000-year level (i.e., load corresponding to the last wind speed on the right). The figures in Section 6 provide the return periods for the different wind speeds and significant wave heights. The capacity to demand ratio indicates a very high reliability index for this design. This is expected given the small utilization ratios and large reserve strength ratio values for this structure at the MA site. The reliability index is 5.42, which corresponds to an annual failure probability

of 2.9×10^{-8} . The ultimate strength limit state does not govern the design for MA site. The monopile design is controlled by the resonance avoidance requirement; therefore, the capacity far exceeds extreme loads for this monopile.

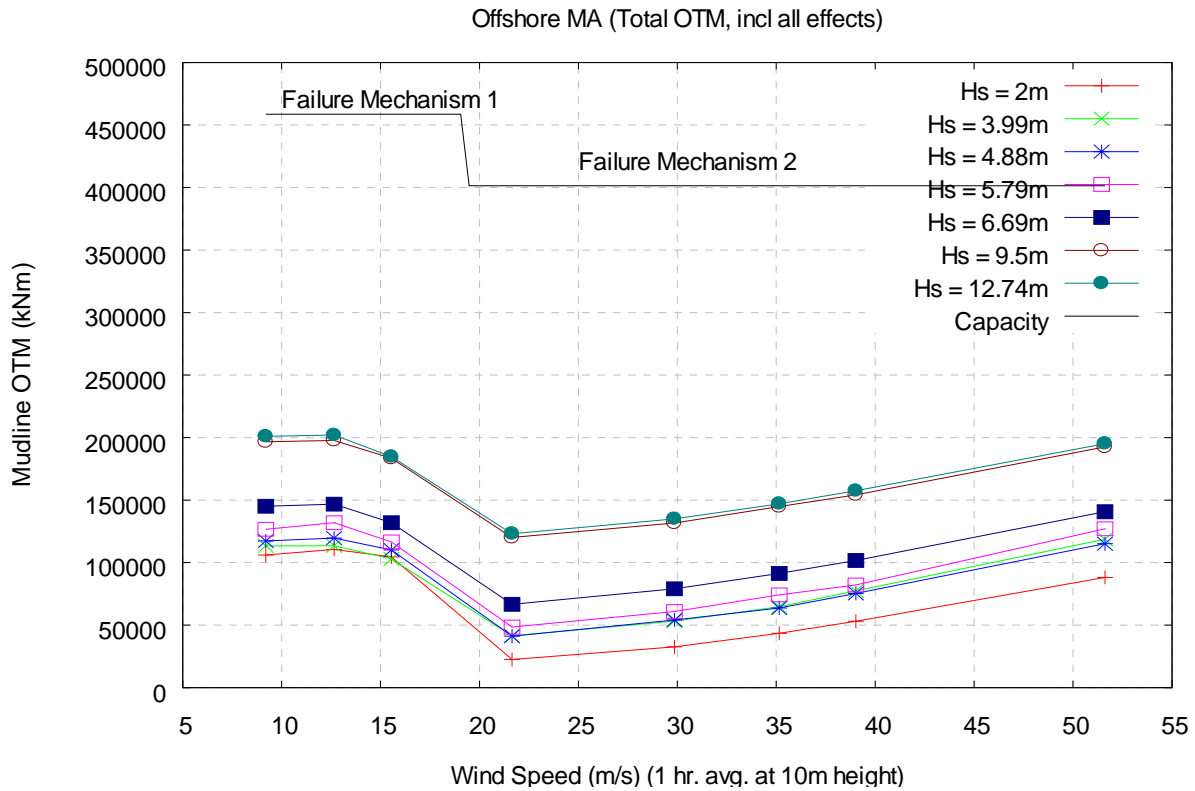


Figure 45: Total load and capacity for MA site as a function of wind speed. (Failure mechanism is different for operating vs. parked modes.)

The overturning moment capacity of the monopile is far greater than the loads analyzed for the range of metocean conditions included. The variation in loads due to slam for values of Hs from 6.69m to 9.5m has no affect on overall reliability.

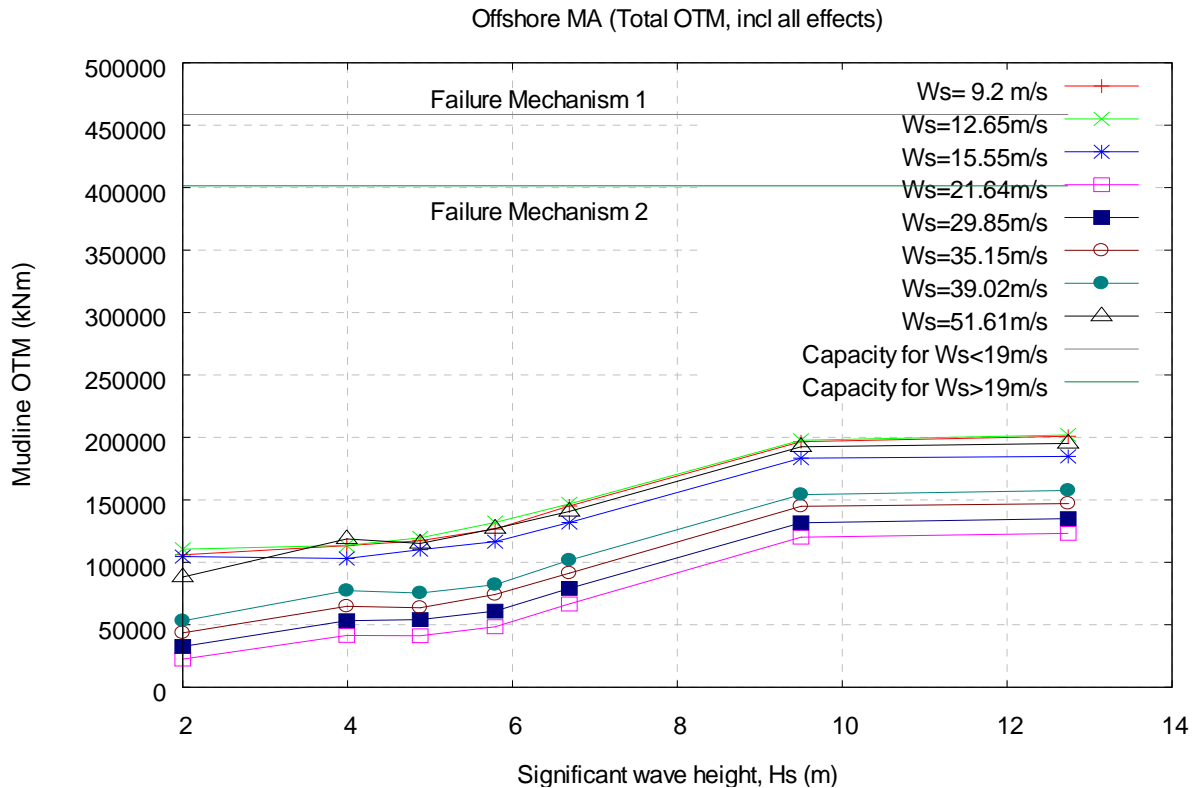


Figure 46: Total load and capacity for MA site as a function of wave height

The 19m/s value of 1hour average at 10m translates to the 25m/s cut out speed for 10-min average at 90m (hub height).

6.5 TEXAS CASE

6.5.1 Design Requirements for Resonance Avoidance

As was the case with the monopile, the initial configuration of the tripod was developed to achieve the maximum 4 second period of vibration. In this case, it was found that minimum size requirements for several of the structural components were controlled by extreme storm loading conditions. However, the increment in size that was needed to meet these strength requirements was not significant, indicating that the resonance avoidance and strength requirements for this design were more balanced. In general, the resonance avoidance requirement controlled the design of the central column while the strength requirements controlled the design of the piles and braces.

6.5.2 Wind and Wave Load Analyses with FAST

A representation of the tripod was developed for input into the FAST program for wind and wave load analysis. In the case of the tripod, the equivalent monopile properties that were needed for the FAST analysis required additional effort. Again, a second model was developed using the CAP program to properly represent the effect of the foundation, additional framing, and the variation of drag and inertia coefficients above and below water. A series of analyses were performed to assess the best overall matching properties for an equivalent monopile in terms of total wave load (Appendix B). The modulus of elasticity of the equivalent monopile model (including the tower) was scaled to set the period at 4 seconds. Table 17 summarizes the resulting equivalent monopile properties that were used for the FAST analyses.

Table 17: FAST input data for TX site

Monopile thickness (m)	0.06
Tower base outer diameter (m)	6
Tower base wall thickness (m)	0.03
Tower top outer diameter (m)	3.87
Tower top wall thickness (m)	0.02
Steel density (effective) (kg/m ³)	8500
Steel Young's modulus (E) (MPa)	1.834×10 ⁵
Steel shear modulus (G) (MPa)	7.055×10 ⁴
Water Depth, d (m)	24
Height monopile extends above MSL (m)	10
Length of Tower+Monopile (m)	111.6
C _d	0.98
C _m	1.18
Structural fore-aft period (s)	4.0

6.5.3 Total Wind and Wave Load Demand

The water depth for Site 2 is deeper than Site 1 and is such that waves for both the 50-year and 100-year are below the breaking wave limit. However, as was the case with the offshore Massachusetts site calculations, some correction to the Stream function wave force calculation

was made to correct for wave steepness. The results of the FAST analysis with these additional components of force are provided in Table 18. These are nominal loads and do not include any load factors.

Table 18: Structural loads at TX site

Storm Type	Base Shear (kN)				
	FAST	Tower Wind	Slam	Addition	Total
Operating Storm	2,050	14	0	0	2,070
50-year Storm	4,500	139	0	0	4,640
100-year Storm	5,470	180	0	95	5,750
Storm Type	Overturning Moment (MN-m)				
	FAST	Tower Wind	Slam	Addition	Total
Operating Storm	121	1	0	0	122
50-year Storm	124	10.3	0	0	134
100-year Storm	153	13.5	0	3.5	170

H: Max Wave Height

W: Wind Speed

RP: Return Period

FAST: Aerodynamic + Drag + Inertia

Addition: Additional Drag & Inertia which was not calculated in stream due to numerical issues

In contrast to the comparison of loads for the MA site, the results for the TX site show that there is a substantial difference in total 100-year load vs. the 50-year load measured either in terms of base shear or overturning. This difference is due to both higher wind speeds and wave heights.

6.5.4 Strength Checks

Each unfactored base shear and overturning moment pair (at mudline) from Table 18 was converted into a shear-moment pair at Elevation -8m and applied to the tripod model in CAP (Figure 47). The analyses were repeated for three wave heading directions (000, 090, 180). In each analysis, the maxima of the axial load, shear, and bending moment demand on the main member types (central column, piles, legs, and braces) were obtained. The first round of design checks showed that the pile dimensions in the preliminary design were insufficient both per API and IEC / ISO. Therefore, the wall thicknesses of the overstressed members were increased and the CAP analyses were repeated.

In the second round of the design checks, the modified tripod passed the IEC/ISO requirements but had some overstress for the API condition. This established the acceptable design for the IEC case. The remaining overstress was addressed again through member resizing and the CAP analyses were repeated. The API design checks with the third set of CAP results showed that the tripod passed the API criteria throughout. This established the acceptable design for the API case. A summary of the differences in the member sizes required for the IEC and API designs are provided in **Table 19**. The only difference between the designs is in the pile wall thickness.

The design check data for the IEC and the API tripods (such as unfactored and factored loads, utilization ratios) are provided in Table 20 through Table 25. In the design checks, a material strength of 290MPa (42 ksi) was considered for all the tripod components.

A set of Eigenvalue analyses were performed to assess the change in dynamic response resulting from the design revisions. This showed that the change in the period of the first mode of the tripod was less than 0.25s. The coupled wind and wave load analyses were therefore not repeated after the design modifications since the change in the dynamic amplification due to such a small shift in the period was negligible.

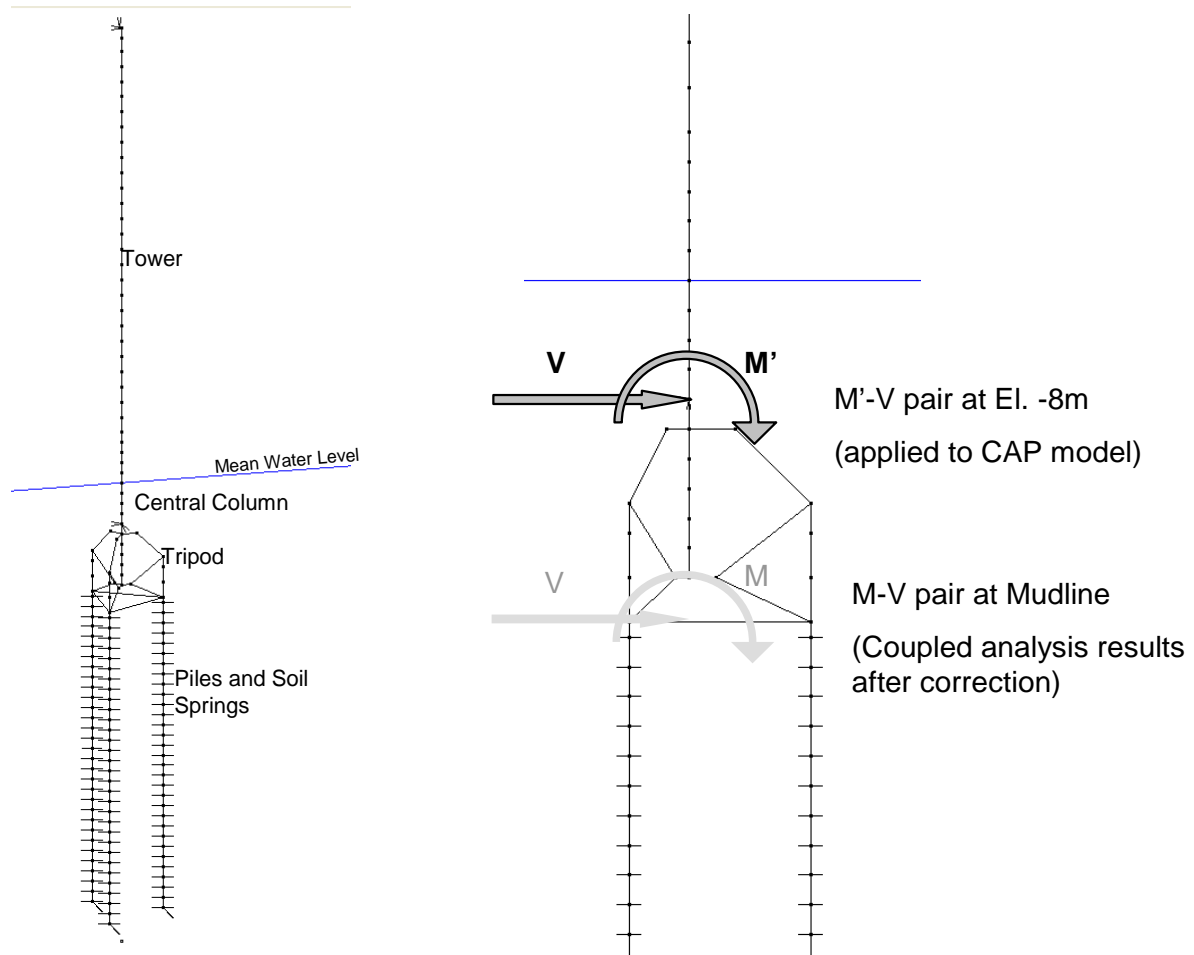


Figure 47: Tripod model in CAP. (Left: Oblique model view; Right: Loads applied to the model.)

Table 19: Member dimensions in API and IEC tripods

	Preliminary Design	IEC Tripod	API Tripod
Central Column (nominal)	6.0m x 60mm	6.0m x 60mm	6.0m x 60mm
Piles	1.4m x 30mm	1.4m x 32mm	1.4m x 35mm
Top Brace	1.2m x 30mm	1.2m x 30mm	1.2m x 30mm
Other Braces	1.2m x 20mm	1.2m x 20mm	1.2m x 20mm
Legs (Pile sleeves)	1.5m x 15mm	1.5m x 15mm	1.5m x 15mm

Table 20: Unfactored design loads for the members of the IEC tripod

Element Type	Member Dimensions	Load ^a	IEC Tripod -Unfactored Loads	
			Power Production	Parked/Idling (50yr Extreme Environmental Load)
Pile	1.4m x 32mm	Axial Load, kN (G)	1,704	1,704
		Axial Load, kN (E)	10,373	11,844
		Bending Moment, kN-m (E)	1,429	4,928
		Shear, kN (E)	739	1,713
Central Column (Nominal Section – 6m)	6m x 60mm	Axial Load, kN (G)	4,778	4,778
		Axial Load, kN (E)	0	0
		Bending Moment, kN-m (E)	93,917	69,585
		Shear, kN (E)	2,080	4,647
Central Column (Bottom End – 3.6m)	3.6m x 36mm	Axial Load, kN (G)	2,765	2,765
		Axial Load, kN (E)	0	0
		Bending Moment, kN-m (E)	21,805	20,205
		Shear, kN (E)	5,181	2,420
Leg (Pile Sleeve)	1.5m x 15mm	Axial Load, kN (G)	483	483
		Axial Load, kN (E)	3,139	3,173
		Bending Moment, kN-m (E)	667	593
		Shear, kN (E)	130	90
Top Brace	1.2m x 30mm	Axial Load, kN (G)	1,270	1,270
		Axial Load, kN (E)	7,535	7,455
		Bending Moment, kN-m (E)	2,950	2,633
		Shear, kN (E)	731	651
Middle Brace	1.2m x 20mm	Axial Load, kN (G)	-720 (Tension)	-720 (Tension)
		Axial Load, kN (E)	5,778	6,096
		Bending Moment, kN-m (E)	646	539
		Shear, kN (E)	149	130
Bottom Brace	1.2m x 20mm	Axial Load, kN (G)	736	736
		Axial Load, kN (E)	1,414	3,765
		Bending Moment, kN-m (E)	1,409	2,203
		Shear, kN (E)	373	551

^a G: Gravity loads; E: Extreme environmental loads

Table 21: Unfactored design loads for the members of the API tripod

Element Type	Member Dimensions	Load ^a	API Tripod -Unfactored Loads	
			Power Production	Parked/Idling (100yr Extreme Environmental Load)
Pile	1.4m x 35mm	Axial Load, kN (G)	1,713	1,713
		Axial Load, kN (E)	10,366	14,992
		Bending Moment, kN-m (E)	1,394	6,089
		Shear, kN (E)	738	2,129
Central Column (Nominal Section – 6m)	6m x 60mm	Axial Load, kN (G)	4,778	4,778
		Axial Load, kN (E)	0	0
		Bending Moment, kN-m (E)	93,903	89,998
		Shear, kN (E)	2,080	5,762
Central Column (Bottom End - 3.6m)	3.6m x 36mm	Axial Load, kN (G)	2,756	2,756
		Axial Load, kN (E)	0	0
		Bending Moment, kN-m (E)	21,749	25,751
		Shear, kN (E)	5,182	3,241
Leg (Pile Sleeve)	1.5m x 15mm	Axial Load, kN (G)	458	458
		Axial Load, kN (E)	2,962	3,812
		Bending Moment, kN-m (E)	648	717
		Shear, kN (E)	126	105
Top Brace	1.2m x 30mm	Axial Load, kN (G)	1,273	1,273
		Axial Load, kN (E)	7,540	9,498
		Bending Moment, kN-m (E)	2,960	3,319
		Shear, kN (E)	736	822
Middle Brace	1.2m x 20mm	Axial Load, kN (G)	-722 (Tension)	-722 (Tension)
		Axial Load, kN (E)	5,774	7,738
		Bending Moment, kN-m (E)	637	661
		Shear, kN (E)	147	155
Bottom Brace	1.2m x 20mm	Axial Load, kN (G)	728	728
		Axial Load, kN (E)	1,401	4,636
		Bending Moment, kN-m (E)	1,386	2,661
		Shear, kN (E)	365	656

^a G: Gravity loads; E: Extreme environmental loads

Table 22: Factored design loads and utilization ratios for the members of the IEC tripod (power production)

IEC Tripod	Diameter (m)	Thickness (m)	Power Production				
			Axial Load, N (kN)	Bending Moment, M (kN-m)	Shear, V (kN)	Utilization Ratio (N+M)	Utilization Ratio (V)
Pile	1.4	0.032	15,900	1,930	998	0.59	0.09
Column (Nominal Section - 6m)	6.0	0.060	5,260	127,000	2,810	0.28	0.03
Column (Bottom End - 3.6m)	3.6	0.036	3,040	29,400	6,990	0.31	0.22
Leg (Pile Sleeve)	1.5	0.015	4,770	900	176	0.40	0.03
Top Brace	1.2	0.030	11,570	3,980	987	0.79	0.11
Middle Brace	1.2	0.020	7,010	872	201	0.51	0.03
Bottom Brace	1.2	0.020	2,720	1,900	504	0.42	0.09

Table 23: Factored design loads and utilization ratios for the members of the IEC tripod (parked/idling)

IEC Tripod	Diameter (m)	Thickness (m)	Parked/Idling (50yr Extreme Environmental Load)				
			Axial Load (kN)	Bending Moment (kN-m)	Shear (kN)	Utilization Ratio (N+M)	Utilization Ratio (V)
Pile	1.4	0.032	17,900	6,650	2,310	0.94	0.21
Column (Nominal Section - 6m)	6.0	0.060	5,260	93,900	6,270	0.21	0.07
Column (Bottom End - 3.6m)	3.6	0.036	3,040	27,300	3,270	0.29	0.10
Leg (Pile Sleeve)	1.5	0.015	4,820	801	122	0.39	0.02
Top Brace	1.2	0.030	11,500	3,560	879	0.74	0.10
Middle Brace	1.2	0.020	7,440	730	176	0.51	0.03
Bottom Brace	1.2	0.020	5,890	2,970	744	0.75	0.13

Table 24: Design loads and utilization ratios for the members of the API tripod (power production)

API Tripod	Diameter (m)	Thickness (m)	Power Production				
			Axial Load (kN)	Bending Moment (kN-m)	Shear (kN)	Utilization Ratio (N+M)	Utilization Ratio (V)
Pile	1.4	0.035	12,100	1,390	738	0.59	0.09
Column (Nominal Section - 6m)	6.0	0.060	4,780	93,900	2,080	0.36	0.03
Column (Bottom End - 3.6m)	3.6	0.036	2,760	21,700	5,182	0.38	0.22
Leg (Pile Sleeve)	1.5	0.015	3,420	648	126	0.44	0.03
Top Brace	1.2	0.030	8,810	2,960	736	0.90	0.12
Middle Brace	1.2	0.020	5,050	637	147	0.54	0.03
Bottom Brace	1.2	0.020	2,130	1,390	365	0.49	0.09

Table 25: Design loads and utilization ratios for the members of the API tripod (parked/idling)

API Tripod	Diameter (m)	Thickness (m)	Parked/Idling (100yr Extreme Environmental Load)				
			Axial Load (kN)	Bending Moment (kN-m)	Shear (kN)	Utilization Ratio (N+M)	Utilization Ratio (V)
Pile	1.4	0.035	16,700	6,090	2,130	0.91	0.18
Column (Nominal Section - 6m)	6.0	0.060	4,780	90,000	5,760	0.26	0.07
Column (Bottom End - 3.6m)	3.6	0.036	2,760	25,800	3,240	0.33	0.10
Leg (Pile Sleeve)	1.5	0.015	4,270	717	105	0.40	0.02
Top Brace	1.2	0.030	10,800	3,320	822	0.79	0.10
Middle Brace	1.2	0.020	7,020	661	155	0.53	0.03
Bottom Brace	1.2	0.020	5,360	2,660	656	0.78	0.12

The maximum member utilization ratios are summarized for the API and IEC tripod designs in Table 26 and Figure 48. In all of the cases, the pile elements were most highly utilized.

Additional combinations of base dimension, number, and size of piles could very likely establish

a configuration for this condition that would be much more optimal and balanced. However, for the purposes of this study, the results provided below illustrate the extent of the difference in API and IEC configurations.

Table 26: Utilization ratio summary

Member Type	IEC Tripod				API Tripod			
	D (m)	t (mm)	Utilization Ratio		D (m)	t (mm)	Utilization Ratio	
			Power Production	Parked / Idling			Power Production	Parked / Idling
Pile	1.4	32	0.59	0.94	1.4	35	0.59	0.91
Column	6.0	60	0.28	0.21	6.0	60	0.36	0.26
Leg (Pile Sleeve)	1.5	15	0.40	0.39	1.5	15	0.38	0.33
Top Brace	1.2	30	0.79	0.74	1.2	30	0.44	0.40
Middle Brace	1.2	20	0.51	0.51	1.2	20	0.90	0.79
Bottom Brace	1.2	20	0.42	0.75	1.2	20	0.54	0.53

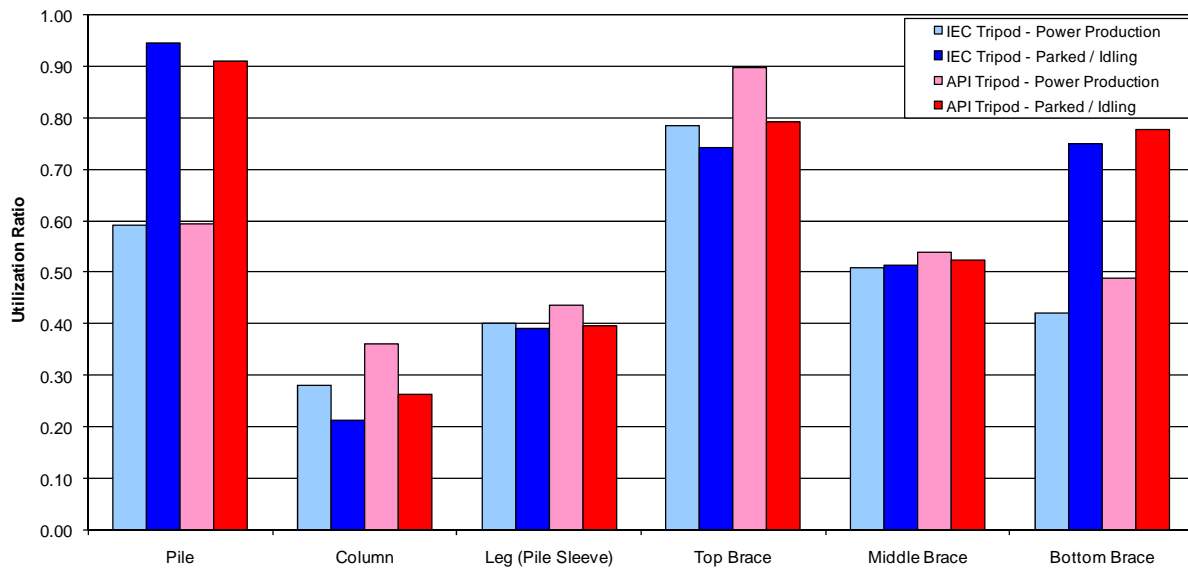


Figure 48: Utilization ratios

All utilization ratios are below 1.0, and most ratios are far below 1.0. The largest ratio is for pile members in parked condition. This implies that factored strength is generally greater than the factored loads in each design code. When weather severity causes ultimate strength failure in the structure, the piles are mostly likely to see the first failure mechanism, given that the piles undergo the greatest stress. The reliability indices for both API and IEC can be expected to come close to the safety levels implicit in these codes, especially for piles where again the utilization ratios are close to 1.

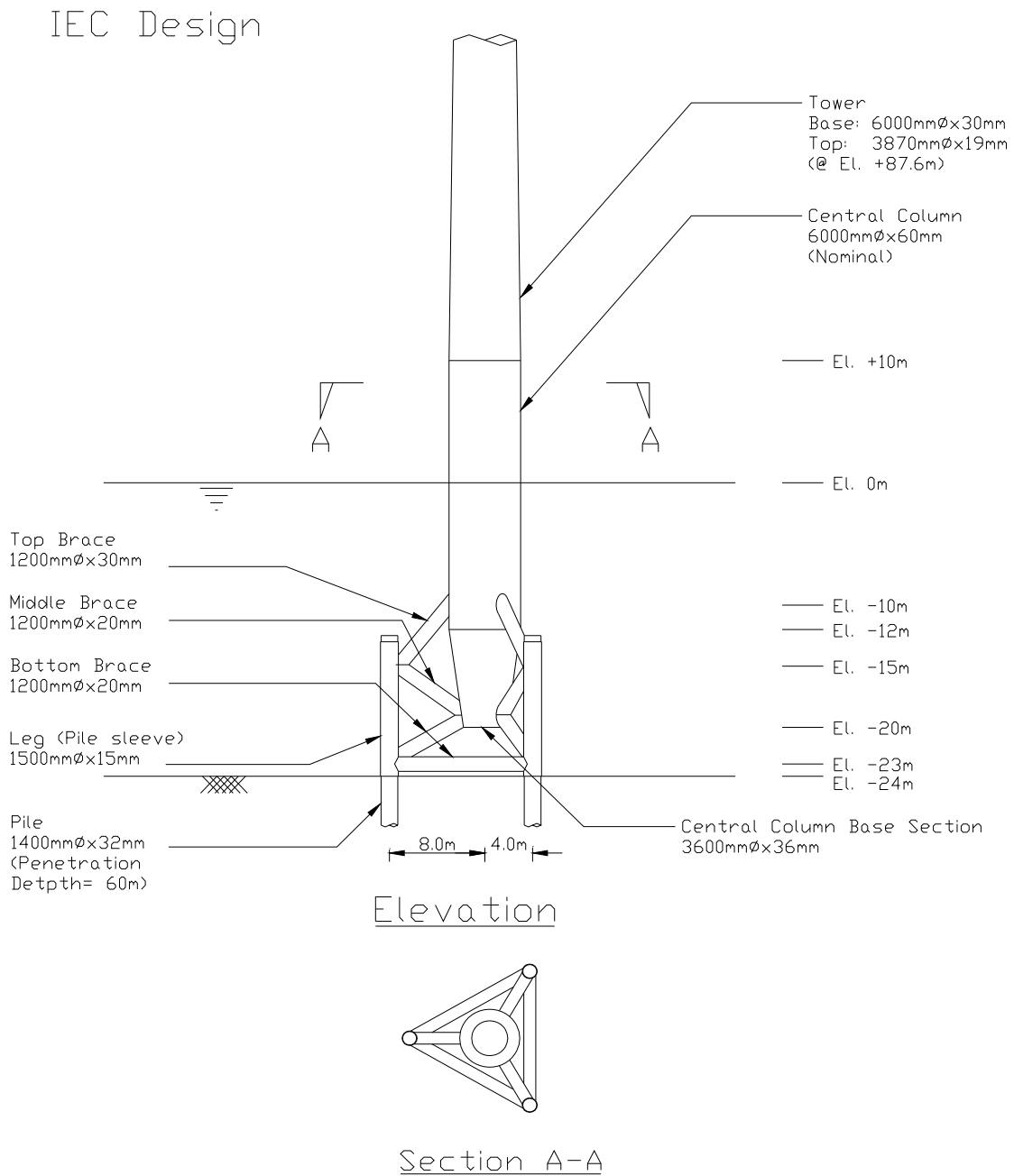


Figure 49: IEC tripod details (final design)

API Design

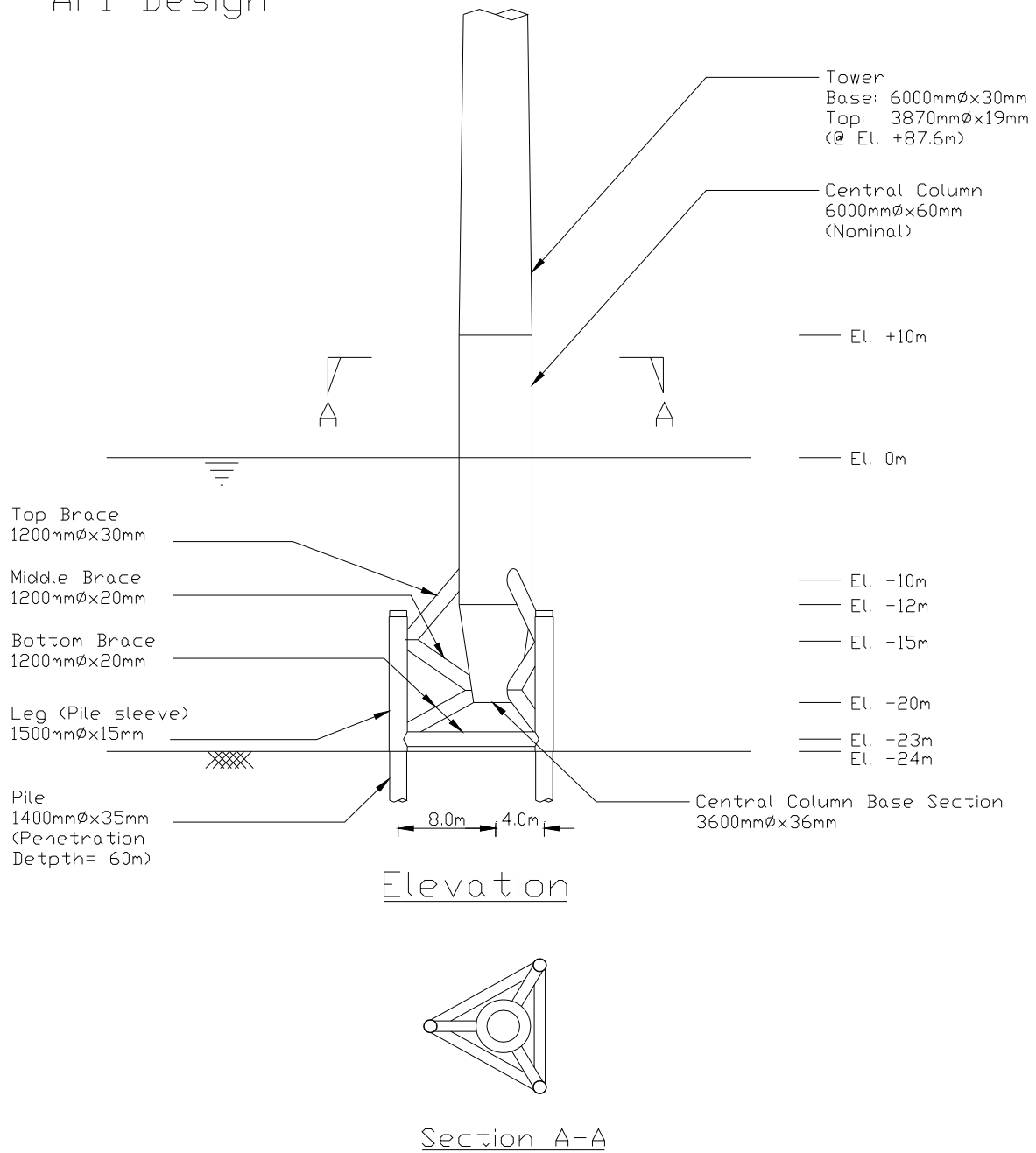


Figure 50: API tripod details (final design)

6.5.5 Capacity Analysis

A nonlinear model of each tripod design was developed using the CAP software and used for a series of lateral pushover analyses. These models included explicitly soil-pile interaction. Figure 51 shows the capacity analysis for the API tripod with the extreme load pattern as an example. The results of these analyses are summarized in Table 27. These analyses indicate that the difference in design is small when measured in terms of ultimate strength. The capacity of the heavier API tripod is only 2% greater than the IEC configuration.

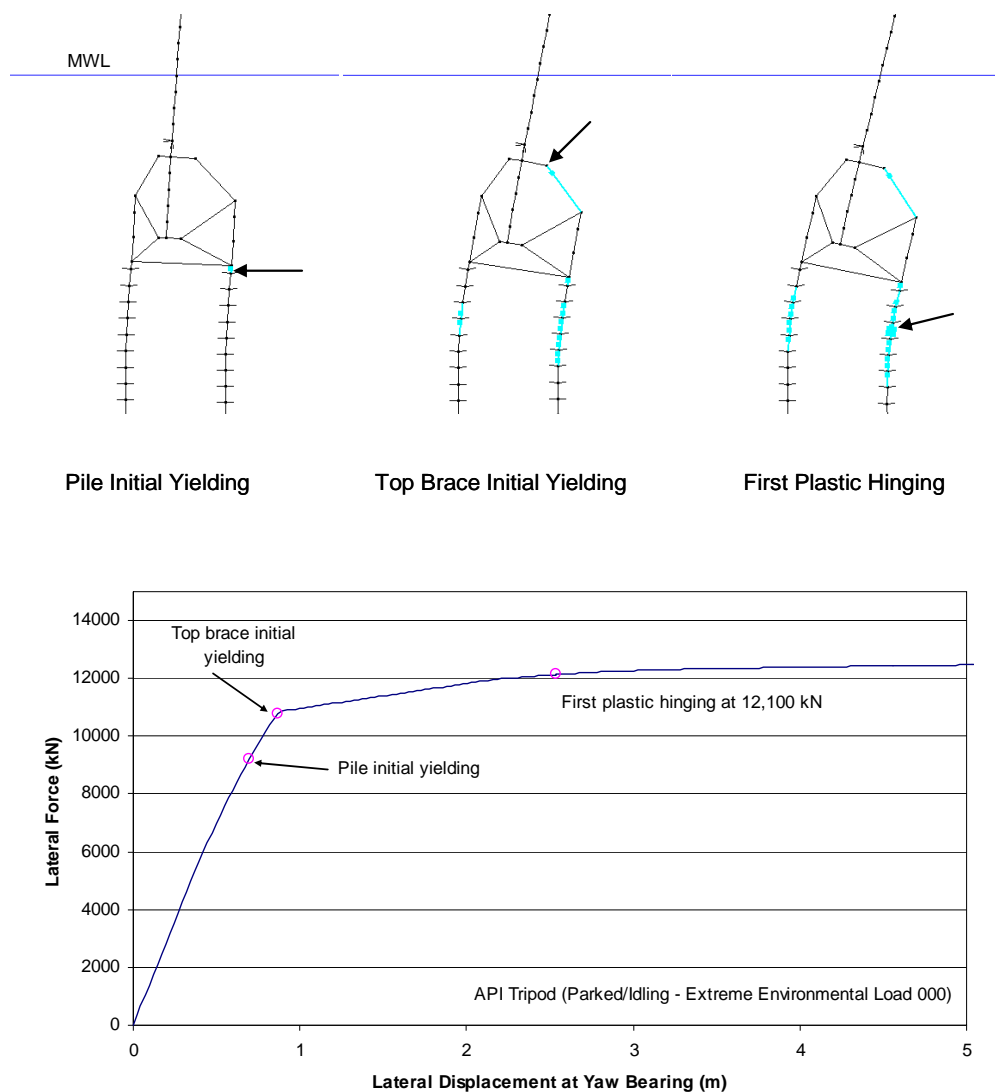


Figure 51: Results of a typical capacity analysis.
(Bottom: load-displacement curve; Top: deflected shape with nonlinear events at important steps.)

Table 27: Capacity analysis results

	IEC Tripod		API Tripod	
	Base Shear (MN)	Base OTM (MN-m)	Base Shear (MN)	Base OTM (MN-m)
Power Production	6.52	384	6.58	388
Parked / Idling	12.3	357	12.1	363

The ratio of the capacity to the design loads provides an initial indication of reliability. Larger ratios imply greater levels of reliability for ultimate strength failure. The ratios for operating cases are about 3.15 and 3.18 for the IEC and API designs, respectively. The IEC capacity to 50-year load ratio is 2.7 and API capacity to 100-year load is 2.1. This is commonly referred to as a Reserve Strength Ratio (RSR). The API ratio is lower than the IEC ratio for the parked case due to the larger load. The ratio of the 100-year load to the 50-year load itself is large, about 1.3, while the capacities of the two designs are essentially the same. This implies that both IEC and API designs could be expected to result in levels of reliability that are higher than what is implicit in each code, given the relatively large reserve strength ratios (a high reserve strength ratio is expected to imply a high reliability, assuming the physics of the load and capacity do not change materially after the 100-year storm condition). A better indication of the reliability levels achieved in each design can be made by comparing the capacities to the same reference load. The IEC and API capacity to 100-year load ratios are both approximately 1.3, indicating similar levels of reliability.

6.5.6 Reliability Analysis

The figures below show the variation of total mudline overturning moment with annual maximum wind speed (Figure 52) and with annual maximum significant wave height (Figure 53 and 55). A comparison of the total load and the resulting capacity for the tripods following API and IEC design guidelines is provided in Figures 56 and 57. The loads are the same for both the tripods since the structure period and the projected areas of the two tripods are similar. However, the API capacity is slightly greater than the IEC capacity so the reliability index for the API design will be slightly greater than that of the IEC design.

The limit state function for the TX site structure is the same as for MA site.

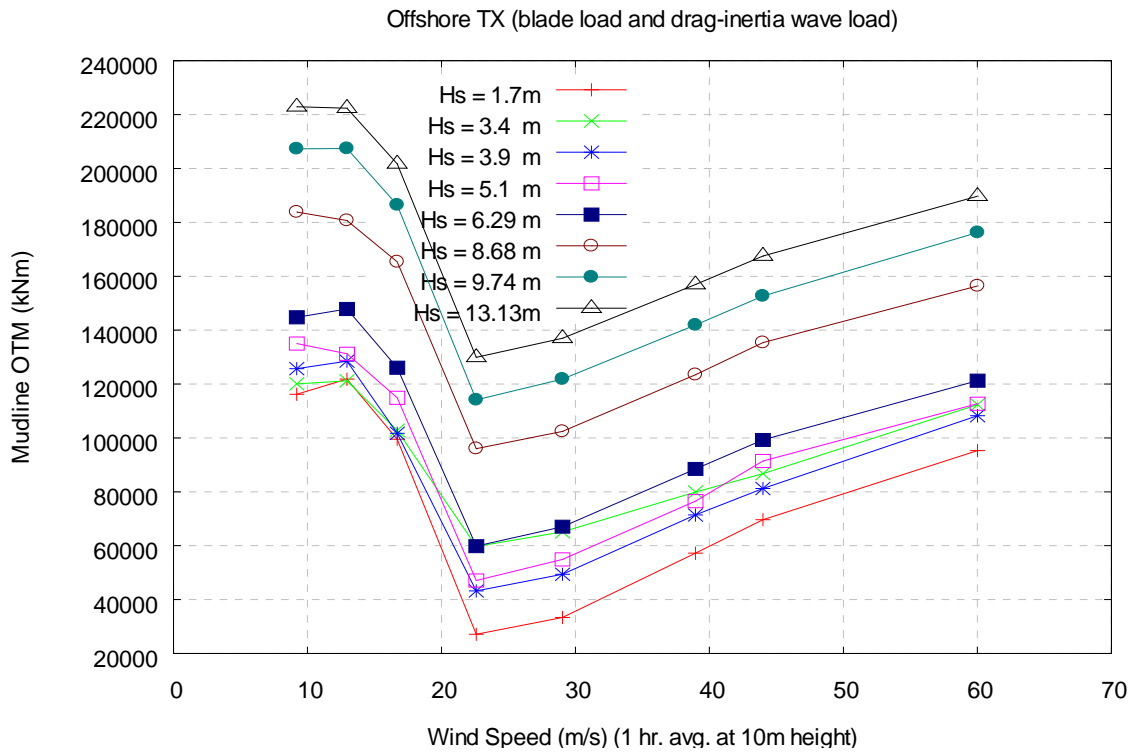


Figure 52: Mudline overturning moment due to aerodynamic wind load and hydrodynamic wave loads. (No breaking wave effect included yet.)

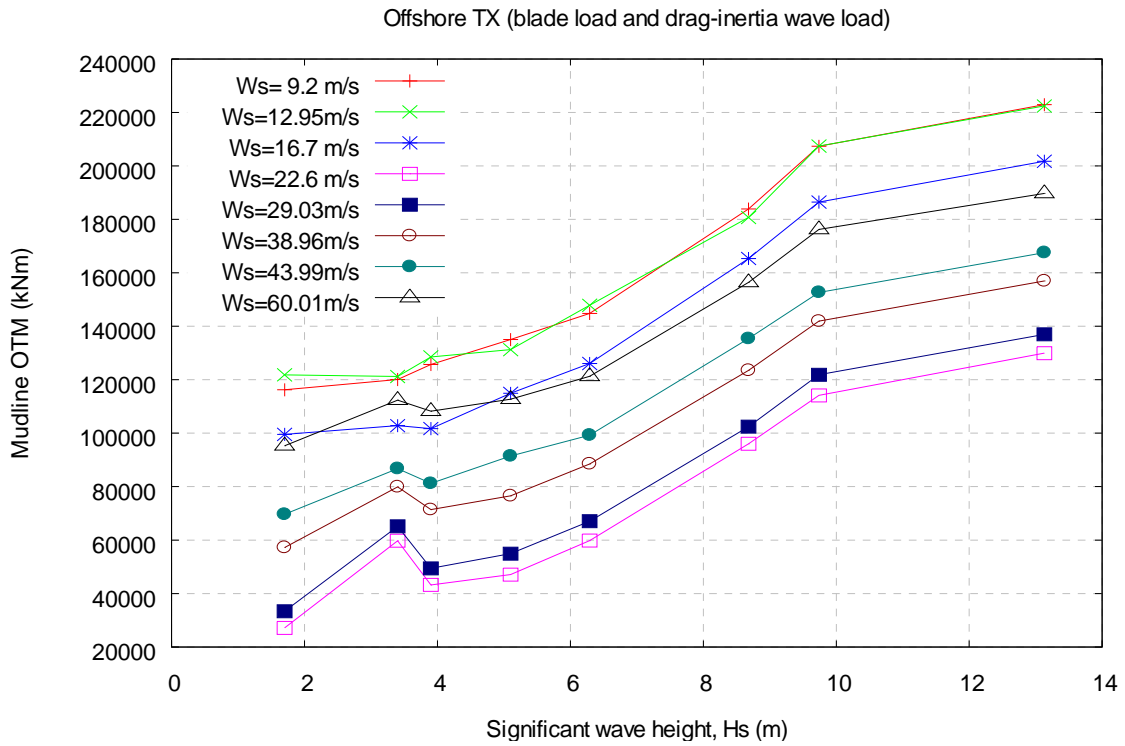


Figure 53: Loads from aerodynamic and hydrodynamic effects (excluding breaking wave effects) vs. Hs

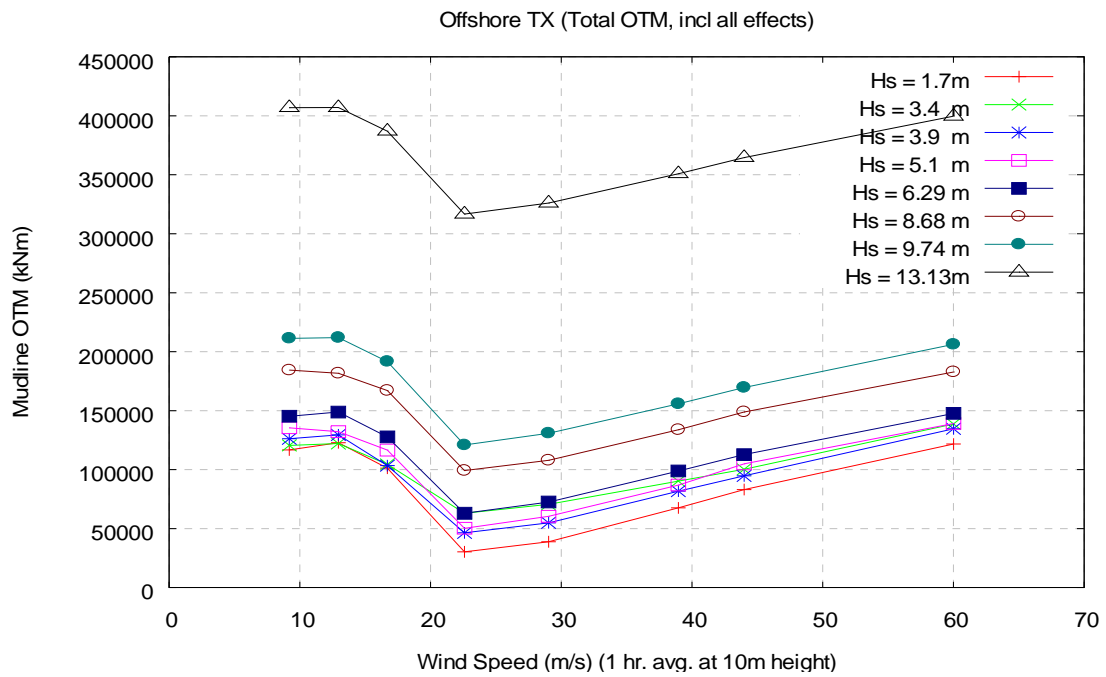


Figure 54: Total load (including all effects) vs wind speed for different Hs values

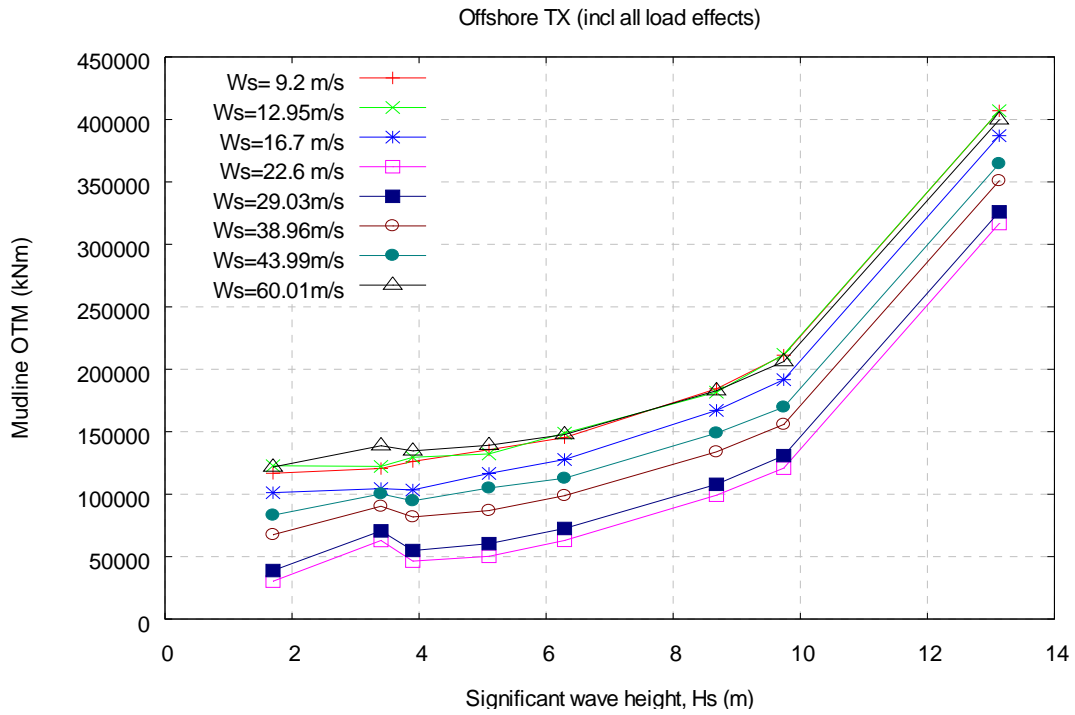


Figure 55: Total load (including all effects) vs Hs for different wind speed values

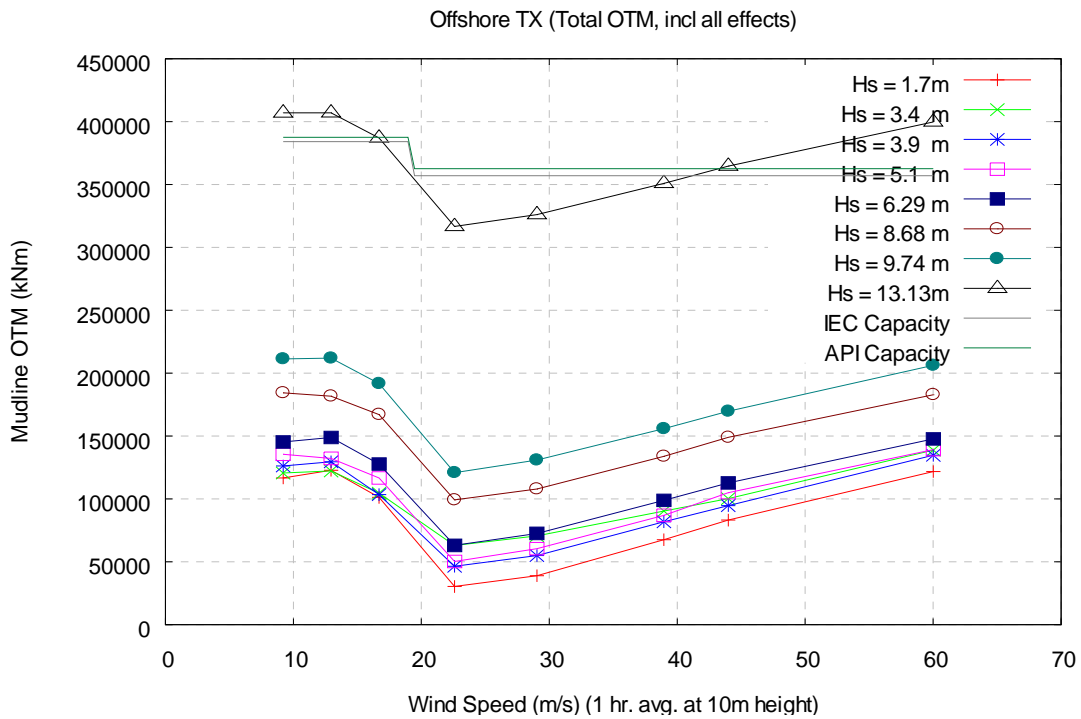


Figure 56: Total load and capacity as a function of wind speed (as reference: $W_{s_{50yr}} \approx 39\text{m/s}$, $W_{s_{100yr}} \approx 44\text{m/s}$)

These figures are meant to show the variation of loads with different combinations of wind speeds and significant wave height. This does not address the likelihood of each W_s and H_s combination. The design codes use the 50-year and the 100-year storms as the basis for design development and these loads are much less than the capacity. The reliability index calculation¹⁵ includes a range of H_s up to the 1000-year value of 13.13m. This is the point at which the load levels come close to ultimate capacity.

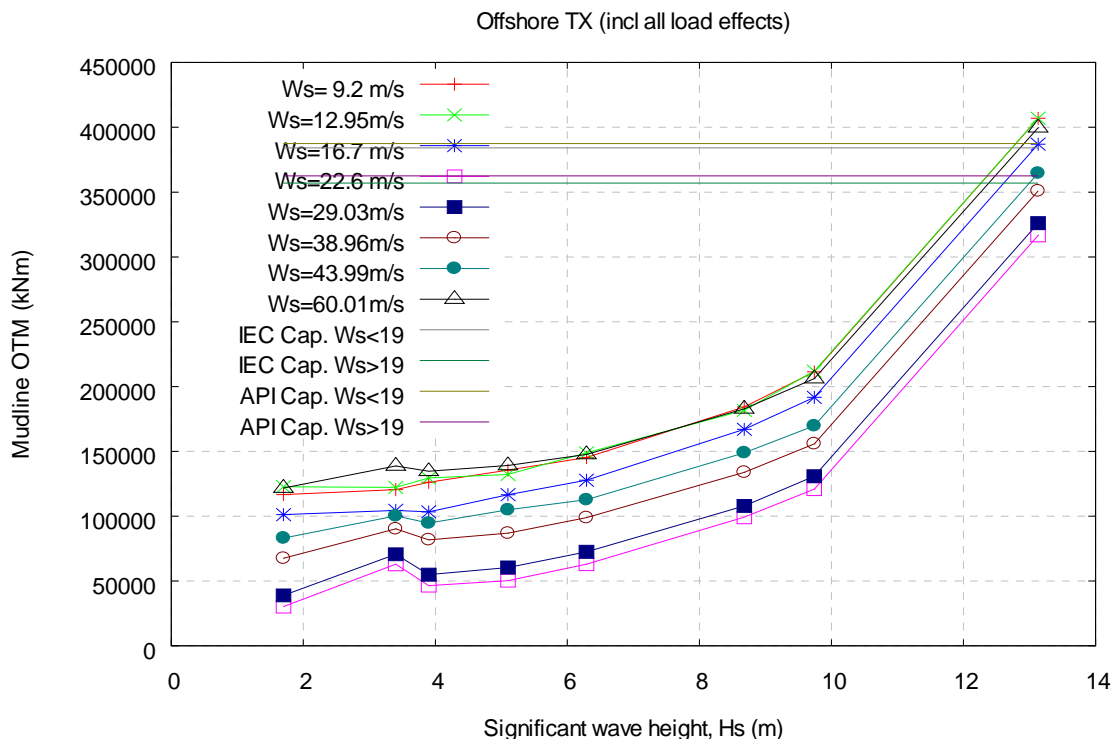


Figure 57: Total load and capacity as a function of H_s (as reference: $H_{s_{50yr}} \approx 8.7m$, $H_{s_{100yr}} \approx 9.74m$)

¹⁵ As additional insight, the pair that corresponds to the 1000-year W_s (60m/s) and the 1000-year H_s (13.13m) is likely to occur in a storm with return period larger than 1000-years. This is due to the correlation between W_s and H_s which is less than 1. A correlation of 1 (100%) would result in the 1000-year storm having the 1000-year W_s value (independent of H_s) and the 1000-year H_s value (independent of W_s). A correlation less than 1 would result in a 1000-year storm having either W_s less than the 1000-year W_s or H_s less than the 1000-year H_s .

Since the capacities of the tripod are closer to the 100-year load than the monopile for the MA site, an addition refinement was included for the TX site to gage whether the ultimate strength failure coming from an operating condition would also contribute materially to the ultimate strength failure from the parked (or extreme metocean) condition. The limit state for operating condition (i.e., up to wind speeds at the blade center of 25 m/s) results in a very high beta value ($\beta > 9$; i.e. $P_f < 10^{-20}$) and does not contribute to the total failure probability. The total failure probability is dictated by the parked condition (extreme environment: i.e., blade center wind speed $> 25\text{m/s}$).

Table 28 includes the reliability index for the two tripods and, as expected, the beta value for the API design is slightly greater than that for the IEC design. The difference in the two beta values is not very significant. The beta values for the TX site are much smaller than that calculated for the MA site. This is due to the greater impact of resonance avoidance on the design of the shallow water monopole and the higher CoV for Ws and Hs for the TX site.

Table 28: Reliability index for tripod for TX site

	β	Prob. of Failure
API	3.32	4.31×10^{-4}
IEC	3.30	4.80×10^{-4}

7.0 SUMMARY AND CONCLUSIONS

This study has included a comparison of API RP-2A (the standard used by the US Minerals Management Service for the regulation of offshore structures in OCS waters) and the IEC 61400-3 (a new standard developed by an international committee specifically to address the design requirements for offshore wind turbine support structures). This review has included a direct comparison of the standards in order to provide an assessment of their applicability to the design of typical wind turbine support structures in U.S. OCS waters.

7.1 KEY FINDINGS

7.1.1 Inherent Safety Level in API and IEC

A study of API and IEC safety factors and design recipe performed for different regions with different metocean variability indicates that the relative safety level generated when using the API or IEC design guidelines depends on the ratio of the 100- to 50-year load. This load ratio is primarily dependent upon the variability in the metocean conditions. For example, the metocean variability for the U.S. OCS regions included in the study appears to be significantly higher than that for the North Sea. As a result, for the U.S. OCS region, the API results in marginally higher safety levels compared to the IEC for a given offshore wind turbine support structure.

The comparison of net safety factors included in the design methods for IEC (50-year) and API (100-year) show that comparable levels of reliability are achieved for a site with metocean variability somewhere between 0.12 (e.g., in North Sea) and 0.25 (e.g., Gulf of Mexico region). In other words, API appears to result in higher reliability than IEC for sites with a metocean coefficient of variation greater than 0.25. For sites with coefficient of variation smaller than 0.12, the IEC appears to result in a higher reliability than API; this is due to the effects of the safety factors in combination with the design storm used in IEC (50-year) versus the API (100-year storm). From a safety standpoint, both codes can be calibrated with appropriate safety factors with either starting point (i.e. either 50-year or 100-year metocean conditions) in order to achieve a predetermined target safety level for offshore wind turbines.

7.1.2 Effect of Period of Vibration Requirements

This study has determined that period of vibration requirements that are specified by most turbine manufacturers to avoid accelerated fatigue will dominate the design requirements for most conditions, especially for monopiles. As a result of this requirement, the difference in the design criteria that is specified within the API and IEC guidelines for extreme storm loading conditions (i.e., 50-year versus 100-year) is irrelevant for these typical conditions. The section properties that are required to ensure resonance-avoidance result in high ultimate strength capacity. This results in high reliability indices for both API and IEC designs. In this case, the difference in the API and IEC indices are irrelevant given that they are both high compared to safety levels suggested by each code.

7.1.3 Effect of Operating versus Extreme Load Conditions

In protected areas that are not subject to extreme wave loading conditions, resonance-avoidance is still likely to be the dominant driver for support structure design. The next important parameter governing design would be wind load demands associated with the power generation or operating load conditions. In this situation, the difference in the design criteria that is specified within the API and IEC standards for extreme storm loading conditions is irrelevant for all types of support structures. When safety levels are compared, the API designs result in marginally higher reliability than the IEC designs, since the net safety factor for API is higher than IEC for operating case.

7.1.4 Effect of Breaking Waves

In shallow water sites, the breaking wave limit may restrict wave heights to the point where both the 50- and 100-year conditions are represented with similar breaking wave conditions (once breaking happens, the slam loads become a dominant contributor to the total loads). In this situation, the difference in the design criteria specified within the API and IEC standards for extreme storm loading conditions is predominantly limited to the difference in wind speeds in a 100-year and a 50-year storm, respectively (wind load varies approximately as the square of the wind speed).

An additional complexity associated with breaking waves is the uncertainty of calculating wave slam forces, which can have a substantial impact on structure design. These problems become further complicated for larger monopile structures that are dominated by wave inertia forces.

7.1.5 Regional Reliability Comparison

The potential for very severe wind speeds and wave heights associated with tropical storms in the Gulf Region and also for the Northeast impacts the level of reliability for offshore structures, regardless of reference level storm condition that is adopted for design. In these locations, a greater safety factor will be required to establish the same level of performance that can be achieved in areas not subject to tropical storms. This additional margin can be established with the use of larger factors of safety for strength or load, with either the 50-year or the 100-year storm as the basis for the load factors. The selection of the best means to achieve consistent reliability across different regions depends on the format of the design guideline that is adopted.

7.2 RECOMMENDATIONS

The study demonstrates that comparison of the reliability levels achieved with the IEC and API guidelines depends on a number of factors. There is no single approach using either the existing form of IEC or API that will result in a consistent reliability index for all conditions of offshore wind farm development in the U.S. OCS region. The study has shown that either guideline can be modified to achieve a target level of reliability and that factors such as metocean variability can be accommodated with adjustments to load and/or resistance factors.

We recommend that the U.S. wind industry address the definition of a minimum acceptable reliability index. This index can be defined either on an absolute basis (e.g., $\beta = 3.5$ or 4) or by means of comparison (e.g., following the API philosophy for oil and gas platforms in the Gulf of Mexico). This definition would allow for the calibration of either an IEC or API approach to offshore wind support structures that would address the variation of key factors across all areas in the U.S. OCS region. Such an approach would define load factors or factors of safety for metocean variability, tropical storm hazard, operating conditions, water depth, breaking waves, etc. on the reliability index to achieve a uniform safety level for all conditions in the U.S. OCS region.

The IEC provides guidance specific to offshore wind turbine support structures that is not addressed in API. This more comprehensive design basis must be addressed in any design guideline adopted in the U.S.

Lastly, the study shows that there are several areas associated with the definition of loading that are critical to the design of the support structure and are subject to significant variability. The methods used for the calculation of wave slam forces, for example, specifically requires further study to improve the overall level of reliability in offshore wind turbine support structure design.

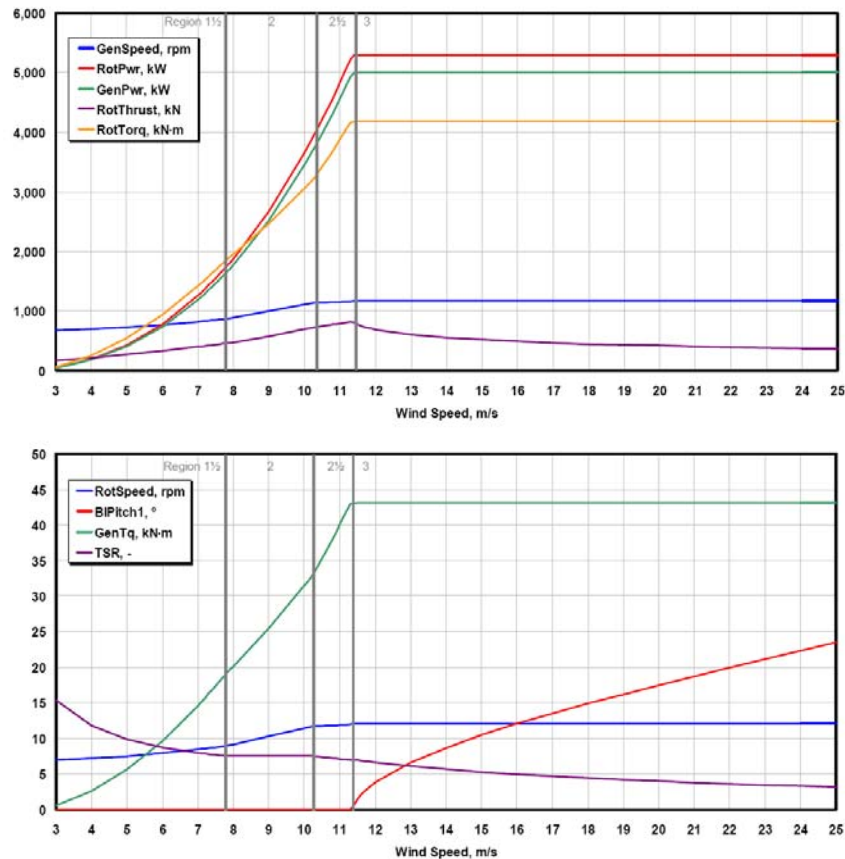
REFERENCES

1. American Petroleum Institute (API), Recommended Practice for Planning, Designing and Constructing Fixed Offshore Platforms – Working Stress Design, API RP-2A-WSD, 21st Edition 2000.
2. International Electrotechnical Commission (IEC), IEC 61400-3 Ed.1, Wind Turbines – Part 3: Design requirements of offshore wind turbines, IEC TC 88 WG3 Committee Draft, December 2005.
3. International Electrotechnical Commission (IEC), IEC 61400-1 Ed.3, Wind Turbines – Part 1: Design requirements, August 2005.
4. Det Norske Veritas (DNV), Design of offshore wind turbine structures, Offshore Standard, DNV-OS-J101, Oslo, Norway, 1st Edition, 2004
5. Germanischer Lloyd (GL), Guideline for the certification of offshore wind turbines, Hamburg Germany, 2nd Edition 2005.
6. International Standardization Organization (ISO), “Petroleum and Natural Gas Industries – Fixed Steel Offshore Structures,” 2004, ISO/DIS 19902, ISO Central Secretariat, Geneva.
7. Tarp-Johansen, N. J., “*Partial safety factors and characteristic values for combined extreme wind and wave load effects,*” Journal of Solar Energy Engineering (2005), 127:242-252.
8. Tarp-Johansen, N. J., Manwell, J.F. and McGowan, J., “*Application of Design Standards to the Design of Offshore Wind Turbines in the U.S.*”, Offshore Technology conference, Houston, Texas May 2006.
9. Der Kiureghian, A., T. Haukaas and K. Fujimura, “*Structural reliability software at the University of California, Berkeley,*” Structural Safety, 28:44-67, 2006.
10. Jonkman, J. Dynamics Modeling and Loads Analysis of an Offshore Floating Turbine, National Renewable Energy Laboratory, Technical Report NREL/TP-500-41958, November 2007.

11. Argyriadis, K., Gill, L. and Schwartz, S., “*Loads for offshore wind turbines; the 2nd edition of the GL wind guideline*”, 2004
12. Clausen, N-E, A. Candelaria, S. Gjerding, S. Hernando, P. Nørgård, S. Ott, N-J Tarp-Johansen. “*Wind farms in regions exposed to tropical cyclones,*” European Wind Energy Conference, Milan, 7-10 May 2007
13. “*Component-Based Calibration of North West European Annex Environmental Load Factor to ISO Fixed Steel Offshore Structures Code 19902,*” 2002, Bomel Ltd, Maidenhead, UK.

APPENDIX A: STEADY-STATE RESPONSE OF THE NREL 5MW BASELINE WIND TURBINE

The steady-state response of the NREL 5MW Baseline Wind Turbine, used in this study, is specified in NREL/TP-500-41958 [10] as follows:



- GenSpeed: The rotational speed of the generator (high-speed shaft).
- RotPwr and GenPwr: The mechanical power within the rotor and the electrical output of the generator, respectively.
- RotThrust: The rotor thrust.
- RotTorq: The mechanical torque in the low-speed shaft.
- RotSpeed: The rotational speed of the rotor (low-speed shaft).
- BIPitch1: The pitch angle of Blade 1.
- GenTq: The electrical torque of the generator.
- TSR: The tip-speed ratio

APPENDIX B: DRAG AND INERTIA COEFFICIENTS FOR LARGE DIAMETER TURBINE COMPONENTS

The calculations below are performed using the approach outlined in API RP2A Section C2.3.1.b7.

Monopile at Site 1 (Offshore Massachusetts):

Monopile diameter= 6m

Assumptions:

- 15m water depth
- 1m surge
- 10-m wave height with 10s period
- 0.1m/s uniform current
- Above high-tide level (smooth), average peak-to-valley height of hard growth, $k = 0.05\text{mm}$; relative surface roughness, $e = k/D = 0.05\text{E-}3 \text{ m} / 6\text{m} = 8\text{E-}6$

Maximum water particle velocity normal to the cylinder axis, $U_m = 8.7 \text{ m/s}$

Wave period, $T = 10\text{s}$

Keulegan-Carpenter Number, $K = U_m T / D = 8.7 \times 10 / 6 = 14.5$

Below high-tide level (rough surface drag and inertia):

$C_{ds} = 1.0$

$K / C_{ds} = 14.5 / 1.0 = 14.5 \rightarrow C_d / C_{ds} = 1.45$ (Figure C2.3.1-5)

$C_d = 1.45 \times 1.0 = 1.45$

$K / C_{ds} = 14.5 \rightarrow C_m = 1.4$ (Figure C2.3.1-8, “rough” curve)

Above high-tide level (smooth):

$$e=8E-6 \rightarrow C_{ds} = 0.62 \text{ (Figure C2.3.1-4)}$$

$$K/C_{ds} = 14.5 / 0.62 = 23.3 \rightarrow C_d/C_{ds} = 1.25 \text{ (Figure C2.3.1-5)}$$

$$C_d = 1.25 \times 0.62 = 0.78$$

$$K/C_{ds} = 23.3 \rightarrow C_m = 1.6 \text{ (Figure C2.3.1-8, "smooth" curve)}$$

Summary:

	Rough	Smooth
C_d	1.45	0.78
C_m	1.4	1.6

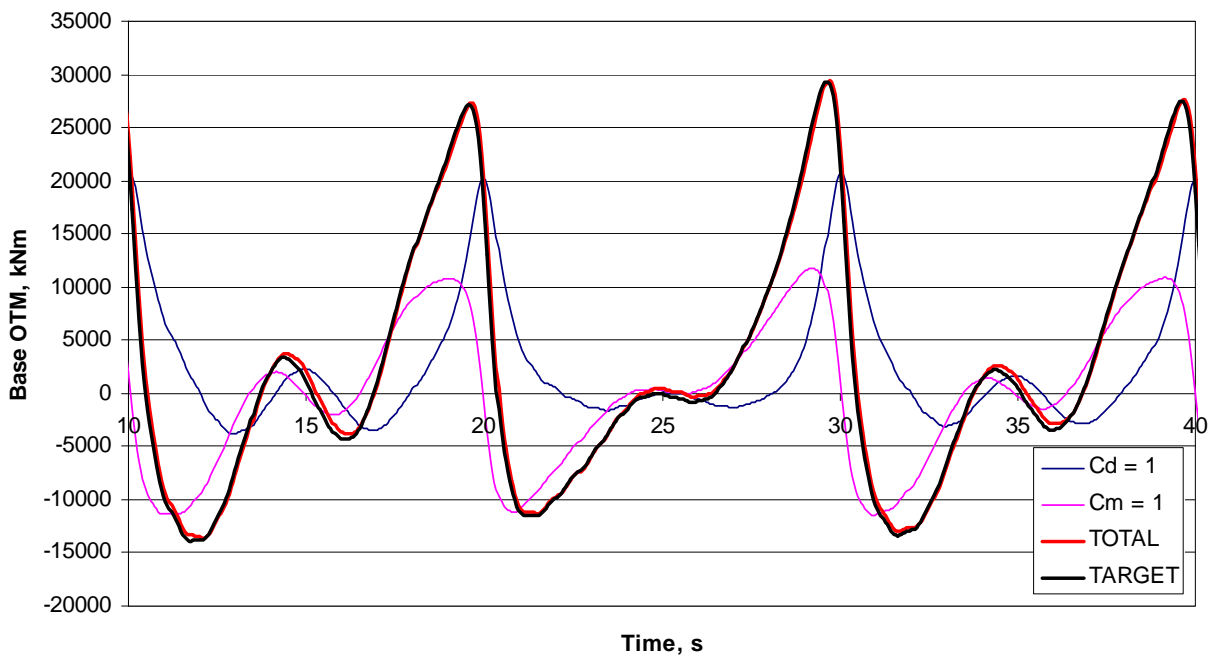
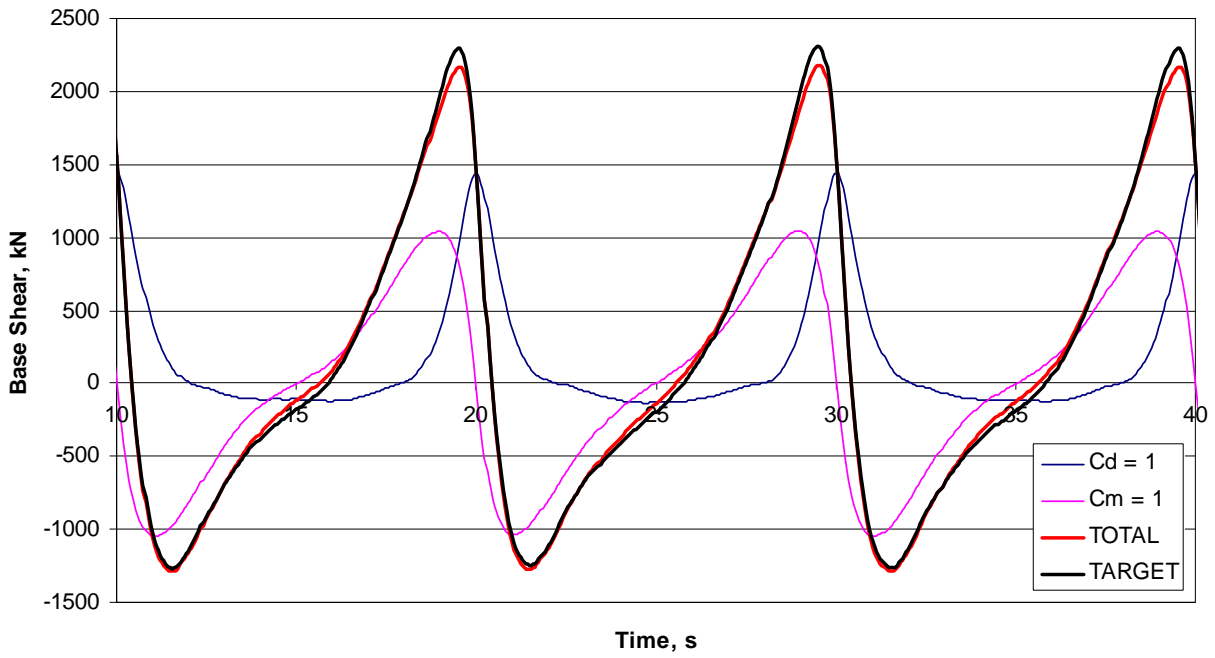
Equivalent Monopile Properties for FAST Analyses:

A wave analysis (with 10-m wave with 10s period) was performed in CAP using a model of a 6-m monopile with the actual C_d/C_m values calculated above per API RP2A. The total base shear and the overturning moment histories are shown in the figures below as “target”. Then the wave analysis was repeated for “ $C_d=1.0$; $C_m=0$ ” and “ $C_d=0$; $C_m=1.0$ ” cases. The results of these analyses are shown in the plots with the blue and the pink curves. The equivalent monopile with uniform properties was estimated to match the base shear and overturning moment histories. The unit C_d and the unit C_m analyses were added to each other in various proportions until the total overturning moment matched the target curve. The best result was obtained for $1.05C_d + 1.43C_m$ case (shown in the plots below). The maximum overturning moment was matched 100%. The maximum base shear is 5.6% below the target.

As a result, the drag and inertia coefficients that are applicable to the equivalent monopile analyses with FAST analyses are as follows:

$$C_d = 1.05$$

$$C_m = 1.43$$



Tripod at Site 2 (Offshore Texas):

Central column diameter= 6m

Assumptions:

- 25m water depth
- 1.5m surge
- 15.4-m wave with 10.8s period
- 1m/s uniform current
- Above high-tide level (smooth), average peak-to-valley height of hard growth, $k = 0.05\text{mm}$; relative surface roughness, $e = k/D = 0.05\text{E-}3 \text{ m} / 6\text{m} = 8\text{E-}6$

Maximum water particle velocity normal to the cylinder axis, $U_m = 11.6 \text{ m/s}$

Wave period, $T = 10.8\text{s}$

Keulegan-Carpenter Number, $K = U_m T / D = 11.6 \times 10.8 / 6 = 21$

Below high-tide level (rough):

$$C_{ds} = 1.0$$

$$K/C_{ds} = 21 / 1.0 = 21 \rightarrow C_d/C_{ds} = 1.28 \text{ (Figure C2.3.1-5)}$$

$$C_d = 1.28 \times 1.0 = 1.28$$

$$K/C_{ds} = 21 \rightarrow C_m = 1.2 \text{ (Figure C2.3.1-8, "rough" curve)}$$

Above high-tide level (smooth):

$$e = 8\text{E-}6 \rightarrow C_{ds} = 0.62 \text{ (Figure C2.3.1-4)}$$

$$K/C_{ds} = 21 / 0.62 = 34 \rightarrow C_d/C_{ds} = 1.1 \text{ (Figure C2.3.1-5)}$$

$$C_d = 1.1 \times 0.62 = 0.68$$

$K/C_{ds} = 34 \rightarrow C_m = 1.6$ (Figure C2.3.1-8, “smooth” curve)

Summary:

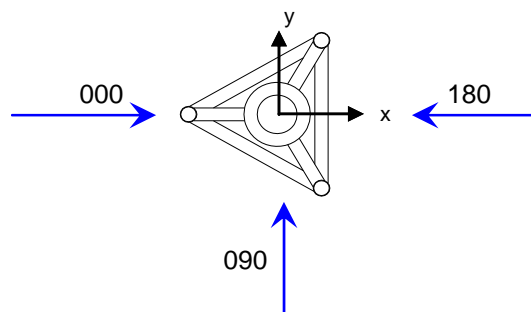
	Rough	Smooth
C_d	1.28	0.68
C_m	1.2	1.6

Equivalent Monopile Properties for FAST Analyses:

Three wave analyses (15.4-m wave with 10.8s period) were performed in CAP using the tripod model with the following C_d/C_m values:

- Below high-tide level (Rough): $C_d= 1.28$; $C_m= 1.2$
- Above high-tide level (Smooth): $C_d= 0.68$; $C_m= 1.6$
- Legs and arms (Rough): $C_d= 1.05$; $C_m= 1.2$

Given the structure is not axis-symmetric, the wave analyses were run in three wave-heading directions (0, 90, 180 degree from x-axis).



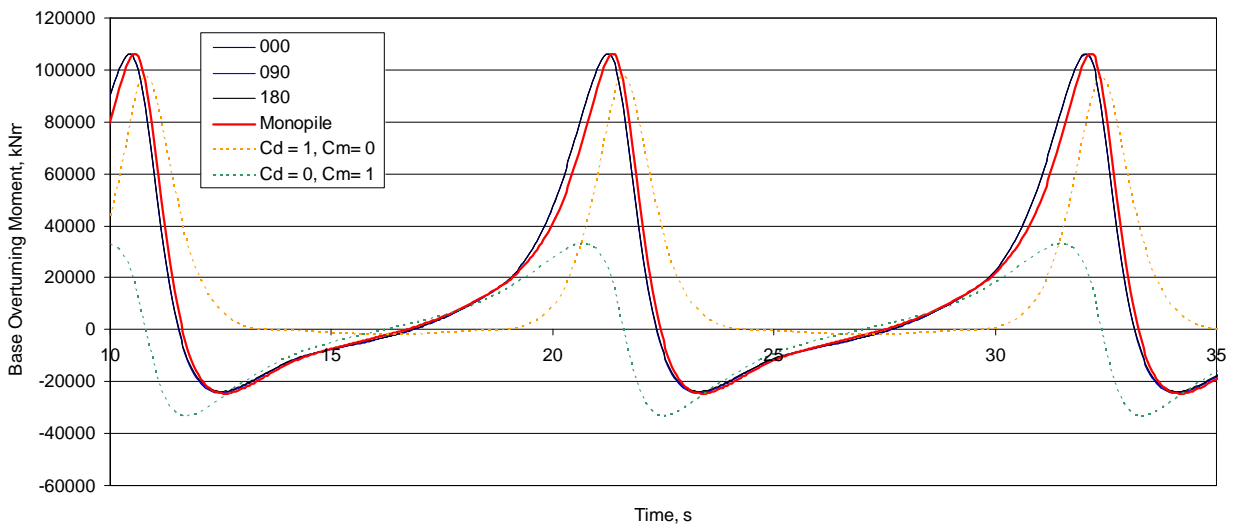
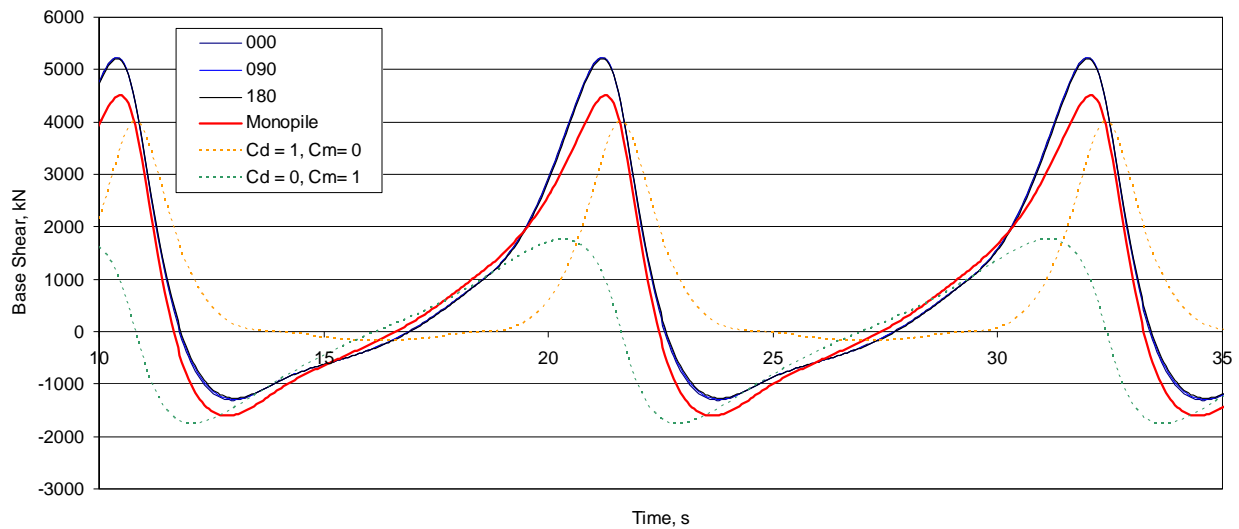
The total base shear and the overturning moment histories are shown in the figures below. Then the wave analysis was repeated with a 6-m monopile model for “ $C_d=1.0$; $C_m= 0$ ” and “ $C_d= 0$; $C_m=1.0$ ” cases. The results of these analyses are shown in the plots with the yellow and the orange curves. The equivalent monopile with uniform properties was estimated to match the base shear and overturning moment histories. The unit C_d and the unit C_m analyses were added to each other in various proportions until the total overturning moment matched the target curve. The

best result was obtained for $0.98C_d + 1.18C_m$ case (shown in the plots below). The maximum overturning moment was matched 100%. The maximum base shear is 13.8% below the target.

As a result, the drag and inertia coefficients that are applicable to the equivalent monopile analyses with FAST analyses are as follows:

$$C_d = 0.98$$

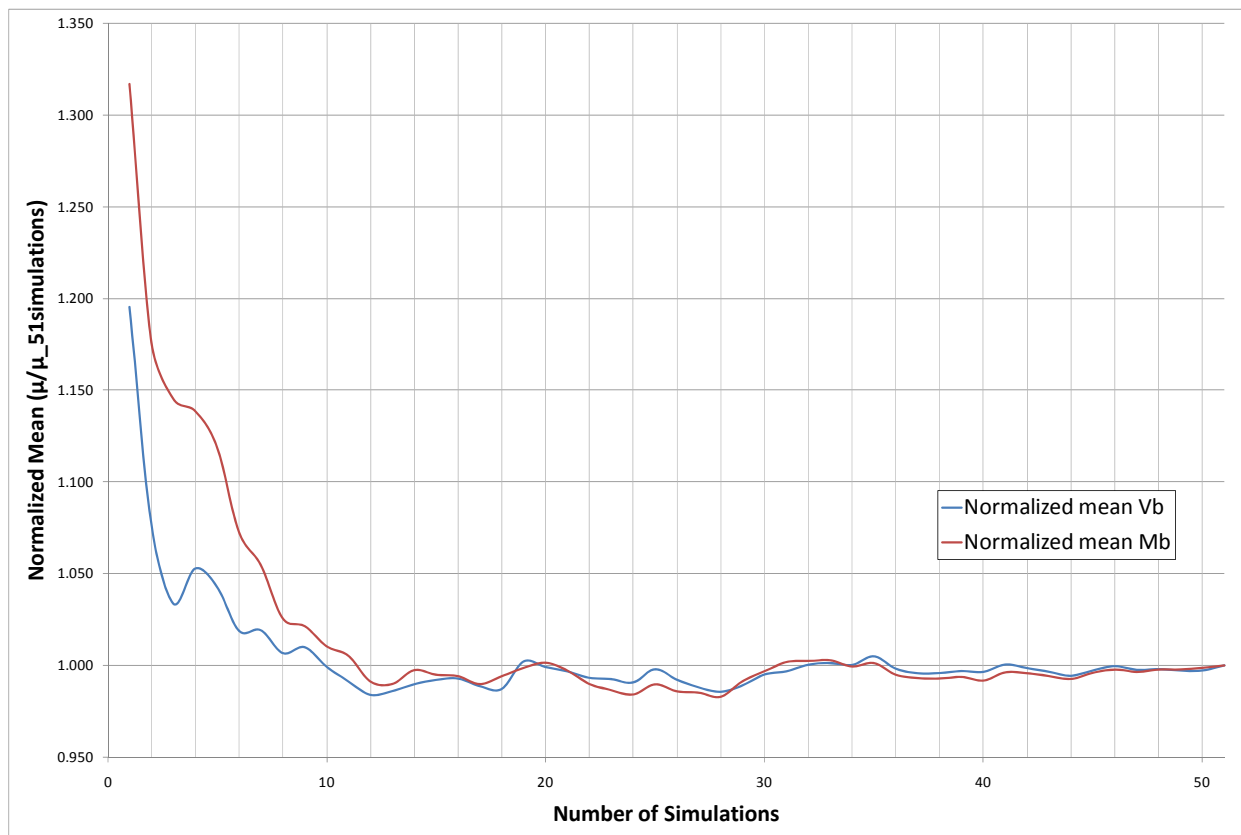
$$C_m = 1.18$$



APPENDIX C: STUDY ON THE SENSITIVITY OF LOAD ANALYSIS RESULTS TO THE NUMBER OF SIMULATIONS

The coupled wave and wind load analysis was performed for a number of simulations due to the stochastic nature of the turbulent wind load. For each simulation the maximum shear force and overturning moment were obtained throughout the time-history. The mean of these maximum values were used for the reliability assessment of the structure.

This study was performed to assess the number of simulations necessary in order to obtain a satisfactory convergence on the mean of maximum base shear and overturning moment. A total of 51 simulations were performed. The mean of the maximum base shear and overturning moment were calculated. Figure below shows the convergence of the mean of each component as more simulations were used in the analysis. It was observed that using 10 simulations gives an estimate within 2% of the mean when 51 simulations.



APPENDIX D: COMPARISON OF API AND IEC GUIDELINES

This appendix presents a comparison of the relevant sections of API and IEC guidelines that pertain to this study on offshore wind turbines. Sections on earthquake and ice loads, for example, are not relevant for this study and are not included in this appendix.

D.1 ENVIRONMENTAL CRITERIA AND PERFORMANCE REQUIREMENTS

In the direct comparison below, the external conditions used for calculating loads specified by the API and IEC standards are compared.

D.1.1 Wind

Table 29: API and IEC standards for wind

	API	IEC
Shear profile	Logarithmic	Power Law
Turbulence spectrum	1 dimensional spectrum given, site specific spectrum may be used	Various 3 dimensional spectra specified.
Gust specification	Stochastic	Stochastic and deterministic

D.1.2 Sea State

Table 30: API and IEC standards for sea state

	API	IEC
Storm return period	100 years, plus less severe storms (less than 5 years) for operational loads	50 years, plus 1 year for use with fault cases
Breaking waves	No guidance	Spilling and plunging. Informative annex suggests calculation method.
Wave period	The period associated with desired storm required for ultimate strength	Loads must be calculated using a range of possible periods
Apparent wave period	Doppler effect must be considered	No consideration specified
Current profiles	Tidal, circulation, and storm	Tidal, wind and surf-generated
Tides	Only extreme storm tides considered	Extreme tides considered in some load cases, normal water level range used in others

D.2 DIRECT COMPARISON BY TOPIC

Taking the API standard section by section, any equivalent guidance in the IEC standard has been identified and its section number recorded in the Tables below. If the two standards gave similar requirements, this was recorded below by “*No difference noted.*” If no equivalent guidance could be found in the IEC, then “*Not included*” was entered instead of an IEC section number, unless it was considered that the guidance was not relevant in the context of a wind turbine specific standard where *N/A* is entered. Guidance given by the IEC which was either not given by API or for which no relevant API section exists was described in the most relevant section of the Tables below.

D.2.1 Planning

The API standard allows for a wider variety of structure than the IEC, and as a result there are many subsections under Planning that are omitted from the IEC. As an example, “Spillage and Contamination” is not addressed by the wind turbine design standard.

Environmental considerations are approached in a different manner by the two standards. The IEC 61400-1 standard specifies sets of generic wind conditions (“classes”), which can be used to specify the wind speed and turbulence parameters; however, the metocean and sea-bed parameters are required to be site specific. To determine the site specific wind conditions, the IEC standard prescribes in more detail how the data should be determined, and refers to wind industry practice (e.g. referring wind speed to hub height).

The API standard gives more detail than the IEC standard in describing the establishment of projected extreme climate; however it does not reflect specific metocean requirements for wind turbine design. The design load cases used in the IEC standard make use of specific return periods to accompany specific turbine operating conditions. It is considered overly conservative to assume that turbine fault conditions occur simultaneously with 50-year storm conditions; instead, the 1-year storm conditions are used for these load cases. Similar principles underly the differences between the tidal considerations of the standards: different load cases are based on different tidal ranges.

Table 31: API and IEC comparison (planning)

API Section	Corresponding IEC Section	Comments on IEC	Comments on API
<i>1. Planning</i>			
1.1.3 Codes and Standards	1.2	No difference noted	
1.2.1 Function	N/A		
1.2.2 Location	12.1 AA	No difference noted	
1.2.3 Orientation	N/A		
1.2.4 Water Depth	12.2 , 6.1.3	No difference noted	
1.2.5 Access and Auxiliary Systems	14.1 ,14.2	No difference noted	
1.2.6 Fire Protection	14.2	Requirement for personnel only	Requirement for personnel and possible destruction of equipment
1.2.7 Deck Elevation	7.3.4 , 14.2	No difference noted	
1.2.8 Wells	N/A		
1.2.9 Equipment and Material Layouts	N/A		
1.2.10 Personnel and Material Handling	Not included		
1.2.11 Spillage and Contamination	Not included		

API Section	Corresponding IEC Section	Comments on IEC	Comments on API
1.3 Environmental Considerations			
1.3.1 General Meteorological and Oceanographic Considerations	6	Electrical conditions included	The estimated reliability resource of all data should be noted
1.3.2 Winds	12.3	Wind turbine classes used for rotor and nacelle.	
		Additionally, the following values should be estimated: ambient turbulence intensity , wind shear , density	The spectrum of wind speed fluctuations about the average should be specified in some instances
		All parameters, except air density, shall be available as functions of wind direction, given as 1-min averages. Reference height is always hub height.	Wind data should be adjusted to a standard elevation, such as 33feet (10m) above mean sea level, with a specified averaging period time, such as one hour.
		Conversion table between averaging periods provided	
1.3.3 Waves	6.1.1 , 12.4	The following parameters shall be estimated: significant wave height with a recurrence period of 50 year, and 1 year. Extreme wave height with a recurrence period of 50 years and 1 year, reduced individual wave height with a recurrence period of 50 years	
		No seasonal variation information required	For normal conditions: data required for each month and season.
			For extreme: the nature, date, and place of the events which produced the historical sea-states used in the development of the projected values should be developed.

API Section	Corresponding IEC Section	Comments on IEC	Comments on API
1.3.4 Tides	6.1.3.2 / 12.6	Normal Water Level Range used with Severe Sea State/Severe Wave Height	Storm tide used with storm waves
		Extreme Water Level Range used with 50-year Sea State/Wave Height	
1.3.5 Currents	6.1.2/12.5	No difference noted	
1.3.8 Marine Growth	6.1.5 , 12.8	IEC refers to ISO 19901-1 for detailed guidance	Detailed guidance provided
1.4 Site Investigation – Foundations	12.15	No difference noted	

D.2.2 Design Criteria

The turbine specific nature of the IEC 61400 standard differs significantly from the API. The IEC approach is built around a specification of many Design Load Cases. In the API standard, there is a distinction between live loads and dead loads that does not easily translate into wind turbine design, since the operating loads are derived from the environmental forces (lift and drag on the blades.)

The API standard neatly separates a static wave analysis from a linear, stochastic, dynamic one. However, a combination of the two is required by the IEC. Structurally dynamic simulations are required, but non-linear wave kinematics must also be accounted for. Various approaches are outlined in annex D.6. Nonetheless, some direct comparisons can be made; the use of non-linear regular wave models is broadly similar, however differences are identified below. For example, the IEC requirement to consider the worst case wavelength adds extra conservatism. There are also some differences in structural modeling assumptions (damping and modal frequencies.)

The models of wind shear and turbulence spectra recommended by the two standards are fundamentally different, so no direct comparison can be made. Differences are also noted in current models, ice models and metocean criteria.

Table 32: API and IEC comparison (design criteria)

API Section	Corresponding IEC Section	Unique to IEC	Unique to API
<i>2.Design Criteria and Procedures</i>			
2.1.1 Dimension System	Not included		
2.1.2.b Dead Loads	7.3	No difference noted	
2.1.2.c Live Loads	7.4.8	No difference noted	
2.1.2.d Environmental Loads	7.3 (11)	Earth movement only included in foundation design	
2.1.2.e Construction Loads	7.4.8	No difference noted	
2.1.2.f Removal and reinstallation Loads	Not included		
2.1.2.g Dynamic Loads	7.3	No difference noted	
2.2.2 Design Loading Conditions	7.4	Replaced by load case description	
2.2.3 Temporary Loading Conditions	7.4.8	No difference noted	

API Section	Corresponding IEC Section	Unique to IEC	Unique to API
2.3.1 Waves	6.1.1.1	“Design calculations shall be based on values of peak spectral period which results in highest loads”. Range of possible period for regular waves also given.	
		Assessment of breaking waves.	
2.3.1.a General	5.2	Dynamic model required	Dynamic model optional
2.3.1.b Static Wave Analysis		Here we compare the detail of the Static Wave Analysis, with the IEC requirements as many of the procedures apply to both	
2.3.1.b.1 Apparent Wave period	Not included	Correction not required	
2.3.1.b.2 Two-Dimensional Wave Kinematics	C.1	No difference noted	
2.3.1.b.3 Wave Kinematics Factor	D.6.2	No difference noted	
2.3.1.b.4 Current Blockage Factor	Not included	Adds conservatism to metocean loads, for jacket-type and tripod structures	
2.3.1.b.5 Combined Wave/Current Kinematics	Not specified	Linear stretching used for waves	Nonlinear stretching preferred for currents
2.3.1.b.6 Marine Growth	6.1.5	Effect on accessibility, corrosion rate and a strategy for inspection and possible removal should be considered.	
2.3.1.b.7 Drag and Inertia Coefficients	D1	“Typical” values are identical.	
2.3.1.b.9 Hydrodynamic Models for Appurtenances	7.3.4, D.5	No difference noted	
2.3.1.b.10 Morison Equation		No difference noted	
2.3.1.b.11 Global Structure Forces	D.1/D.2	No difference noted	
2.3.1.b.12 Local Member Design	D.2/D.3	No difference noted	

API Section	Corresponding IEC Section	Unique to IEC	Unique to API
2.3.1.c Dynamic Wave Analysis			
2.3.1.c.2 Waves	B.4	Both random and deterministic wave models can be used.	
		Unidirectional sea states should be used.	Wave spreading should be considered
			Wave group effects may also cause important dynamic responses in compliant structures.
2.3.1.c.3 Currents	6.1.2	No difference noted	
2.3.1.c.4 Winds	6	No difference noted	
2.3.1.c.5 Fluid Force on a Member	D.1		Relative velocity used in Morrison's equation for guyed towers or TLPs.
2.3.1.c.6 Structural Modelling	D.1, 7.5.4		A damping value of 2-3% of critical for extreme wave analyses and 2 % of critical for fatigue analyses may be used.
			It may be appropriate to consider a stiffer foundation for fatigue analyses than for extreme wave responds analyses.
		The designer shall take particular account of the nonlinearities of the interaction of the foundation and seabed, and the uncertainty and potential long term time variation of the dynamic properties due to scour, sand waves, etc. The robustness of the design to changes in the resonant frequencies of the support structure and to the changes in the foundation loading shall be assessed.	

API	IEC	Unique to IEC	Unique to API
2.3.1.c.7 Analysis Method		No difference noted for time domain methods	
			Frequency domain methods are generally appropriate for small wave fatigue analyses.
2.3.2 Wind		Different wind models used.	
		In the absence of information defining the long term joint probability distribution of extreme wind and waves, it shall be assumed that the extreme 10-min mean wind speed with 50-year recurrence period occurs during the extreme sea state with 50-year recurrence period. The same assumption shall apply with regard to the combination of the extreme 10-min wind speed and the extreme sea state each with a 1-year recurrence period.	
2.3.2.e Shape Coefficients	Not included	No guidance provided	Shape factors provided for wind calculations
2.3.2.f Shielding Coefficients	N/A		Left to designer's judgement
2.3.1.g Wind Tunnel Data	7.2	No difference noted	
2.3.3 Current	6.1.2, 12.5	No difference noted	
	6.1.2	Near shore currents	
	6.1.2.4	Normal current used with Severe Sea State	
2.3.4 Hydrodynamic Force Guidelines for U.S. Waters	Not included	No metocean data in IEC	Detailed guidance provided for U.S. Waters

D.2.3 Member Design

The IEC standard does not provide guidance on the calculation of the design strength of the structure; instead, the user is referred to the appropriate ISO standard (in this case, ISO 19902). The use of other design standards is also permitted as long as the designer demonstrates that at least the same level of structural reliability has been achieved.

API RP 2A-WSD follows the Working Stress Design format, however ISO 19902, is a Load and Resistance Factor Design code. This makes direct comparison of the structural steel design aspect difficult. Section numbers that are preceded by “ISO” refer to 19902.

In API design, the member stresses are limited to

$$\text{Allowable stress} = \text{API Allowable Stress Factor} \times \text{Yield Stress};$$

whereas in IEC design, the stress limit is

$$\text{Member strength} = \text{Yield Stress} / \text{IEC Resistance Factor}.$$

API RP2A also allows the increase of allowable stresses by 33% for the extreme load cases.

Note that the extreme load demand on the members is defined as the 100-yr load demand per API and 50-yr load demand multiplied by load factor of 1.35 per IEC. The design equations can be formularized as follows:

Per API:

$$1.33 \times \text{API Allowable Stress Factor} \times \text{Yield Stress} > 100\text{-yr load demand}$$

Per IEC:

$$\text{Yield Stress} / \text{IEC Resistance Factor} > \text{IEC Load Factor} \times 50\text{-yr load demand}$$

Table 33: API and IEC/ISO comparison (member design)

API Section	Corresponding IEC/ISO Section	Unique to IEC/ISO	Unique to API
3. Structural steel design.			
3.1.1 Basic Stresses	Not included		Allowable stresses specified in AISC.
3.1.2 Increased Allowable Stresses	Not included		Increase on AISC values by a third allowed.
3.1.3 Design Considerations			Minimum of 12 directions for tripod plus or minus 5 degrees
3.2.1 Axial Tension	ISO 13.2.2	Resistance factor of 1.05	0.6 (to be increased by 1/3 for extreme loads)
3.2.2.b Local Buckling	ISO 13.2.3.2	Similar equations for elastic buckling, different equations for inelastic buckling for sections with high D/t (diameter-to-wall thickness) ratios	
3.2.3 Bending	ISO 13.2.4	Resistance factor of 1.05 with variation based on D/t ratio	0.75 (to be increased by 1/3 for extreme loads) and smaller depending on D/t ratio
3.2.4 Shear	ISO 13.2.3.5	Resistance factor of $1.05 \times \sqrt{3}$	0.4 (to be increased 1/3 for extreme loads)
			Reduced allowable torsional shear stress for cylindrical members, when local shear deformations are substantial due to cylinder geometry

D.2.4 Fatigue

Table 34: API and IEC comparison for fatigue

API Section	Corresponding IEC Section	Unique to IEC	Unique to API
<i>5. Fatigue</i>			
5.1 Fatigue Design	Not included	Detailed fatigue analyses always needed in IEC	
5.2 Fatigue Analysis	6.1.4	Ice loading should be considered	
5.2.1	7.4.1	No difference noted	
5.2.2	ISO 16	Dynamic effects always needed.	Dynamic effect should be considered for sea states having significant energy near a platform's natural period.
			Joint stiffness should be considered
		Appropriate assessment needed to neglect currents for fatigue.	
5.2.3	ISO 16.7	No difference noted	
5.2.4	ISO 16.12.1	No difference noted	
5.2.5	ISO 16.12.2	Fatigue damage design factors given as a function of inspection ability and criticality.	No specific guidance.
5.3 S-N Curves	ISO 16.11.1		ANSI document reference
5.4 S-N Curves, Tubular Connections	ISO 16.11.1	Different S-N curves.	
5.5 Stress Concentration Factors	ISO A 6.15.4	No difference noted	

D.2.5 Foundation

Table 35: API and IEC comparison for foundation

API Section	Corresponding IEC Section	Unique to IEC	Unique to API
6. Foundation design			
6.1 General	ISO 17.1	Alternative designs procedures permitted.	
6.3.4 Pile penetration	ISO 17.3.4	Different pile partial resistance factor for extreme conditions:	
		1.25 (extreme), 1.50(operating), plus factor of 1.35 on loads.	1.5 (extreme), 2.0(operating).

APPENDIX E: CODE CHECKS FOR MONOPILE (PER API AND IEC)

The tables presented below provide a summary of the detailed calculations for the monopile design per API and IEC/ISO. The highlighted section on the left side of the tables indicates the input data for the calculations. The rest of the data is calculated using the input data. The calculated quantities can be divided into four main categories (from top to bottom): (1) Geometric properties for the section such as area, modulus of inertia, section modulus, etc.; (2) Allowable stresses; (3) Acting stresses on the section; (4) Utilization ratios.

The design loads used here are provided in Table 14. These loads include load factors in the case of IEC/ISO design. Also note that the material factors (γ factors) in IEC/ISO design are provided in the tables.

Monopile section below mudline:*Power production load case per API:*

D (m)	t (m)	A (m ²)	I (m ⁴)	r(m)	S (m ³)	Z (m ³)
6.0	0.06	1.12	4.94	2.10	1.65	2.12

k	L (m)	kL/r	D/t
2.4	102.6	117.25	100.00

F_v (MPa)	E (MPa)
250	200,000

Per API RP2A, Allowable stresses (without any increase factor):

F _{xe} (MPa)	F _{xc} (MPa)	C _c	(kL/r)/C _c
1200	228	131.5	0.89

F _a (MPa)	F _t (MPa)	F _b (MPa)	F _v (MPa)
72	150	162	100

F _e ' (MPa)
75

Acting stresses on the section:**Design loads**

N (kN)	8,486
M (kNm)	123,921
V (kN)	2,454

f _a (MPa)	f _b (MPa)	f _v (MPa)
7.6	75.3	4.4

C_m	0.85
----------------------	-------------

Allowable stress increase factor:
1.00

Utilization Ratio Calculations:

Combined Axial Compression and Bending (EXCEPT PILES)

Eqn 3.3.1-1 0.55

Eqn 3.3.1-2 0.52

Eqn 3.3.1-3 0.57

UR= 0.570

Shear

UR= 0.044

Combined Axial Compression and Bending (PILES ONLY)

UR= 0.520 (Eqn 3.3.1-5)

Parked/Idling load case per API (100-yr Return Period Metocean Loads):

D (m)	t (m)	A (m ²)	I (m ⁴)	r(m)	S (m ³)	Z (m ³)
6.0	0.06	1.12	4.94	2.10	1.65	2.12

k	L (m)	kL/r	D/t
2.4	102.6	117.25	100.00

F_v (MPa)	E (MPa)
250	200,000

Per API RP2A, Allowable stresses (without any increase factor):

F _{xe} (MPa)	F _{xc} (MPa)	C _c	(kL/r)/C _c
1200	228	131.5	0.89

F _a (MPa)	F _t (MPa)	F _b (MPa)	F _v (MPa)
72	150	162	100

F _e ' (MPa)
75

Acting stresses on the section:

Design loads

N (kN)	8,486
M (kNm)	186,474
V (kN)	6,907

f _a (MPa)	f _b (MPa)	f _v (MPa)
7.6	113.3	12.3

C_m	0.85
----------------------	-------------

Allowable stress increase factor:
1.33

Utilization Ratio Calculations:

Combined Axial Compression and Bending (EXCEPT PILES)

Eqn 3.3.1-1 0.58

Eqn 3.3.1-2 0.56

Eqn 3.3.1-3 0.61

UR= 0.605

Shear

UR= 0.093

Combined Axial Compression and Bending (PILES ONLY)

UR= 0.568 (Eqn 3.3.1-5)

Power production load case per IEC/ISO:

D (m)	t (m)	A (m ²)	I (m ⁴)	r(m)	S (m ³)	Z (m ³)
6.0	0.06	1.12	4.94	2.10	1.65	2.12

k	L (m)	kL/r	D/t
2.4	102.6	117.25	100.00

Fy (MPa)	E (MPa)
250	200,000

Per ISO 19902:

F _{xe} (MPa)	F _{yc} (MPa)	λ	F _v D/(Et)
1200	247	1.3	0.125

F _c (MPa)	F _t (MPa)	F _b (MPa)	F _v (MPa)	F _e (MPa)
129	250	272	144	144

γ _{R,c}	γ _{R,t}	γ _{R,b}	γ _{R,v}
1.18	1.05	1.05	1.05

Design loads

N (kN)	9,335
M (kNm)	167,293
V (kN)	3,313

Stress on the section due to factored loads:

f _c (MPa)	f _b (MPa)	f _v (MPa)
8.3	101.6	5.9

Utilization Ratio Calculations:

Combined Axial Compression and Bending (EXCEPT PILES)

Eqn 13.3-3 0.431

Eqn 13.3-4 0.433

UR= 0.433

Shear

UR= 0.043

Combined Axial Compression and Bending (PILES ONLY)

UR= 0.433 (Eqn13.3-4)

Cm	0.85
-----------	-------------

Parked/Idling load case per IEC/ISO (50-yr Return Period Metocean Loads)

D (m)	t (m)	A (m²)	I (m⁴)	r(m)	S (m³)	Z (m³)
6.0	0.06	1.12	4.94	2.10	1.65	2.12

k	L (m)	kL/r	D/t
2.4	102.6	117.25	100.00

F_y (MPa)	E (MPa)
250	200,000

Per ISO 19902:

F_{xe} (MPa)	F_{yc} (MPa)	λ	F_yD/(Et)
1200	247	1.3	0.125

F_c (MPa)	F_t (MPa)	F_b (MPa)	F_v (MPa)	F_e (MPa)
129	250	272	144	144

γ_{R,c}	γ_{R,t}	γ_{R,b}	γ_{R,v}
1.18	1.05	1.05	1.05

Design loads

N (kN)	9,335
M (kNm)	236,300
V (kN)	9,104

Stress on the section due to factored loads:

f_c (MPa)	f_b (MPa)	f_v (MPa)
8.3	143.5	16.3

Utilization Ratio Calculations:

Combined Axial Compression and Bending (EXCEPT PILES)

Eqn 13.3-3 0.577

Eqn 13.3-4 0.595

UR= 0.595

Shear

UR= 0.118

Combined Axial Compression and Bending (PILES ONLY)

UR= 0.595 (Eqn13.3-4)

C_m	0.85
----------------------	-------------

APPENDIX F: CODE CHECKS FOR IEC TRIPOD

The tables presented below provide a summary for the detailed calculations for the tripod design per API and IEC/ISO. The highlighted section on the left side of the tables indicates the input data for the calculations. The rest of the data is calculated using the input data. The calculated quantities can be divided into four main categories (from top to bottom): (1) Geometric properties for the section such as area, modulus of inertia, section modulus, etc.; (2) Allowable stresses; (3) Acting stresses on the section; (4) Utilization ratios.

The design loads used here are provided in Table 22 and Table 23. These loads include load factors in the case of IEC/ISO design. Also note that the material factors (γ factors) in IEC/ISO design are provided in the tables.

Piles below mudline:*Power production load case per IEC/ISO:*

D (m)	t (m)	A (m ²)	I (m ⁴)	r(m)	S (m ³)	Z (m ³)
1.4	0.032	0.14	0.03	0.48	0.05	0.06

k	L (m)	kL/r	D/t
1	14	28.94	43.75

F_v (MPa)	E (MPa)
290	200,000

Per ISO 19902:

F _{xe} (MPa)	F _{vc} (MPa)	λ	F _v D/(Et)
2743	290	0.4	0.063

F _c (MPa)	F _t (MPa)	F _b (MPa)	F _v (MPa)	F _e (MPa)
280	290	365	167	2357

γ _{R,c}	γ _{R,t}	γ _{R,b}	γ _{R,v}
1.18	1.05	1.05	1.05

Design loads (factored):

N (kN)	15,878
M (kNm)	1,929
V (kN)	998

Stress on the section due to factored loads:

f _c (MPa)	f _b (MPa)	f _v (MPa)
115.5	41.9	14.5

C_m	0.85
----------------------	-------------

Utilization Ratio Calculations:

Combined Axial Compression and Bending (EXCEPT PILES)

Eqn 13.3-3 0.594

Eqn 13.3-4 0.590

UR= 0.594

Shear

UR= 0.091

Combined Axial Compression and Bending (PILES ONLY)

UR= 0.590 (Eqn 13.3-4)

Parked/Idling load case per IEC/ISO (50-yr Return Period Metocean Loads):

D (m)	t (m)	A (m ²)	I (m ⁴)	r(m)	S (m ³)	Z (m ³)
1.4	0.032	0.14	0.03	0.48	0.05	0.06
k	L (m)	kL/r	D/t			
1	14	28.94	43.75			
F_v (MPa)	E (MPa)	Per ISO 19902:				
290	200,000	F _{xe} (MPa)	F _{yc} (MPa)	λ	F _v D/(Et)	
		2743	290	0.4	0.063	
		F _c (MPa)	F _t (MPa)	F _b (MPa)	F _v (MPa)	F _e (MPa)
		280	290	365	167	2357
		γ _{R,c}	γ _{R,t}	γ _{R,b}	γ _{R,v}	
		1.18	1.05	1.05	1.05	
Design loads (factored):		Stress on the section due to factored loads:				
N (kN)	17,864	f _c (MPa)	f _b (MPa)	f _v (MPa)		
M (kNm)	6,653	129.9	144.7	33.6		
V (kN)	2,313					
C_m	0.85	Utilization Ratio Calculations:				
		Combined Axial Compression and Bending (EXCEPT PILES)				
		Eqn 13.3-3 0.922				
		Eqn 13.3-4 0.945				
		UR= 0.945				
		Shear				
		UR= 0.211				
		Combined Axial Compression and Bending (PILES ONLY)				
		UR= 0.945 (Eqn13.3-4)				

Central column (nominal section):*Power production load case per IEC/ISO:*

D (m)	t (m)	A (m ²)	I (m ⁴)	r(m)	S (m ³)	Z (m ³)
6	0.06	1.12	4.94	2.10	1.65	2.12

k	L (m)	kL/r	D/t
2.4	97.6	111.53	100.00

F_v (MPa)	E (MPa)
290	200,000

Per ISO 19902:

F _{xe} (MPa)	F _{yc} (MPa)	λ	F _v D/(Et)
1200	284	1.3	0.145

F _c (MPa)	F _t (MPa)	F _b (MPa)	F _v (MPa)	F _e (MPa)
143	290	309	167	159

γ _{R,c}	γ _{R,t}	γ _{R,b}	γ _{R,v}
1.18	1.05	1.05	1.05

Design loads (factored):

N (kN)	5,256
M (kNm)	126,788
V (kN)	2,808

Stress on the section due to factored loads:

f _c (MPa)	f _b (MPa)	f _v (MPa)
4.7	77.0	5.0

C_m	0.85
----------------------	-------------

Utilization Ratio Calculations:

Combined Axial Compression and Bending (EXCEPT PILES)

Eqn 13.3-3 0.268

Eqn 13.3-4 0.281

UR= 0.281

Shear

UR= 0.031

Combined Axial Compression and Bending (PILES ONLY)

UR= 0.281 (Eqn 13.3-4)

Parked/Idling load case per IEC/ISO (50-yr Return Period Metocean Loads):

D (m)	t (m)	A (m²)	I (m⁴)	r(m)	S (m³)	Z (m³)
6	0.06	1.12	4.94	2.10	1.65	2.12

k	L (m)	kL/r	D/t
2.4	97.6	111.53	100.00

F_y (MPa)	E (MPa)
290	200,000

Per ISO 19902:

F_{xe} (MPa)	F_{yc} (MPa)	λ	F_yD/(Et)
1200	284	1.3	0.145

F_c (MPa)	F_t (MPa)	F_b (MPa)	F_v (MPa)	F_e (MPa)
143	290	309	167	159

γ_{R,c}	γ_{R,t}	γ_{R,b}	γ_{R,v}
1.18	1.05	1.05	1.05

Design loads (factored):

N (kN)	5,256
M (kNm)	93,940
V (kN)	6,273

Stress on the section due to factored loads:

f_c (MPa)	f_b (MPa)	f_v (MPa)
4.7	57.1	11.2

C_m	0.85
----------------------	-------------

Utilization Ratio Calculations:

Combined Axial Compression and Bending (EXCEPT PILES)

Eqn 13.3-3 0.208

Eqn 13.3-4 0.213

UR= 0.213

Shear

UR= 0.070

Combined Axial Compression and Bending (PILES ONLY)

UR= 0.213 (Eqn13.3-4)

Central column (base section):*Power production load case per IEC/ISO:*

D (m)	t (m)	A (m ²)	I (m ⁴)	r(m)	S (m ³)	Z (m ³)
3.6	0.036	0.40	0.64	1.26	0.36	0.46

k	L (m)	kL/r	D/t
1	10	7.94	100.00

F_v (MPa)	E (MPa)
290	200,000

Per ISO 19902:

F _{xe} (MPa)	F _{vc} (MPa)	λ	F _v D/(Et)
1200	284	0.1	0.145

F _c (MPa)	F _t (MPa)	F _b (MPa)	F _v (MPa)	F _e (MPa)
284	290	309	167	31344

γ _{R,c}	γ _{R,t}	γ _{R,b}	γ _{R,v}
1.18	1.05	1.05	1.05

Design loads (factored):

N (kN)	3,042
M (kNm)	29,437
V (kN)	6,994

Stress on the section due to factored loads:

f _c (MPa)	f _b (MPa)	f _v (MPa)
7.5	82.8	34.7

C_m	0.85
----------------------	-------------

Utilization Ratio Calculations:

Combined Axial Compression and Bending (EXCEPT PILES)

Eqn 13.3-3 0.270

Eqn 13.3-4 0.312

UR= 0.312

Shear

UR= 0.218

Combined Axial Compression and Bending (PILES ONLY)

UR= 0.312 (Eqn 13.3-4)

Parked/Idling load case per IEC/ISO (50-yr Return Period Metocean Loads):

D (m)	t (m)	A (m ²)	I (m ⁴)	r(m)	S (m ³)	Z (m ³)
3.6	0.036	0.40	0.64	1.26	0.36	0.46
k	L (m)	kL/r	D/t			
1	10	7.94	100.00			
F_v (MPa)	E (MPa)	Per ISO 19902:				
290	200,000	F _{xe} (MPa)	F _{yc} (MPa)	λ	F _v D/(Et)	
		1200	284	0.1	0.145	
		F _c (MPa)	F _t (MPa)	F _b (MPa)	F _v (MPa)	F _e (MPa)
		284	290	309	167	31344
		γ _{R,c}	γ _{R,t}	γ _{R,b}	γ _{R,v}	
		1.18	1.05	1.05	1.05	
Design loads (factored):		Stress on the section due to factored loads:				
N (kN)	3,042	f _c (MPa)	f _b (MPa)	f _v (MPa)		
M (kNm)	27,277	7.5	76.7	16.2		
V (kN)	3,268					
C_m	0.85	Utilization Ratio Calculations:				
		Combined Axial Compression and Bending (EXCEPT PILES)				
		Eqn 13.3-3 0.253				
		Eqn 13.3-4 0.292				
		UR= 0.292				
		Shear				
		UR= 0.102				
		Combined Axial Compression and Bending (PILES ONLY)				
		UR= 0.292 (Eqn13.3-4)				

Leg section (Pile sleeve):*Power production load case per IEC/ISO:*

D (m)	t (m)	A (m ²)	I (m ⁴)	r(m)	S (m ³)	Z (m ³)
1.5	0.015	0.07	0.02	0.53	0.03	0.03

k	L (m)	kL/r	D/t
1	8	15.24	100.00

F _v (MPa)	E (MPa)
290	200,000

Per ISO 19902:

F _{xe} (MPa)	F _{vc} (MPa)	λ	F _v D/(Et)
1200	284	0.2	0.145

F _c (MPa)	F _t (MPa)	F _b (MPa)	F _v (MPa)	F _e (MPa)
282	290	309	167	8503

γ _{R,c}	γ _{R,t}	γ _{R,b}	γ _{R,v}
1.18	1.05	1.05	1.05

Design loads (factored):

N (kN)	4,769
M (kNm)	900
V (kN)	176

Stress on the section due to factored loads:

f _c (MPa)	f _b (MPa)	f _v (MPa)
68.1	35.0	5.0

C _m	0.85
----------------	------

Utilization Ratio Calculations:

Combined Axial Compression and Bending (EXCEPT PILES)

Eqn 13.3-3 0.387

Eqn 13.3-4 0.401

UR= 0.401

Shear

UR= 0.032

Combined Axial Compression and Bending (PILES ONLY)

UR= 0.401 (Eqn 13.3-4)

Parked/Idling load case per IEC/ISO (50-yr Return Period Metocean Loads):

D (m)	t (m)	A (m ²)	I (m ⁴)	r(m)	S (m ³)	Z (m ³)
1.5	0.015	0.07	0.02	0.53	0.03	0.03

k	L (m)	kL/r	D/t
1	8	15.24	100.00

F _v (MPa)	E (MPa)
290	200,000

Per ISO 19902:

F _{xe} (MPa)	F _{vc} (MPa)	λ	F _v D/(Et)
1200	284	0.2	0.145

F _c (MPa)	F _t (MPa)	F _b (MPa)	F _v (MPa)	F _e (MPa)
282	290	309	167	8503

γ _{R,c}	γ _{R,t}	γ _{R,b}	γ _{R,v}
1.18	1.05	1.05	1.05

Design loads (factored):

N (kN)	4,815
M (kNm)	801
V (kN)	122

Stress on the section due to factored loads:

f _c (MPa)	f _b (MPa)	f _v (MPa)
68.8	31.1	3.5

C _m	0.85
----------------	------

Utilization Ratio Calculations:

Combined Axial Compression and Bending (EXCEPT PILES)

Eqn 13.3-3 0.379

Eqn 13.3-4 0.391

UR= 0.391

Shear

UR= 0.022

Combined Axial Compression and Bending (PILES ONLY)

UR= 0.391 (Eqn13.3-4)

Top Brace:*Power production load case per IEC/ISO:*

D (m)	t (m)	A (m ²)	I (m ⁴)	r(m)	S (m ³)	Z (m ³)
1.2	0.03	0.11	0.02	0.41	0.03	0.04

k	L (m)	kL/r	D/t
0.8	7.1	13.73	40.00

F_v (MPa)	E (MPa)
290	200,000

Per ISO 19902:

F _{xe} (MPa)	F _{yc} (MPa)	λ	F _v D/(Et)
3000	290	0.2	0.058

F _c (MPa)	F _t (MPa)	F _b (MPa)	F _v (MPa)	F _e (MPa)
288	290	371	167	10476

γ _{R,c}	γ _{R,t}	γ _{R,b}	γ _{R,v}
1.18	1.05	1.05	1.05

Design loads (factored):

N (kN)	11,569
M (kNm)	3,983
V (kN)	987

Stress on the section due to factored loads:

f _c (MPa)	f _b (MPa)	f _v (MPa)
104.9	126.6	17.9

Utilization Ratio Calculations:

Combined Axial Compression and Bending (EXCEPT PILES)

Eqn 13.3-3 0.738

Eqn 13.3-4 0.785

UR= 0.785

Shear

UR= 0.112

Combined Axial Compression and Bending (PILES ONLY)

UR= 0.785 (Eqn 13.3-4)

C_m	0.85
----------------------	-------------

Parked/Idling load case per IEC/ISO (50-yr Return Period Metocean Loads):

D (m)	t (m)	A (m ²)	I (m ⁴)	r(m)	S (m ³)	Z (m ³)
1.2	0.03	0.11	0.02	0.41	0.03	0.04
k	L (m)	kL/r	D/t			
0.8	7.1	13.73	40.00			
F_v (MPa)	E (MPa)	Per ISO 19902:				
290	200,000	F _{xe} (MPa)	F _{yc} (MPa)	λ	F _v D/(Et)	
		3000	290	0.2	0.058	
		F _c (MPa)	F _t (MPa)	F _b (MPa)	F _v (MPa)	F _e (MPa)
		288	290	371	167	10476
		γ _{R,c}	γ _{R,t}	γ _{R,b}	γ _{R,v}	
		1.18	1.05	1.05	1.05	
Design loads (factored):		Stress on the section due to factored loads:				
N (kN)	11,461	f _c (MPa)	f _b (MPa)	f _v (MPa)		
M (kNm)	3,555	103.9	113.0	15.9		
V (kN)	879					
C_m	0.85	Utilization Ratio Calculations:				
		Combined Axial Compression and Bending (EXCEPT PILES)				
		Eqn 13.3-3 0.701				
		Eqn 13.3-4 0.743				
		UR= 0.743				
		Shear				
		UR= 0.100				
		Combined Axial Compression and Bending (PILES ONLY)				
		UR= 0.743 (Eqn13.3-4)				

Middle Brace:

Power production load case per IEC/ISO:

D (m)	t (m)	A (m ²)	I (m ⁴)	r(m)	S (m ³)	Z (m ³)
1.2	0.02	0.07	0.01	0.42	0.02	0.03

k	L (m)	kL/r	D/t
0.8	8	15.34	60.00

F_v (MPa)	E (MPa)
290	200,000

Per ISO 19902:

F _{xe} (MPa)	F _{yc} (MPa)	λ	F _v D/(Et)
2000	290	0.2	0.087

F _c (MPa)	F _t (MPa)	F _b (MPa)	F _v (MPa)	F _e (MPa)
287	290	340	167	8390

γ _{R,c}	γ _{R,t}	γ _{R,b}	γ _{R,v}
1.18	1.05	1.05	1.05

Design loads (factored):

N (kN)	7,008
M (kNm)	872
V (kN)	201

Stress on the section due to factored loads:

f _c (MPa)	f _b (MPa)	f _v (MPa)
94.5	40.5	5.4

Utilization Ratio Calculations:

Combined Axial Compression and Bending (EXCEPT PILES)

Eqn 13.3-3 0.496

Eqn 13.3-4 0.510

UR= 0.510

Shear

UR= 0.034

Combined Axial Compression and Bending (PILES ONLY)

UR= 0.510 (Eqn 13.3-4)

C_m	0.85
----------------------	-------------

Parked/Idling load case per IEC/ISO (50-yr Return Period Metocean Loads):

D (m)	t (m)	A (m ²)	I (m ⁴)	r(m)	S (m ³)	Z (m ³)
1.2	0.02	0.07	0.01	0.42	0.02	0.03

k	L (m)	kL/r	D/t
0.8	8	15.34	60.00

F_v (MPa)	E (MPa)
290	200,000

Per ISO 19902:

F _{xe} (MPa)	F _{yc} (MPa)	λ	F _v D/(Et)
2000	290	0.2	0.087

F _c (MPa)	F _t (MPa)	F _b (MPa)	F _v (MPa)	F _e (MPa)
287	290	340	167	8390

γ _{R,c}	γ _{R,t}	γ _{R,b}	γ _{R,v}
1.18	1.05	1.05	1.05

Design loads (factored):

N (kN)	7,438
M (kNm)	728
V (kN)	176

Stress on the section due to factored loads:

f _c (MPa)	f _b (MPa)	f _v (MPa)
100.3	33.8	4.7

Utilization Ratio Calculations:

Combined Axial Compression and Bending (EXCEPT PILES)

Eqn 13.3-3 0.502

Eqn 13.3-4 0.513

UR= 0.513

Shear

UR= 0.030

Combined Axial Compression and Bending (PILES ONLY)

UR= 0.513 (Eqn13.3-4)

C_m	0.85
----------------------	-------------

Bottom Brace:*Power production load case per IEC/ISO:*

D (m)	t (m)	$A (m^2)$	$I (m^4)$	$r(m)$	$S (m^3)$	$Z (m^3)$
1.2	0.02	0.07	0.01	0.42	0.02	0.03

k	L (m)	kL/r	D/t
0.8	6.9	13.23	60.00

F_v (MPa)	E (MPa)
290	200,000

Per ISO 19902:

F_{xe} (MPa)	F_{yc} (MPa)	λ	$F_v D/(Et)$
2000	290	0.2	0.087

F_c (MPa)	F_t (MPa)	F_b (MPa)	F_v (MPa)	F_e (MPa)
288	290	340	167	11278

$\gamma_{R,c}$	$\gamma_{R,t}$	$\gamma_{R,b}$	$\gamma_{R,v}$
1.18	1.05	1.05	1.05

Design loads (factored):

N (kN)	2,719
M (kNm)	1,902
V (kN)	504

Stress on the section due to factored loads:

f_c (MPa)	f_b (MPa)	f_v (MPa)
36.7	88.4	13.6

C_m	0.85
-------------------------	-------------

Utilization Ratio Calculations:

Combined Axial Compression and Bending (EXCEPT PILES)

Eqn 13.3-3 0.383

Eqn 13.3-4 0.422

UR= 0.422

Shear

UR= 0.085

Combined Axial Compression and Bending (PILES ONLY)

UR= 0.422 (Eqn 13.3-4)

Parked/Idling load case per IEC/ISO (50-yr Return Period Metocean Loads):

D (m)	t (m)	A (m ²)	I (m ⁴)	r(m)	S (m ³)	Z (m ³)
1.2	0.02	0.07	0.01	0.42	0.02	0.03

k	L (m)	kL/r	D/t
0.8	6.9	13.23	60.00

F_v (MPa)	E (MPa)
290	200,000

Per ISO 19902:

F _{xe} (MPa)	F _{yc} (MPa)	λ	F _v D/(Et)
2000	290	0.2	0.087

F _c (MPa)	F _t (MPa)	F _b (MPa)	F _v (MPa)	F _e (MPa)
288	290	340	167	11278

γ _{R,c}	γ _{R,t}	γ _{R,b}	γ _{R,v}
1.18	1.05	1.05	1.05

Design loads (factored):

N (kN)	5,892
M (kNm)	2,974
V (kN)	744

Stress on the section due to factored loads:

f _c (MPa)	f _b (MPa)	f _v (MPa)
79.5	138.2	20.1

Utilization Ratio Calculations:

Combined Axial Compression and Bending (EXCEPT PILES)

Eqn 13.3-3 0.691

Eqn 13.3-4 0.750

UR= 0.750

Shear

UR= 0.126

Combined Axial Compression and Bending (PILES ONLY)

UR= 0.750 (Eqn13.3-4)

C_m	0.85
----------------------	-------------

APPENDIX G: CODE CHECKS FOR API TRIPOD

The tables presented below provide a summary for the detailed calculations for the tripod design per API and IEC/ISO. The highlighted section on the left side of the tables indicates the input data for the calculations. The rest of the data is calculated using the input data. The calculated quantities can be divided into four main categories (from top to bottom): (1) Geometric properties for the section such as area, modulus of inertia, section modulus, etc.; (2) Allowable stresses; (3) Acting stresses on the section; (4) Utilization ratios.

The design loads used here are provided in Table 24 and Table 25.

Piles below mudline:*Power production load case per API:*

D (m)	t (m)	A (m²)	I (m⁴)	r(m)	S (m³)	Z (m³)
1.4	0.04	0.17	0.04	0.48	0.06	0.07

k	L (m)	kL/r	D/t
1	14	29.10	35.00

F_v (MPa)	E (MPa)
290	200,000

Per API RP2A, Allowable stresses (without any increase factor):

F_{xe} (MPa)	F_{xc} (MPa)	C_c	(kL/r)/C_c
3429	290	116.7	0.25

F_a (MPa)	F_t (MPa)	F_b (MPa)	F_v (MPa)
160	174	218	116

F_e' (MPa)
1216

Acting stresses on the section:

f_a (MPa)	f_b (MPa)	f_v (MPa)
70.9	25.3	8.6

Design loads:

N (kN)	12,110
M (kNm)	1,431
V (kN)	734

C_m	0.85
----------------------	-------------

Allowable stress increase factor
1.00

Utilization Ratio Calculations:

Combined Axial Compression and Bending (EXCEPT PILES)

Eqn 3.3.1-1	0.55
Eqn 3.3.1-2	0.52
Eqn 3.3.1-3	0.56
UR=	0.549

Shear

UR= 0.074

Combined Axial Compression and Bending (PILES ONLY)

UR= 0.524 (Eqn 3.3.1-5)

Parked/Idling load case per API (100-yr Return Period Metocean Loads):

D (m)	t (m)	A (m²)	I (m⁴)	r(m)	S (m³)	Z (m³)
1.4	0.04	0.17	0.04	0.48	0.06	0.07

k	L (m)	kL/r	D/t
1	14	29.10	35.00

F_y (MPa)	E (MPa)
290	200,000

Per API RP2A, Allowable stresses (without any increase factor):

F_{xe} (MPa)	F_{xc} (MPa)	C_c	(kL/r)/C_c
3429	290	116.7	0.25

F_a (MPa)	F_t (MPa)	F_b (MPa)	F_v (MPa)
160	174	218	116

F_e' (MPa)
1216

Acting stresses on the section:

Design loads:

N (kN)	20,633
M (kNm)	7,272
V (kN)	2,535

f_a (MPa)	f_b (MPa)	f_v (MPa)
120.7	128.7	29.7

C_m	0.85
----------------------	-------------

Allowable stress increase factor
1.33

Utilization Ratio Calculations:

Combined Axial Compression and Bending (EXCEPT PILES)

Eqn 3.3.1-1	0.99
Eqn 3.3.1-2	0.97
Eqn 3.3.1-3	1.01
UR=	0.988

Shear

UR= 0.192

Combined Axial Compression and Bending (PILES ONLY)

UR= 0.967 (Eqn 3.3.1-5)

Central column (nominal section):*Power production load case per API:*

D (m)	t (m)	A (m²)	I (m⁴)	r(m)	S (m³)	Z (m³)
6	0.06	1.12	4.94	2.10	1.65	2.12

k	L (m)	kL/r	D/t
2.4	97.6	111.53	100.00

F_v (MPa)	E (MPa)
290	200,000

Per API RP2A, Allowable stresses (without any increase factor):

F_{xe} (MPa)	F_{xc} (MPa)	C_c	(kL/r)/C_c
1200	265	122.1	0.91

F_a (MPa)	F_t (MPa)	F_b (MPa)	F_v (MPa)
81	174	184	116

F_e' (MPa)
83

Acting stresses on the section:**Design loads:**

N (kN)	4,778
M (kNm)	93,706
V (kN)	2,079

f_a (MPa)	f_b (MPa)	f_v (MPa)
4.3	56.9	3.7

C_m	0.85
----------------------	-------------

Allowable stress increase factor
1.00

Utilization Ratio Calculations:

Combined Axial Compression and Bending (EXCEPT PILES)

Eqn 3.3.1-1 0.33

Eqn 3.3.1-2 0.33

Eqn 3.3.1-3 0.36

UR= 0.362

Shear

UR= 0.032

Combined Axial Compression and Bending (PILES ONLY)

UR= 0.336 (Eqn 3.3.1-5)

Parked/Idling load case per API (100-yr Return Period Metocean Loads):

D (m)	t (m)	A (m²)	I (m⁴)	r(m)	S (m³)	Z (m³)
6	0.06	1.12	4.94	2.10	1.65	2.12
k	L (m)	kL/r	D/t			
2.4	97.6	111.53	100.00			
F_y (MPa)	E (MPa)	Per API RP2A, Allowable stresses (without any increase factor):				
290	200,000	F_{xe} (MPa)	F_{xc} (MPa)	C_c	(kL/r)/C_c	
		1200	265	122.1	0.91	
		F_a (MPa)	F_t (MPa)	F_b (MPa)	F_v (MPa)	
		81	174	184	116	
		F_e' (MPa)				
		83				
Design loads:		Acting stresses on the section:				
N (kN)	4,778	f_a (MPa)	f_b (MPa)	f_v (MPa)		
M (kNm)	118,247	4.3	71.8	12.3		
V (kN)	6,911					
C_m	0.85	Utilization Ratio Calculations:				
Allowable stress increase factor	1.33	Combined Axial Compression and Bending (EXCEPT PILES)				
		Eqn 3.3.1-1	0.30			
		Eqn 3.3.1-2	0.31			
		Eqn 3.3.1-3	0.33			
		UR=	0.333			
		Shear				
		UR=	0.080			
		Combined Axial Compression and Bending (PILES ONLY)				
		UR=	0.313	(Eqn 3.3.1-5)		

Central column (base section):*Power production load case per API:*

D (m)	t (m)	A (m ²)	I (m ⁴)	r(m)	S (m ³)	Z (m ³)
3.6	0.036	0.40	0.64	1.26	0.36	0.46

k	L (m)	kL/r	D/t
1	10	7.94	100.00

F_v (MPa)	E (MPa)
290	200,000

Per API RP2A, Allowable stresses (without any increase factor):

F _{xe} (MPa)	F _{xc} (MPa)	C _c	(kL/r)/C _c
1200	265	122.1	0.06

F _a (MPa)	F _t (MPa)	F _b (MPa)	F _v (MPa)
156	174	184	116

F _e ' (MPa)
16354

Acting stresses on the section:**Design loads:**

N (kN)	2,760
M (kNm)	21,076
V (kN)	5,213

f _a (MPa)	f _b (MPa)	f _v (MPa)
6.8	59.3	25.9

C_m	0.85
----------------------	-------------

Allowable stress increase factor
1.00

Utilization Ratio Calculations:

Combined Axial Compression and Bending (EXCEPT PILES)

Eqn 3.3.1-1 0.32

Eqn 3.3.1-2 0.36

Eqn 3.3.1-3 0.37

UR= 0.365

Shear

UR= 0.223

Combined Axial Compression and Bending (PILES ONLY)

UR= 0.365 (Eqn 3.3.1-5)

Parked/Idling load case per API (100-yr Return Period Metocean Loads):

D (m)	t (m)	A (m²)	I (m⁴)	r(m)	S (m³)	Z (m³)
3.6	0.036	0.40	0.64	1.26	0.36	0.46

k	L (m)	kL/r	D/t
1	10	7.94	100.00

F_y (MPa)	E (MPa)
290	200,000

Per API RP2A, Allowable stresses (without any increase factor):

F_{xe} (MPa)	F_{xc} (MPa)	C_c	(kL/r)/C_c
1200	265	122.1	0.06

F_a (MPa)	F_t (MPa)	F_b (MPa)	F_v (MPa)
156	174	184	116

F_e' (MPa)
16354

Acting stresses on the section:

Design loads:

N (kN)	2,760
M (kNm)	32,095
V (kN)	4,620

f_a (MPa)	f_b (MPa)	f_v (MPa)
6.8	90.3	22.9

C_m	0.85
----------------------	-------------

Allowable stress increase factor
1.33

Utilization Ratio Calculations:

Combined Axial Compression and Bending (EXCEPT PILES)

Eqn 3.3.1-1 0.35

Eqn 3.3.1-2 0.40

Eqn 3.3.1-3 0.40

UR= 0.401

Shear

UR= 0.149

Combined Axial Compression and Bending (PILES ONLY)

UR= 0.400 (Eqn 3.3.1-5)

Leg section (Pile sleeve):*Power production load case per API:*

D (m)	t (m)	A (m²)	I (m⁴)	r(m)	S (m³)	Z (m³)
1.5	0.015	0.07	0.02	0.53	0.03	0.03

k	L (m)	kL/r	D/t
1	8	15.24	100.00

F_y (MPa)	E (MPa)
290	200,000

Per API RP2A, Allowable stresses (without any increase factor):

F_{xe} (MPa)	F_{xc} (MPa)	C_c	(kL/r)/C_c
1200	265	122.1	0.12

F_a (MPa)	F_t (MPa)	F_b (MPa)	F_v (MPa)
153	174	184	116

F_e' (MPa)
4436

Acting stresses on the section:**Design loads:**

N (kN)	3,137
M (kNm)	570
V (kN)	112

f_a (MPa)	f_b (MPa)	f_v (MPa)
44.8	22.2	3.2

C_m	0.85
----------------------	-------------

Allowable stress increase factor
1.00

Utilization Ratio Calculations:

Combined Axial Compression and Bending (EXCEPT PILES)

Eqn 3.3.1-1	0.40
Eqn 3.3.1-2	0.38
Eqn 3.3.1-3	0.41
UR=	0.396

Shear

UR=	0.028
------------	--------------

Combined Axial Compression and Bending (PILES ONLY)

UR=	0.402	(Eqn 3.3.1-5)
------------	--------------	---------------

Parked/Idling load case per API (100-yr Return Period Metocean Loads):

D (m)	t (m)	A (m²)	I (m⁴)	r(m)	S (m³)	Z (m³)
1.5	0.015	0.07	0.02	0.53	0.03	0.03

k	L (m)	kL/r	D/t
1	8	15.24	100.00

F_y (MPa)	E (MPa)
290	200,000

Per API RP2A, Allowable stresses (without any increase factor):

F_{xe} (MPa)	F_{xc} (MPa)	C_c	(kL/r)/C_c
1200	265	122.1	0.12

F_a (MPa)	F_t (MPa)	F_b (MPa)	F_v (MPa)
153	174	184	116

F_e' (MPa)
4436

Acting stresses on the section:

Design loads:

N (kN)	4,850
M (kNm)	769
V (kN)	121

f_a (MPa)	f_b (MPa)	f_v (MPa)
69.3	29.9	3.5

C_m	0.85
----------------------	-------------

Allowable stress increase factor
1.33

Utilization Ratio Calculations:

Combined Axial Compression and Bending (EXCEPT PILES)

Eqn 3.3.1-1	0.45
Eqn 3.3.1-2	0.42
Eqn 3.3.1-3	0.46
UR=	0.445

Shear

UR=	0.022
------------	--------------

Combined Axial Compression and Bending (PILES ONLY)

UR=	0.450	(Eqn 3.3.1-5)
------------	--------------	---------------

Top Brace:*Power production load case per API:*

D (m)	t (m)	A (m ²)	I (m ⁴)	r(m)	S (m ³)	Z (m ³)
1.2	0.035	0.13	0.02	0.41	0.04	0.05

k	L (m)	kL/r	D/t
0.8	7.1	13.78	34.29

F_y (MPa)	E (MPa)
290	200,000

Per API RP2A, Allowable stresses (without any increase factor):

F _{xe} (MPa)	F _{xc} (MPa)	C _c	(kL/r)/C _c
3500	290	116.7	0.12

F _a (MPa)	F _t (MPa)	F _b (MPa)	F _v (MPa)
168	174	218	116

F _e ' (MPa)
5421

Acting stresses on the section:**Design loads:**

N (kN)	8,869
M (kNm)	3,044
V (kN)	750

f _a (MPa)	f _b (MPa)	f _v (MPa)
69.2	84.0	11.7

C_m	0.85
----------------------	-------------

Allowable stress increase factor
1.00

Utilization Ratio Calculations:

Combined Axial Compression and Bending (EXCEPT PILES)

Eqn 3.3.1-1 0.74
 Eqn 3.3.1-2 0.78
 Eqn 3.3.1-3 0.80
UR= 0.784

Shear

UR= 0.101

Combined Axial Compression and Bending (PILES ONLY)

UR= 0.784 (Eqn 3.3.1-5)

Parked/Idling load case per API (100-yr Return Period Metocean Loads):

D (m)	t (m)	A (m²)	I (m⁴)	r(m)	S (m³)	Z (m³)
1.2	0.035	0.13	0.02	0.41	0.04	0.05

k	L (m)	kL/r	D/t
0.8	7.1	13.78	34.29

F_v (MPa)	E (MPa)
290	200,000

Per API RP2A, Allowable stresses (without any increase factor):

F_{xe} (MPa)	F_{xc} (MPa)	C_c	(kL/r)/C_c
3500	290	116.7	0.12

F_a (MPa)	F_t (MPa)	F_b (MPa)	F_v (MPa)
168	174	218	116

F_e' (MPa)
5421

Acting stresses on the section:

Design loads:

N (kN)	13,428
M (kNm)	4,266
V (kN)	1,044

f_a (MPa)	f_b (MPa)	f_v (MPa)
104.8	117.7	16.3

C_m	0.85
----------------------	-------------

Allowable stress increase factor
1.33

Utilization Ratio Calculations:

Combined Axial Compression and Bending (EXCEPT PILES)

Eqn 3.3.1-1	0.82
Eqn 3.3.1-2	0.86
Eqn 3.3.1-3	0.88
UR=	0.860

Shear

UR=	0.106
------------	--------------

Combined Axial Compression and Bending (PILES ONLY)

UR=	0.860	(Eqn 3.3.1-5)
------------	--------------	---------------

Middle Brace:*Power production load case per API:*

D (m)	t (m)	A (m ²)	I (m ⁴)	r(m)	S (m ³)	Z (m ³)
1.2	0.025	0.09	0.02	0.42	0.03	0.03

k	L (m)	kL/r	D/t
0.8	8	15.40	48.00

F_v (MPa)	E (MPa)
290	200,000

Per API RP2A, Allowable stresses (without any increase factor):

F _{xe} (MPa)	F _{xc} (MPa)	C _c	(kL/r)/C _c
2500	290	116.7	0.13

F _a (MPa)	F _t (MPa)	F _b (MPa)	F _v (MPa)
168	174	208	116

F _e ' (MPa)
4341

Acting stresses on the section:**Design loads:**

N (kN)	5,062
M (kNm)	812
V (kN)	180

f _a (MPa)	f _b (MPa)	f _v (MPa)
54.9	30.6	3.9

C_m	0.85
----------------------	-------------

Allowable stress increase factor
1.00

Utilization Ratio Calculations:

Combined Axial Compression and Bending (EXCEPT PILES)

Eqn 3.3.1-1 0.45
 Eqn 3.3.1-2 0.46
 Eqn 3.3.1-3 0.47
UR= 0.462

Shear

UR= 0.034

Combined Axial Compression and Bending (PILES ONLY)

UR= 0.462 (Eqn 3.3.1-5)

Parked/Idling load case per API (100-yr Return Period Metocean Loads):

D (m)	t (m)	A (m²)	I (m⁴)	r(m)	S (m³)	Z (m³)
1.2	0.025	0.09	0.02	0.42	0.03	0.03

k	L (m)	kL/r	D/t
0.8	8	15.40	48.00

F_v (MPa)	E (MPa)
290	200,000

Per API RP2A, Allowable stresses (without any increase factor):

F_{xe} (MPa)	F_{xc} (MPa)	C_c	(kL/r)/C_c
2500	290	116.7	0.13

F_a (MPa)	F_t (MPa)	F_b (MPa)	F_v (MPa)
168	174	208	116

F_e' (MPa)
4341

Acting stresses on the section:

Design loads:

N (kN)	9,074
M (kNm)	1,103
V (kN)	247

f_a (MPa)	f_b (MPa)	f_v (MPa)
98.3	41.5	5.4

C_m	0.85
----------------------	-------------

Allowable stress increase factor
1.33

Utilization Ratio Calculations:

Combined Axial Compression and Bending (EXCEPT PILES)

Eqn 3.3.1-1 0.57

Eqn 3.3.1-2 0.57

Eqn 3.3.1-3 0.59

UR= 0.575

Shear

UR= 0.035

Combined Axial Compression and Bending (PILES ONLY)

UR= 0.575 (Eqn 3.3.1-5)

Bottom Brace:*Power production load case per API:*

D (m)	t (m)	A (m ²)	I (m ⁴)	r(m)	S (m ³)	Z (m ³)
1.2	0.025	0.09	0.02	0.42	0.03	0.03

k	L (m)	kL/r	D/t
0.8	6.9	13.28	48.00

F_v (MPa)	E (MPa)
290	200,000

Per API RP2A, Allowable stresses (without any increase factor):

F _{xe} (MPa)	F _{xc} (MPa)	C _c	(kL/r)/C _c
2500	290	116.7	0.11

F _a (MPa)	F _t (MPa)	F _b (MPa)	F _v (MPa)
169	174	208	116

F _e ' (MPa)
5836

Acting stresses on the section:**Design loads:**

N (kN)	2,155
M (kNm)	1,338
V (kN)	335

f _a (MPa)	f _b (MPa)	f _v (MPa)
23.4	50.4	7.3

C_m	0.85
----------------------	-------------

Allowable stress increase factor
1.00

Utilization Ratio Calculations:

Combined Axial Compression and Bending (EXCEPT PILES)

Eqn 3.3.1-1	0.34
Eqn 3.3.1-2	0.38
Eqn 3.3.1-3	0.38
UR=	0.380

Shear

UR=	0.063
------------	--------------

Combined Axial Compression and Bending (PILES ONLY)

UR=	0.376	(Eqn 3.3.1-5)
-----	-------	---------------

Parked/Idling load case per API (100-yr Return Period Metocean Loads):

D (m)	t (m)	A (m²)	I (m⁴)	r(m)	S (m³)	Z (m³)
1.2	0.025	0.09	0.02	0.42	0.03	0.03

k	L (m)	kL/r	D/t
0.8	6.9	13.28	48.00

F_y (MPa)	E (MPa)
290	200,000

Per API RP2A, Allowable stresses (without any increase factor):

F_{xe} (MPa)	F_{xc} (MPa)	C_c	(kL/r)/C_c
2500	290	116.7	0.11

F_a (MPa)	F_t (MPa)	F_b (MPa)	F_v (MPa)
169	174	208	116

F_e' (MPa)
5836

Acting stresses on the section:

Design loads:

N (kN)	6,288
M (kNm)	3,188
V (kN)	754

f_a (MPa)	f_b (MPa)	f_v (MPa)
68.1	120.0	16.3

Utilization Ratio Calculations:

Combined Axial Compression and Bending (EXCEPT PILES)

Eqn 3.3.1-1	0.68
Eqn 3.3.1-2	0.73
Eqn 3.3.1-3	0.74
UR=	0.727

Shear

UR=	0.106
------------	--------------

Combined Axial Compression and Bending (PILES ONLY)

UR=	0.727	(Eqn 3.3.1-5)
------------	--------------	---------------

APPENDIX H: EFFECT OF NONLINEARITY

To better understand the effect of nonlinearity in the calculated forces, wave height is kept constant as 10.67 m and the force on the structure is calculated with different surges.

Table 36: Base shear for the broken waves

Surge (m)	Current (m/sec)	Crest height above mudline (m)	Water Velocity (m/sec)	Base Shear (kN)	Wave Height/depth
0.69	0.180	24.0	10.9	3,450	0.68
0.85	0.185	24.2	10.6	3,390	0.68
1.50	0.200	24.6	9.74	3,210	0.68

Figure 58, Figure 59, and Figure 60 show that the kinematics and the force on the structure decrease as environmental conditions get more severe, i.e., as current and surge increase. This is due to the fact that particle kinematics is higher in shallower water.

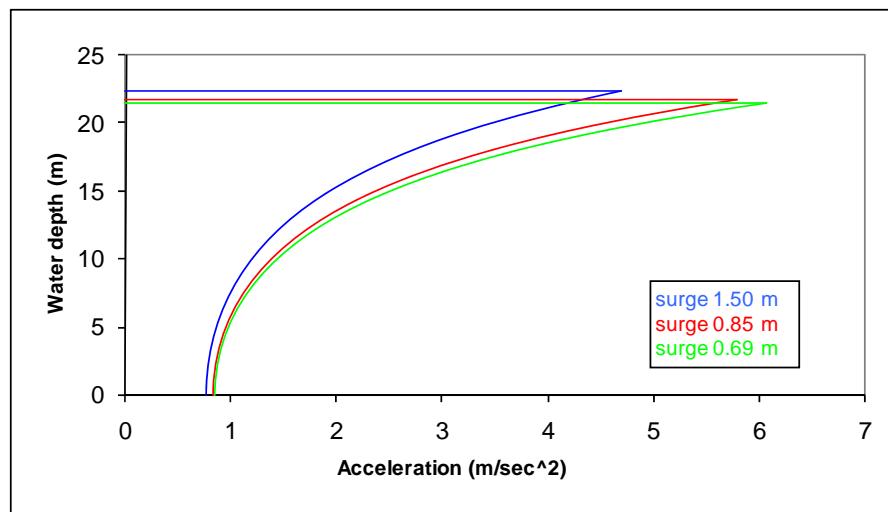


Figure 58: Change in acceleration due to different environmental conditions

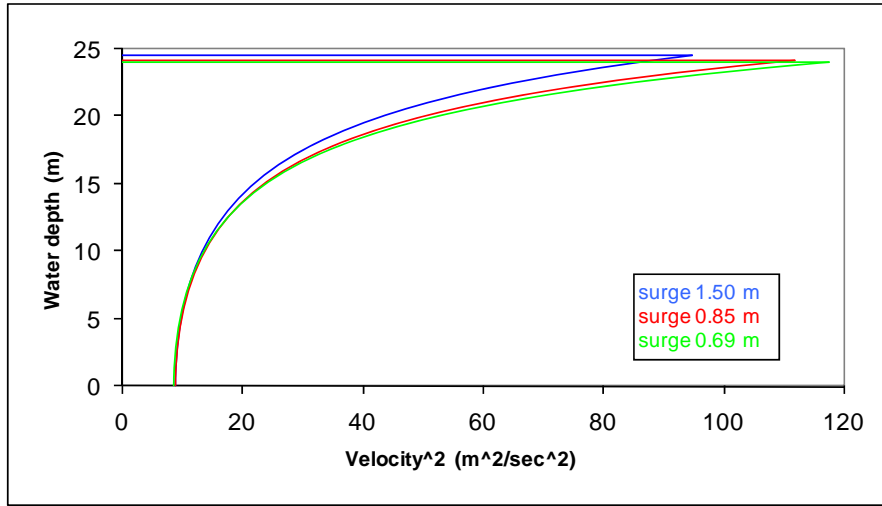


Figure 59: Change in square of velocity due to different environmental conditions

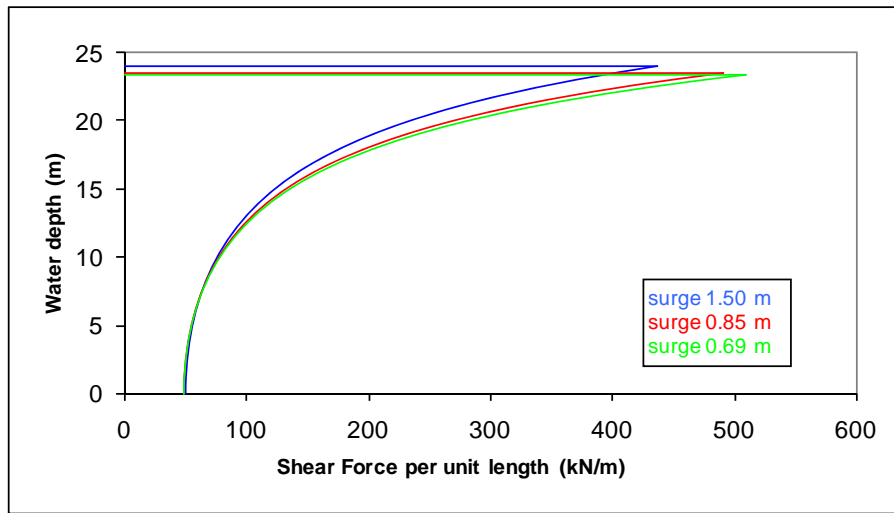


Figure 60: Change in force due to different environmental conditions